Designation: E1820 – 20b

Standard Test Method for
Measurement of Fracture Toughness[1]

1. Scope

1.1 This test method covers procedures and guidelines for the determination of fracture toughness of metallic materials using the following parameters: *K, J,* and CTOD (δ). Toughness can be measured in the *R*-curve format or as a point value. The fracture toughness determined in accordance with this test method is for the opening mode (Mode I) of loading.

NOTE 1—Until this version, K_{Ic} could be evaluated using this test method as well as by using Test Method E399. To avoid duplication, the evaluation of K_{Ic} has been removed from this test method and the user is referred to Test Method E399.

1.2 The recommended specimens are single-edge bend, [SE(B)], compact, [C(T)], and disk-shaped compact, [DC(T)]. All specimens contain notches that are sharpened with fatigue cracks.

1.2.1 Specimen dimensional (size) requirements vary according to the fracture toughness analysis applied. The guidelines are established through consideration of material toughness, material flow strength, and the individual qualification requirements of the toughness value per values sought.

NOTE 2—Other standard methods for the determination of fracture toughness using the parameters *K, J,* and CTOD are contained in Test Methods E399, E1290, and E1921. This test method was developed to provide a common method for determining all applicable toughness parameters from a single test.

1.3 The values stated in SI units are to be regarded as standard. The values given in parentheses after SI units are provided for information only and are not considered standard.

1.4 *This standard does not purport to address all of the safety concerns, if any, associated with its use. It is the responsibility of the user of this standard to establish appropriate safety, health, and environmental practices and determine the applicability of regulatory limitations prior to use.*

1.5 *This international standard was developed in accordance with internationally recognized principles on standardization established in the Decision on Principles for the Development of International Standards, Guides and Recommendations issued by the World Trade Organization Technical Barriers to Trade (TBT) Committee.*

2. Referenced Documents

2.1 *ASTM Standards:*[2]

E4 Practices for Force Verification of Testing Machines

E8/E8M Test Methods for Tension Testing of Metallic Materials

E21 Test Methods for Elevated Temperature Tension Tests of Metallic Materials

E23 Test Methods for Notched Bar Impact Testing of Metallic Materials

E399 Test Method for Linear-Elastic Plane-Strain Fracture Toughness of Metallic Materials

E1290 Test Method for Crack-Tip Opening Displacement (CTOD) Fracture Toughness Measurement (Withdrawn 2013)[3]

E1823 Terminology Relating to Fatigue and Fracture Testing

E1921 Test Method for Determination of Reference Temperature, T_o, for Ferritic Steels in the Transition Range

E1942 Guide for Evaluating Data Acquisition Systems Used in Cyclic Fatigue and Fracture Mechanics Testing

E2298 Test Method for Instrumented Impact Testing of Metallic Materials

2.2 *ASTM Data Sets:*[4]

E1820/1–DS1(2016) Standard data set 1 to evaluate computer algorithms for evaluation of J_{Ic} using Annex 9 of E1820

E1820/2–DS2(2020) Standard data set 2 to evaluate computer algorithms for evaluation of J_{Ic} using Annex 9 of E1820

E1820/3–DS3(2020) Standard data set 3 to evaluate computer algorithms for evaluation of J_{Ic} using Annex 9 of E1820

3. Terminology

3.1 Terminology E1823 is applicable to this test method. Only items that are exclusive to Test Method E1820, or that have specific discussion items associated, are listed in this section.

3.2 *Definitions of Terms Specific to This Standard:*

3.2.1 *compliance [LF⁻¹], n*—the ratio of displacement increment to force increment.

3.2.2 *crack opening displacement (COD) [L], n*—force-induced separation vector between two points at a specific gage length. The direction of the vector is normal to the crack plane.

3.2.2.1 *Discussion*—In this practice, *displacement,* v, is the total displacement measured by clip gages or other devices spanning the crack faces.

3.2.3 *crack extension, Δa [L], n*—an increase in crack size.

3.2.4 *crack-extension force, G [FL⁻¹ or FLL⁻²], n*—the elastic energy per unit of new separation area that is made available at the front of an ideal crack in an elastic solid during a virtual increment of forward crack extension.

3.2.5 *crack-tip opening displacement (CTOD), δ [L], n*—crack displacement resulting from the total deformation (elastic plus plastic) at variously defined locations near the original (prior to force application) crack tip.
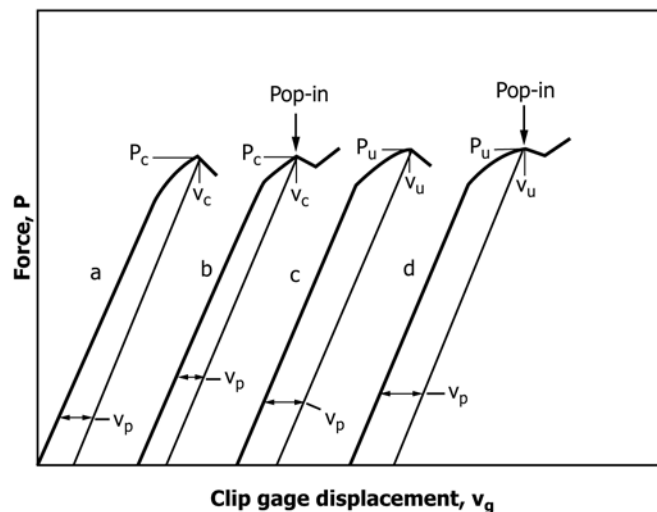
3.2.5.1 *Discussion*—In this test method, CTOD is the displacement of the crack surfaces normal to the original (unloaded) crack plane at the tip of the fatigue precrack, a_o. In this test method, CTOD is calculated at the original crack size, a_o, from measurements made from the force versus displacement record.

3.2.5.2 *Discussion*—In CTOD testing, δ_{Ic} [L] is a value of CTOD near the onset of slow stable crack extension, here defined as occurring at Δa_p = 0.2 mm (0.008 in.) + $0.7\delta_{Ic}$.

3.2.5.3 *Discussion*—In CTOD testing, δ_c [L] is the value of CTOD at the onset of unstable crack extension (see 3.2.36) or pop-in (see 3.2.22) when Δa_p < 0.2 mm (0.008 in.) + $0.7\delta_c$. δ_c corresponds to the force P_c and clip-gage displacement v_c (see Fig. 1). It may be size-dependent and a function of test specimen geometry.

3.2.5.4 *Discussion*—In CTOD testing, δ_u [L] is the value of CTOD at the onset of unstable crack extension (see 3.2.36) or pop-in (see 3.2.22) when the event is preceded by Δa_p >0.2 mm (0.008 in.) + $0.7\delta_u$. The δ_u corresponds to the force P_u and the clip gage displacement v_u (see Fig. 1). It may be size-dependent and a function of test specimen geometry. It can be useful to define limits on ductile fracture behavior.

3.2.5.5 *Discussion*—In CTOD testing, δ_c^* [L] characterizes the CTOD fracture toughness of materials at fracture instability prior to the onset of significant stable tearing crack extension. The value of δ_c^* determined by this test method represents a measure of fracture toughness at instability without significant stable crack extension that is independent of in-plane dimensions. However, there may be a dependence of toughness on thickness (length of crack front).

NOTE 1—Construction lines drawn parallel to the elastic loading slope to give v_p, the plastic component of total displacement, v_g.

NOTE 2—In curves b and d, the behavior after pop-in is a function of machine/specimen compliance, instrument response, and so forth.

FIG. 1 Types of Force versus Clip gage Displacement Records

3.2.6 *dial energy, KV [FL]*—absorbed energy as indicated by the impact machine encoder or dial indicator, as applicable.

3.2.7 *dynamic stress intensity factor, K_{Jd}*—The dynamic equivalent of the stress intensity factor K_J, calculated from J using the equation specified in this test method.

3.2.8 *effective thickness, B_e [L]* , *n*—for side-grooved specimens $B_e = B − (B − B_N)^2/B$. This is used for the elastic unloading compliance measurement of crack size.

3.2.9 *effective yield strength, σ_Y [FL^{-2}], n*—an assumed value of uniaxial yield strength that represents the influence of plastic yielding upon fracture test parameters.

3.2.9.1 *Discussion*—It is calculated as the average of the 0.2 % offset yield strength σ_{YS}, and the ultimate tensile strength, σ_{TS} as follows:

$$\sigma_Y = \frac{\sigma_{YS} + \sigma_{TS}}{2} \tag{1}$$

3.2.9.2 *Discussion*—In estimating σ_Y, influences of testing conditions, such as loading rate and temperature, should be considered.

3.2.9.3 *Discussion*—The dynamic effective yield strength, σ_{Yd}, is the dynamic equivalent of the effective yield strength.

3.2.10 *general yield force, P_{gy} [F]*—in an instrumented impact test, applied force corresponding to general yielding of the specimen ligament. It corresponds to F_{gy}, as used in Test Method E2298.

3.2.11 *J-integral, J [FL^{-1}], n*—a mathematical expression, a line or surface integral that encloses the crack front from one crack surface to the other, used to characterize the local stress-strain field around the crack front.

3.2.11.1 *Discussion*—The *J*-integral expression for a two-dimensional crack, in the *x-z* plane with the crack front parallel to the *z*-axis, is the line integral as follows:

$$J = \int_\Gamma \left(W dy - \bar{T} \cdot \frac{\partial \bar{u}}{\partial x} ds \right) \tag{2}$$

where:

W	=	loading work per unit volume or, for elastic bodies, strain energy density,
Γ	=	path of the integral, that encloses (that is, contains) the crack tip,
ds	=	increment of the contour path,
$\bar{T}$	=	outward traction vector on ds,
$\bar{u}$	=	displacement vector at ds,
x, y, z	=	rectangular coordinates, and
$\bar{T} \cdot \frac{\partial \bar{u}}{\partial x} ds$	=	rate of work input from the stress field into the area enclosed by Γ.

3.2.11.2 *Discussion*—The value of *J* obtained from this equation is taken to be path-independent in test specimens commonly used, but in service components (and perhaps in test specimens) caution is needed to adequately consider loading interior to Γ such as from rapid motion of the crack or the service component, and from residual or thermal stress.

3.2.11.3 *Discussion*—In elastic (linear or nonlinear) solids, the *J*-integral equals the crack-extension force, *G*. (See *crack extension force*.)

3.2.11.4 *Discussion*—In elastic (linear and nonlinear) solids for which the mathematical expression is path independent, the

J-integral is equal to the value obtained from two identical bodies with infinitesimally differing crack areas each subject to stress. The parameter *J* is the difference in work per unit difference in crack area at a fixed value of displacement or, where appropriate, at a fixed value of force (**1**)[5].

3.2.11.5 *Discussion*—The dynamic equivalent of J_c is $J_{cd,X}$, with *X* = order of magnitude of *J*-integral rate.

3.2.12 *J_c [FL^{-1}]* —The property J_c determined by this test method characterizes the fracture toughness of materials at fracture instability prior to the onset of significant stable tearing crack extension. The value of J_c determined by this test method represents a measure of fracture toughness at instability without significant stable crack extension that is independent of in-plane dimensions; however, there may be a dependence of toughness on thickness (length of crack front).

3.2.13 *J_u [FL^{-1}]*—The quantity J_u determined by this test method measures fracture instability after the onset of significant stable tearing crack extension. It may be size-dependent and a function of test specimen geometry. It can be useful to define limits on ductile fracture behavior.

3.2.13.1 *Discussion*—The dynamic equivalent of J_u is $J_{ud,X}$, with *X* = order of magnitude of *J*-integral rate.

3.2.14 *J-integral rate, $\dot{J}$ [$FL^{-1}T^{-1}$]*—derivative of J with respect to time.

3.2.15 *machine capacity, MC [FL]*—maximum available energy of the impact testing machine.

3.2.16 *maximum force, P_{max} [F]*—in an instrumented impact test, maximum value of applied force. It corresponds to F_m, as used in Test Method E2298.

3.2.17 *net thickness, B_N [L], n*—distance between the roots of the side grooves in side-grooved specimens.

3.2.18 *original crack size, a_o [L]* , *n*—the physical crack size at the start of testing.

3.2.18.1 *Discussion*—In this test method, a_{oq} is used to denote original crack size estimated from compliance.

3.2.19 *original remaining ligament, b_o [L], n*—distance from the original crack front to the back edge of the specimen, that is ($b_o = W − a_o$).

3.2.20 *physical crack size, a_p [L]* , *n*—the distance from a reference plane to the observed crack front. This distance may represent an average of several measurements along the crack front. The reference plane depends on the specimen form, and it is normally taken to be either the boundary, or a plane containing either the load-line or the centerline of a specimen or plate. The reference plane is defined prior to specimen deformation.

3.2.21 *plane-strain fracture toughness, J_{Ic} [FL^{-1}], K_{JIc} [$FL^{-3/2}$]* , *n*—the crack-extension resistance under conditions of crack-tip plane-strain.

3.2.21.1 *Discussion*—For example, in Mode I for slow rates of loading and substantial plastic deformation, plane-strain fracture toughness is the value of the *J*-integral designated J_{Ic} [FL^{-1}] as measured using the operational procedure (and

---

[5] The boldface numbers in parentheses refer to the list of references at the end of this standard.

satisfying all of the qualification requirements) specified in this test method, that provides for the measurement of crack-extension resistance near the onset of stable crack extension.

3.2.21.2 *Discussion*—For example, in Mode I for slow rates of loading, plane-strain fracture toughness is the value of the stress intensity designated K_{JIc} calculated from J_{Ic} using the equation (and satisfying all of the qualification requirements) specified in this test method, that provides for the measurement of crack-extension resistance near the onset of stable crack extension under dominant elastic conditions (2).

3.2.21.3 *Discussion*—The dynamic equivalent of J_{Ic} is $J_{Icd,X}$, with X = order of magnitude of J-integral rate.

3.2.22 *pop-in, n*—a discontinuity in the force versus clip gage displacement record. The record of a pop-in shows a sudden increase in displacement and, generally a decrease in force. Subsequently, the displacement and force increase to above their respective values at pop-in.

3.2.23 *R-curve or J-R curve, n*—a plot of crack extension resistance as a function of stable crack extension, Δa_p or Δa_e.

3.2.23.1 *Discussion*—In this test method, the J-R curve is a plot of the far-field J-integral versus the physical crack extension, Δa_p. It is recognized that the far-field value of J may not represent the stress-strain field local to a growing crack.

3.2.24 *remaining ligament, b [L], n*—distance from the physical crack front to the back edge of the specimen, that is ($b = W − a_p$).

3.2.25 *specimen center of pin hole distance, H* [L], n*—the distance between the center of the pin holes on a pin-loaded specimen.

3.2.26 *specimen gage length, d [L], n*—the distance between the points of displacement measure (for example, clip gage, gage length).

3.2.27 *specimen span, S [L], n*—the distance between specimen supports.

3.2.28 *specimen thickness, B [L], n*—the side-to-side dimension of the specimen being tested.

3.2.29 *specimen width, W [L], n*—a physical dimension on a test specimen measured from a reference position such as the front edge in a bend specimen or the load-line in the compact specimen to the back edge of the specimen.

3.2.30 *stable crack extension [L], n*—a displacement-controlled crack extension beyond the stretch-zone width (see 3.2.34). The extension stops when the applied displacement is held constant.

3.2.31 *strain rate, $\dot{\varepsilon}$*—derivative of strain ε with respect to time.

3.2.32 *stress-intensity factor, K, K_1, K_2, K_3, K_I, K_{II}, K_{III} [FL$^{−3/2}$], n*—the magnitude of the ideal-crack-tip stress field (stress-field singularity) for a particular mode in a homogeneous, linear-elastic body.

3.2.32.1 *Discussion*—Values of K for the Modes 1, 2, and 3 are given by the following equations:

$$K_1 = \lim_{r \to 0} [\sigma_{yy}(2\pi r)^{1/2}] \qquad (3)$$

$$K_2 = \lim_{r \to 0} [\tau_{xy}(2\pi r)^{1/2}] \qquad (4)$$

$$K_3 = \lim_{r \to 0} [\tau_{yz}(2\pi r)^{1/2}] \qquad (5)$$

where r = distance directly forward from the crack tip to a location where the significant stress is calculated.

3.2.32.2 *Discussion*—In this test method, Mode 1 or Mode I is assumed. See Terminology E1823 for definition of mode.

3.2.33 *stress-intensity factor rate, $\dot{K}$ [FL$^{-3/2}T^{-1}$]*—derivative of K with respect to time.

3.2.34 *stretch-zone width, SZW [L], n*—the length of crack extension that occurs during crack-tip blunting, for example, prior to the onset of unstable brittle crack extension, pop-in, or slow stable crack extension. The SZW is in the same plane as the original (unloaded) fatigue precrack and refers to an extension beyond the original crack size.

3.2.35 *time to fracture, t_f [T]*—time corresponding to specimen fracture.

3.2.36 *unstable crack extension [L], n*—an abrupt crack extension that occurs with or without prior stable crack extension in a standard test specimen under crosshead or clip gage displacement control.

3.3 *Symbols:*

3.3.1 t_i *[T]*—time corresponding to the onset of crack propagation.

3.3.2 v_0 *[LT^{-1}]*—in an instrumented impact test, striker velocity at impact.

3.3.3 W_m *[FL]*—in an instrumented impact test, absorbed energy at maximum force.

3.3.4 W_t *[FL]*—in an instrumented impact test, total absorbed energy calculated from the complete force/displacement test record.

3.3.5 W_0 *[FL]*—in an instrumented impact test, available impact energy.

4. Summary of Test Method

4.1 The objective of this test method is to load a fatigue precracked test specimen to induce either or both of the following responses (*1*) unstable crack extension, including significant pop-in, referred to as "fracture instability" in this test method; (*2*) stable crack extension, referred to as "stable tearing" in this test method. Fracture instability results in a single point-value of fracture toughness determined at the point of instability. Stable tearing results in a continuous fracture toughness versus crack-extension relationship (*R*-curve) from which significant point-values may be determined. Stable tearing interrupted by fracture instability results in an *R*-curve up to the point of instability.

4.2 This test method requires continuous measurement of force versus load-line displacement or crack mouth opening displacement, or both. If any stable tearing response occurs, then an *R*-curve is developed and the amount of slow-stable crack extension shall be measured.

4.3 Two alternative procedures for measuring crack extension are presented, the basic procedure and the resistance curve procedure. The basic procedure involves physical marking of the crack advance and multiple specimens used to develop a plot from which a single point initiation toughness value can be

evaluated. The resistance curve procedure is an elastic-compliance method where multiple points are determined from a single specimen. In the latter case, high precision of signal resolution is required. These data can also be used to develop an *R*-curve. Other procedures for measuring crack extension are allowed.

4.4 The commonality of instrumentation and recommended testing procedure contained herein permits the application of data to more than one method of evaluating fracture toughness. Annex A4 and Annex A6 – Annex A11 define the various data treatment options that are available, and these should be reviewed to optimize data transferability.

4.5 Data that are generated following the procedures and guidelines contained in this test method are labeled qualified data. Data that meet the size criteria in Annex A4 and Annex A6 – Annex A11 are insensitive to in-plane dimensions.

4.6 Supplementary information about the background of this test method and rationale for many of the technical requirements of this test method are contained in (**3**). The formulas presented in this test method are applicable over the range of crack size and specimen sizes within the scope of this test method.

5. Significance and Use

5.1 Assuming the presence of a preexisting, sharp, fatigue crack, the material fracture toughness values identified by this test method characterize its resistance to: *(1)* fracture of a stationary crack, *(2)* fracture after some stable tearing, *(3)* stable tearing onset, and *(4)* sustained stable tearing. This test method is particularly useful when the material response cannot be anticipated before the test. Application of procedures in Test Method E1921 is recommended for testing ferritic steels that undergo cleavage fracture in the ductile-to-brittle transition.

5.1.1 These fracture toughness values may serve as a basis for material comparison, selection, and quality assurance. Fracture toughness can be used to rank materials within a similar yield strength range.

5.1.2 These fracture toughness values may serve as a basis for structural flaw tolerance assessment. Awareness of differences that may exist between laboratory test and field conditions is required to make proper flaw tolerance assessment.

5.2 The following cautionary statements are based on some observations.

5.2.1 Particular care must be exercised in applying to structural flaw tolerance assessment the fracture toughness value associated with fracture after some stable tearing has occurred. This response is characteristic of ferritic steel in the transition regime. This response is especially sensitive to material inhomogeneity and to constraint variations that may be induced by planar geometry, thickness differences, mode of loading, and structural details.

5.2.2 The *J-R* curve from bend-type specimens recommended by this test method (SE(B), C(T), and DC(T)) has been observed to be conservative with respect to results from tensile loading configurations.

5.2.3 The values of δ_c, δ_u, J_c, and J_u may be affected by specimen dimensions.

6. Apparatus

6.1 Apparatus is required for measurement of applied force, load-line displacement, and crack-mouth opening displacement. Force versus load-line displacement and force versus crack-mouth opening displacement may be recorded digitally for processing by computer or autographically with an *x-y* plotter. Test fixtures for each specimen type are described in the applicable Annex.

6.2 *Displacement Gages:*

6.2.1 Displacement measurements are needed for the following purposes: to evaluate *J* from the area under the force versus load-line displacement record, CTOD from the force versus crack-mouth opening displacement record and, for the elastic compliance method, to infer crack extension, Δa_p, from elastic compliance calculations.

6.2.2 The recommended displacement gage has a working range of not more than twice the displacement expected during the test. When the expected displacement is less than 3.75 mm (0.15 in.), the gage recommended in Fig. 2 may be used. When a greater working range is needed, an enlarged gage such as the one shown in Fig. 3 is recommended. Accuracy shall be within ±1 % of the full working range. In calibration, the maximum deviation of the individual data points from a fit (linear or curve) to the data shall be less than ±0.2 % of the working range of the gage when using the elastic compliance method and ±1 % otherwise. Knife edges are required for seating the gage. Parallel alignment of the knife edges shall be maintained to within 1°. Direct methods for measuring load-line displacement are described in Refs (**3-6**).

6.2.2.1 *Gage Attachment Methods*—The specimen shall be provided with a pair of accurately machined knife edges that support the gage arms and serve as the displacement reference points. These knife edges can be machined integral with the specimen or they may be attached separately. Experience has shown that razor blades serve as effective attachable knife edges. The knife edges shall be positively attached to the specimen to prevent shifting of the knife edges during the test method. Experience has shown that machine screws or spot welds are satisfactory attachment methods.

6.2.3 For the elastic compliance method, the recommended signal resolution for displacement should be at least 1 part in 32 000 of the transducer signal range, and signal stability should be ±4 parts in 32 000 of the transducer signal range measured over a 10-min period. Signal noise should be less than ±2 parts in 32 000 of the transducer signal range.

6.2.4 Gages other than those recommended in 6.2.2 are permissible if the required accuracy and precision can be met or exceeded.

6.3 *Force Transducers:*

6.3.1 Testing is performed in a testing machine conforming to the requirements of Practices E4. Applied force may be measured by any force transducer capable of being recorded continuously. Accuracy of force measurements shall be within ±1 % of the working range. In calibration, the maximum deviation of individual data points from a fit to the data shall be
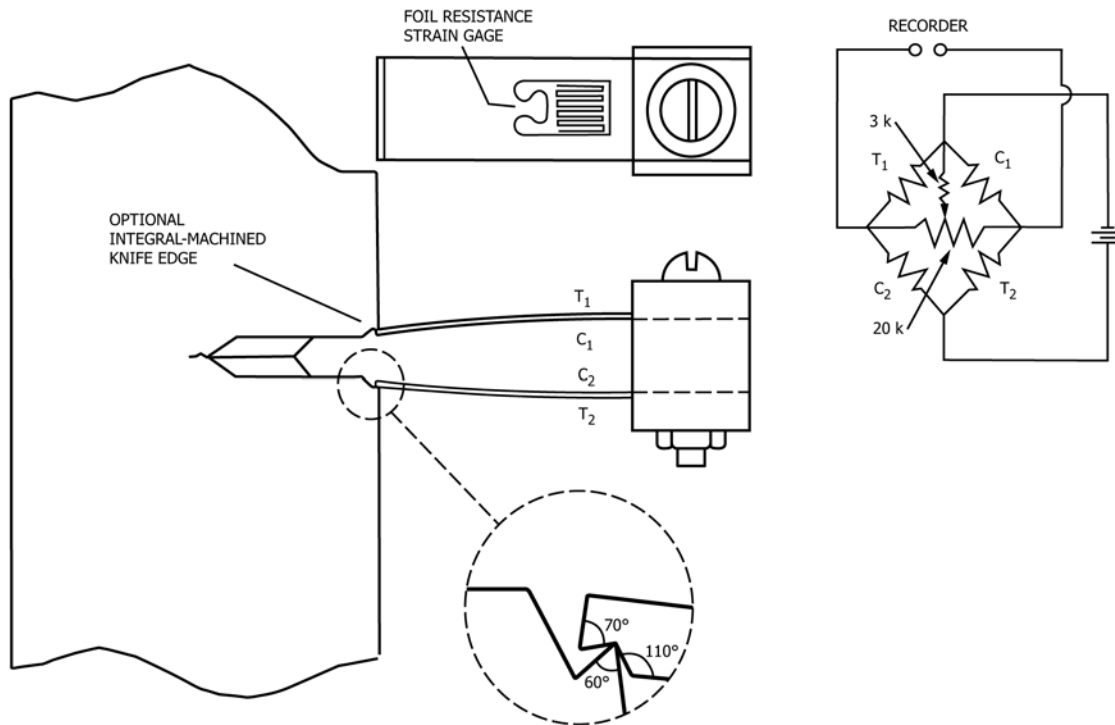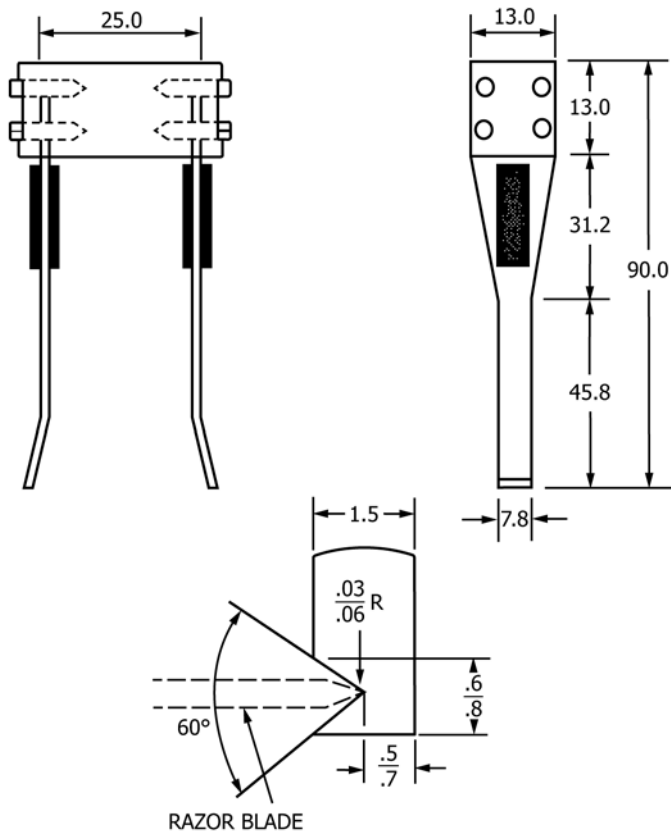
FIG. 2 Double-Cantilever Clip-In Displacement gage Mounted by Means of Integral Knife Edges

NOTE 1—All dimensions are in millimeters.
**FIG. 3 Clip Gage Design for 8.0 mm (0.3 in.)
and More Working Range**

less than ±0.2 % of the calibrated range of the transducer when using elastic compliance, and ±1 % otherwise.

6.3.2 For the elastic compliance method, the signal resolution on force should be at least 1 part in 4000 of the transducer signal range and signal stability should be ±4 parts in 4000 of the transducer signal range measured over a 10-min period. Recommended maximum signal noise should be less than ±2 parts in 4000 of the transducer signal range.

6.4 *System Verification*—It is recommended that the performance of the force and displacement measuring systems be verified before beginning a series of continuous tests. Calibration accuracy of displacement transducers shall be verified with due consideration for the temperature and environment of the test. Force calibrations shall be conducted periodically and documented in accordance with the latest revision of Practices E4.

6.5 *Fixtures:*

6.5.1 *Bend-Test Fixture*—The general principles of the bend-test fixture are illustrated in Fig. 4. This fixture is designed to minimize frictional effects by allowing the support rollers to rotate and move apart slightly as the specimen is loaded, thus permitting rolling contact. Thus, the support rollers are allowed limited motion along plane surfaces parallel to the notched side of the specimen, but are initially positively positioned against stops that set the span length and are held in place by low-tension springs (such as rubber bands). Fixtures and rolls shall be made of high hardness (greater than 40 HRC) steels.

6.5.2 *Tension Testing Clevis:*

6.5.2.1 A loading clevis suitable for testing compact specimens is shown in Fig. 5. Both ends of the specimen are held in such a clevis and loaded through pins, in order to allow rotation
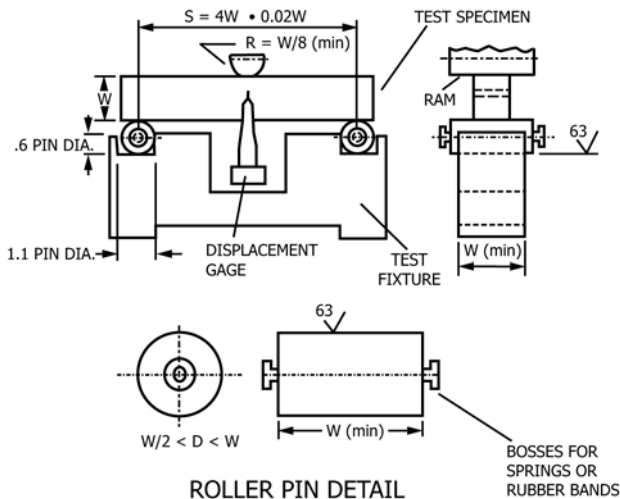
6

FIG. 4 Bend Test Fixture Design

of the specimen during testing. In order to provide rolling contact between the loading pins and the clevis holes, these holes are provided with small flats on the loading surfaces. Other clevis designs may be used if it can be demonstrated that they will accomplish the same result as the design shown. Clevises and pins should be fabricated from steels of sufficient strength (greater than 40 HRC) to elastically resist indentation of the clevises or pins.

6.5.2.2 The critical tolerances and suggested proportions of the clevis and pins are given in Fig. 5. These proportions are based on specimens having W/B = 2 for B > 12.7 mm (0.5 in.) and W/B = 4 for $B \leq 12.7$ mm. If a 1930-MPa (280 000-psi) yield strength maraging steel is used for the clevis and pins, adequate strength will be obtained. If lower-strength grip material is used, or if substantially larger specimens are required at a given σ_{YS}/E ratio, then heavier grips will be required. As indicated in Fig. 5 the clevis corners may be cut off sufficiently to accommodate seating of the clip gage in specimens less than 9.5 mm (0.375 in.) thick.

6.5.2.3 Careful attention should be given to achieving good alignment through careful machining of all auxiliary gripping fixtures.

7. Specimen Size, Configuration, and Preparation

7.1 *Specimen Configurations*—The configurations of the standard specimens are shown in Annex A1 – Annex A3.

7.2 *Crack Plane Orientation*—The crack plane orientation shall be considered in preparing the test specimen. This is discussed in Terminology E1823.

7.3 *Alternative Specimens*—In certain cases, it may be desirable to use specimens having W/B ratios other than two. Suggested alternative proportions for the single-edge bend specimen are $1 \leq W/B \leq 4$ and for the compact (and disk shaped compact) specimen are $2 \leq W/B \leq 4$. However, any thickness can be used as long as the qualification requirements are met.

7.4 *Specimen Precracking*—All specimens shall be pre-cracked in fatigue. Experience has shown that it is impractical to obtain a reproducibly sharp, narrow machined notch that will simulate a natural crack well enough to provide a

satisfactory fracture toughness test result. The most effective artifice for this purpose is a narrow notch from which extends a comparatively short fatigue crack, called the precrack. (A fatigue precrack is produced by cyclically loading the notched specimen for a number of cycles usually between about 10^4 and 10^6 depending on specimen size, notch preparation, and stress intensity level.) The dimensions of the notch and the precrack, and the sharpness of the precrack shall meet certain conditions that can be readily met with most engineering materials since the fatigue cracking process can be closely controlled when careful attention is given to the known contributory factors. However, there are some materials that are too brittle to be fatigue-cracked since they fracture as soon as the fatigue crack initiates; these are outside the scope of the present test method.

7.4.1 *Fatigue Crack Starter Notch*—Three forms of fatigue crack starter notches are shown in Fig. 6. To facilitate fatigue cracking at low stress intensity factor levels, the root radius for a straight-through slot terminating in a *V*-notch should be 0.08 mm (0.003 in.) or less. If a chevron form of notch is used, the root radius may be 0.25 mm (0.010 in.) or less. In the case of a slot tipped with a hole it will be necessary to provide a sharp stress raiser at the end of the hole. The combination of starter notch and fatigue precrack shall conform to the requirements of Fig. 7.

7.4.2 *Fatigue Crack Size*—The crack size (total average length of the crack starter configuration plus the fatigue crack) shall be between 0.45 and 0.70 W for J and δ determination.

7.4.3 *Equipment*—The equipment for fatigue cracking should be such that the stress distribution is uniform through the specimen thickness; otherwise the crack will not grow uniformly. The stress distribution should also be symmetrical about the plane of the prospective crack; otherwise the crack may deviate from that plane and the test result can be significantly affected. The K calibration for the specimen, if it is different from the one given in this test method, shall be known with an uncertainty of less than 5 %. Fixtures used for precracking should be machined with the same tolerances as those used for testing.

7.4.4 *Fatigue Loading Requirements*—Allowable fatigue force values are limited to keep the maximum stress intensity applied during precracking, K_{MAX}, well below the material fracture toughness measured during the subsequent test. The fatigue precracking shall be conducted with the specimen fully heat-treated to the condition in which it is to be tested. No intermediate treatments between precracking and testing are allowed. There are several ways of promoting early crack initiation: *(1)* by providing a very sharp notch tip, *(2)* by using a chevron notch (Fig. 6), *(3)* by statically preloading the specimen in such a way that the notch tip is compressed in a direction normal to the intended crack plane (to a force not to exceed P_m as defined in Annex A1 – Annex A3), and *(4)* by using a negative fatigue force ratio; for a given maximum fatigue force, the more negative the force ratio, the earlier crack initiation is likely to occur. The peak compressive force shall not exceed P_m as defined in Annex A1 – Annex A3.

7.4.5 *Fatigue Precracking Procedure*—Fatigue precracking can be conducted under either force control or displacement
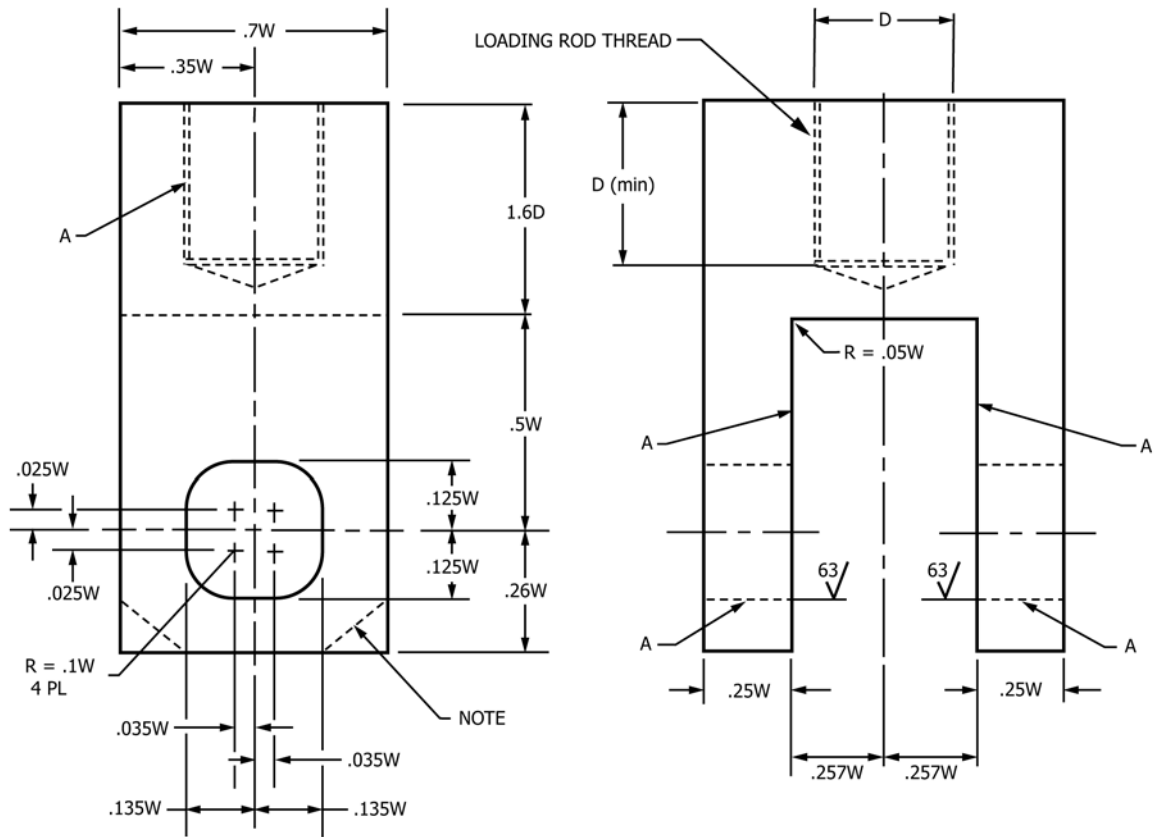
A - SURFACES MUST BE FLAT, IN-LINE AND PERPENDICULAR,
AS APPLICABLE, TO WITHIN 0.002 in. T. I. R. (0.05 mm)

NOTE 1—Corners may be removed as necessary to accommodate the clip gage.
FIG. 5 Tension Testing Clevis Design

FIG. 6 Fatigue Crack Starter Notch Configurations
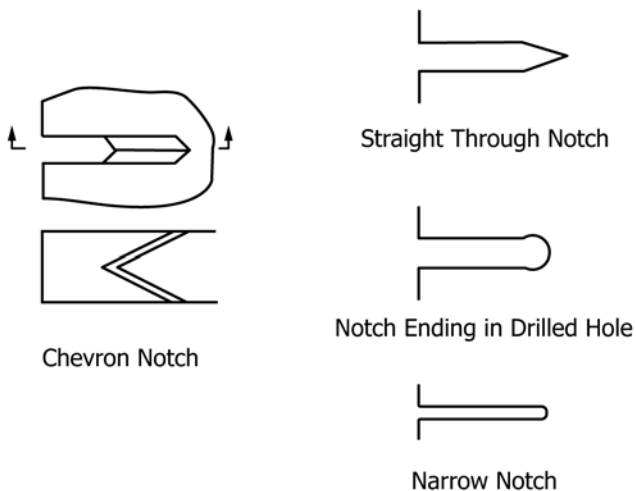
control. If the force cycle is maintained constant, the maximum K and the K range will increase with crack size; if the displacement cycle is maintained constant, the reverse will happen. The initial value of the maximum fatigue force should be less than P_m. The specimen shall be accurately located in the loading fixture. Fatigue cycling is then begun, usually with a sinusoidal waveform and near to the highest practical frequency. There is no known marked frequency effect on fatigue precrack formation up to at least 100 Hz in the absence of adverse environments. The specimen should be carefully monitored until crack initiation is observed on one side. If crack initiation is not observed on the other side before appreciable growth is observed on the first, then fatigue cycling should be stopped to try to determine the cause and find a remedy for the unsymmetrical behavior. Sometimes, simply turning the specimen around in relation to the fixture will solve the problem.

7.4.5.1 The fatigue precrack extension from the machined notch at the nine measurement points along the crack front (see 8.5.3) shall not be less than $0.5h$ where h is the notch height, or 0.25 mm, whichever is larger, and the combination of precrack size and sharpened notch length shall not be less than

8

NOTE 1—The crack-starter notch shall be centered between the top and bottom specimen edges within 0.005 W.

FIG. 7 Envelope of Fatigue Crack and Crack Starter Notches

2.0h. Precracking shall be accomplished in at least two steps. For the first step the maximum stress intensity factor applied to the specimen shall be limited by:

$$K_{MAX} = \left(\frac{\sigma_{YS}^f}{\sigma_{YS}^T}\right)\left(0.063\sigma_{YS}^f \text{ MPa}\sqrt{\text{m}}\right) \quad (6)$$

or

$$K_{MAX} = \left(\frac{\sigma_{YS}^f}{\sigma_{YS}^T}\right)\left(0.4\sigma_{YS}^f \text{ ksi}\sqrt{\text{in.}}\right)$$

where:

σ_{YS}^f and σ_{YS}^T = the material yield stresses at the fatigue precrack and test temperatures respectively.

7.4.5.2 It is generally most effective to use $R = P_{MIN}/P_{MAX}$ = 0.1. The accuracy of the maximum force values shall be known within ±5 %. Precracking should be conducted at as low a K_{MAX} as practical. For some aluminum alloys and high strength steels the above K_{MAX} relationship can give very high precracking forces. This is especially true if precracking and testing are conducted at the same temperature. It is suggested that the user start with approximately 0.7 K_{MAX} given by the above relationship, and if the precrack does not grow after 10^5 cycles the loading can be incrementally increased until the crack begins to extend. For the second precracking step, which shall include at least the final 50 % of the fatigue precrack, the maximum stress intensity factor that may be applied to the specimen shall be given by:

$$K_{MAX} = 0.6\frac{\sigma_{YS}^f}{\sigma_{YS}^T}K_F \quad (7)$$

where:

K_F = K_Q, K_{JQ}, K_{JQc} or K_{JQu} depending on the result of the test, and K_F is calculated from the corresponding J_F using the relationship that:

$$K_F = \sqrt{\frac{EJ_F}{(1-v^2)}} \quad (8)$$

7.4.5.3 To transition between steps, intermediate levels of force shedding can be used if desired.

7.5 *Side Grooves*—Side grooves are highly recommended when the compliance method of crack size prediction is used. The specimen may also need side grooves to ensure a straight crack front as specified in Annex A4 – Annex A11. The total thickness reduction shall not exceed 0.25*B*. A total reduction of 0.20*B* has been found to work well for many materials. Any included angle of side groove less than 90° is allowed. Root radius shall be 0.5 ± 0.2 mm (0.02 ± 0.01 in.). In order to produce nearly straight fatigue precrack fronts, the precracking should be performed prior to the side-grooving operation. B_N is the minimum thickness measured at the roots of the side grooves. The root of the side groove should be located along the specimen centerline.

8. Procedure

8.1 *Objective and Overview:*

8.1.1 The overall objective of the test method is to develop a force-displacement record that can be used to evaluate *K, J,* or CTOD. Two procedures can be used: *(1)* a basic procedure directed toward evaluation of a single *K, J,* or CTOD value without the use of crack extension measurement equipment, or *(2)* a procedure directed toward evaluation of a complete fracture toughness resistance curve using crack extension measurement equipment. This also includes the evaluation of single-point toughness values.

8.1.2 The basic procedure utilizes a force versus displacement plot and is directed toward obtaining a single fracture toughness value such as J_c, K_{JIc}, or δ_c. Optical crack measurements are utilized to obtain both the initial and final physical crack sizes in this procedure. Multiple specimens can be used to evaluate *J* at the initiation of ductile cracking, J_{Ic} or δ_{Ic}.

8.1.3 The resistance curve procedure utilizes an elastic unloading procedure or equivalent procedure to obtain a *J-* or CTOD-based resistance curve from a single specimen. Crack size is measured from compliance in this procedure and

9

verified by post-test optical crack size measurements. An alternative procedure using the normalization method is presented in Annex A15: Normalization Data Reduction Technique.

8.1.4 Three or more determinations of the fracture toughness parameter are suggested to ascertain the effects of material and test system variability. If fracture occurs by cleavage of ferritic steel, the testing and analysis procedures of Test Method E1921 are recommended.

8.2 *System and Specimen Preparation:*

8.2.1 *Specimen Measurement*—Measure the dimensions, B_N, B, W, H^*, and d to the nearest 0.050 mm (0.002 in.) or 0.5 %, whichever is larger.

8.2.2 *Specimen Temperature:*

8.2.2.1 The temperature of the specimen shall be stable and uniform during the test. Hold the specimen at test temperature ±3°C for ½ h/25 mm of specimen thickness.

8.2.2.2 Measure the temperature of the specimen during the test to an accuracy of ±3°C, where the temperature is measured on the specimen surface within W/4 from the crack tip. (See Test Methods E21 for suggestions on temperature measurement.)

8.2.2.3 For the duration of the test, the difference between the indicated temperature and the nominal test temperature shall not exceed ±3°C.

8.2.2.4 The term "indicated temperature" means the temperature that is indicated by the temperature measuring device using good-quality pyrometric practice.

NOTE 3—It is recognized that specimen temperature may vary more than the indicated temperature. The permissible indicated temperature variations in 8.2.2.3 are not to be construed as minimizing the importance of good pyrometric practice and precise temperature control. All laboratories should keep both indicated and specimen temperature variations as small as practicable. It is well recognized, in view of the dependency of fracture toughness of materials on temperature, that close temperature control is necessary. The limits prescribed represent ranges that are common practice.

8.3 *Alignment:*

8.3.1 *Bend Testing*—Set up the bend test fixture so that the line of action of the applied force passes midway between the support roll centers within ±1 % of the distance between the centers. Measure the span to within ±0.5 % of the nominal length. Locate the specimen so that the crack tip is midway between the rolls to within 1 % of the span and square to roll axes within ±2°.

8.3.1.1 When the load-line displacement is referenced from the loading jig, there is potential for introduction of error from two sources. They are the elastic compression of the fixture as the force increases and indentation of the specimen at the loading points. Direct methods for load-line displacement measurement are described in Refs (4-7). If a remote transducer is used for load-line displacement measurement, take care to exclude the elastic displacement of the load-train measurement and brinelling displacements at the load points (8).

8.3.2 *Compact Testing*—Loading pin friction and eccentricity of loading can lead to errors in fracture toughness determination. The centerline of the upper and lower loading rods should be coincident within 0.25 mm (0.01 in.). Center the

specimen with respect to the clevis opening within 0.76 mm (0.03 in.). Seat the displacement gage in the knife edges firmly by wiggling the gage lightly.

8.4 *Basic Procedure*—Load all specimens under displacement gage or machine crosshead or actuator displacement control. If a loading rate that exceeds that specified here is desired, please refer to Annex A14 ("Special Requirements for Rapid-Load J-Integral Fracture Toughness Testing").

8.4.1 The basic procedure involves loading a specimen to a selected displacement level and determining the amount of crack extension that occurred during loading.

8.4.2 Load specimens at a constant rate such that the time taken to reach the force P_m, as defined in Annex A1 – Annex A3, lies between 0.1 and 3 min.

8.4.3 If the test ends by fracture instability, measure the initial crack size and any ductile crack extension by the procedure in 9. Ductile crack extension may be difficult to distinguish but should be defined on one side by the fatigue precrack and on the other by the brittle region. Proceed to Section 9 to evaluate fracture toughness in terms of K, J, or CTOD.

8.4.4 If stable tearing occurs, test additional specimens to evaluate an initiation value of the toughness. Use the procedure in 8.5 to evaluate the amount of stable tearing that has occurred and thus determine the displacement levels needed in the additional tests. Five or more points favorably positioned are required to generate an R curve for evaluating an initiation point. See Annex A9 and Annex A11 to see how points shall be positioned for evaluating an initiation toughness value.

8.5 *Optical Crack Size Measurement:*

8.5.1 After unloading the specimen, mark the crack according to one of the following methods. For steels and titanium alloys, heat tinting at about 300°C (570°F) for 30 min works well. For other materials, fatigue cycling can be used. The use of liquid penetrants is not recommended. For both recommended methods, the beginning of stable crack extension is marked by the end of the flat fatigue precracked area. The end of crack extension is marked by the end of heat tint or the beginning of the second flat fatigue area.

8.5.2 Break the specimen to expose the crack, with care taken to minimize additional deformation. Cooling ferritic steel specimens to ensure brittle behavior may be helpful. Cooling nonferritic materials may help to minimize deformation during final fracture.

8.5.3 Along the front of the fatigue crack and the front of the marked region of stable crack extension, measure the size of the original crack and the final physical crack size at nine equally spaced points centered about the specimen centerline and extending to 0.005 W from the root of the side groove or surface of plane-sided specimens. Calculate the original crack size, a_o, and the final physical crack size, a_p, as follows: average the two near-surface measurements, combine the result with the remaining seven crack size measurements and determine the average. Calculate the physical crack extension, $\Delta a_p = a_p - a_o$. The measuring instrument shall have an accuracy of 0.025 mm (0.001 in.).

10

Eqr {tki j v'd{ "CUVO "Kpvgtcpcvki j u''tgugtxgf +='Hkl'Lcp''4: '37:4: -25'T O V'4244
Fqy pmqcf gf lr tkpv''d{
Rtkpegvqp"Wpkxgtukv{ "*Rtkpegvqp"Wpkxgtukv{+"r wtuwcpv"vq"Nkegpug"Ci tggo gpv0'P q'hwtvj gt 'tgr tqf wevkqp"cwj qtk| gf 0

8.5.4 None of the nine measurements of original crack size and final physical crack size may differ by more than $0.1(b_oB_N)^{1/2}$ from the average physical crack size defined in 8.5.3.

8.6 *Resistance Curve Procedure:*

8.6.1 The resistance curve procedure involves using an elastic compliance technique or other technique to obtain the *J* or CTOD resistance curve from a single specimen test. The elastic compliance technique is described here, while the normalization technique is described in Annex A15.

8.6.2 Load the specimens under displacement gage or machine crosshead or actuator displacement control. Load the specimens at a rate such that the time taken to reach the force P_m, as defined in Annex A1 – Annex A3, lies between 0.1 and 3.0 min, not including the time required to preform unload/reload cycles to estimate compliance. The time to perform an unload/reload sequence should be as needed to accurately estimate crack size, but not more than 10 min. If a higher loading rate is desired, please refer to Annex A14 ("Special Requirements for Rapid-Load J-Integral Fracture Toughness Testing").

8.6.3 Take each specimen individually through the following steps:

8.6.3.1 Measure compliance to estimate the original crack size, a_o, using unloading/reloading sequences over a force range of 0.5 to 1.0 times the final maximum precracking force. Estimate a provisional initial crack size, a_{oq}, from at least three unloading/reloading sequences. No individual value shall differ from the mean by more than ± 0.002 *W*.

8.6.3.2 Proceed with the test using unload/reload sequences that produce crack extension measurements at intervals prescribed by the applicable data analysis section of Annex A8 or Annex A10. Note that at least eight (Δa, *J*) data points are required before the specimen achieves maximum force. If crack size values change negatively by more than $0.005\ a_o$ (backup), stop the test and check the alignment of the loading train. Crack size values determined at forces lower than the maximum precracking force should be ignored.

8.6.4 For many materials, stress relaxation may occur prior to conducting compliance measurements, causing a time-dependent nonlinearity in the unloading slope. One method that may be used to remedy this effect is to hold the specimen for a period of time until the force becomes stable at a constant displacement prior to initiating the unloading.

8.6.5 The maximum recommended range of unload/reload for crack extension measurement should not exceed either 50 % of P_m, as defined in Annex A1 – Annex A3, or 50 % of the current force, whichever is smaller.

8.6.6 Experience has shown that satisfactory results may be obtained with unloads of 10-20% of P_m. A consistent force range should be used for all unloadings in a test.

8.6.7 A minimum of twenty (crack opening displacement, force) data points, uniformly spaced over the unload interval, are required to estimate the specimen compliance. The uncertainty of the compliance estimates can be improved by increasing the number of data points used in the regression analysis. It is recommended that forty or more data points be used in the regression analysis of each unload (reload).

8.6.8 After completing the final unloading cycle, return the force to zero without additional crosshead displacement beyond the then current maximum displacement.

8.6.9 After unloading the specimen, use the procedure in 8.5 to optically measure the crack sizes.

8.7 *Alternative Methods:*

8.7.1 Alternative methods of measuring crack extension, such as the direct current electric potential difference method described in Annex A18, are allowed. Methods shall meet the qualification criteria given in 9.1.5.2 or in the case of the potential difference method, in A18.16.2. If an alternative method is used to obtain J_{Ic}, at least one additional, confirmatory specimen shall be tested at the same test rate and under the same test conditions. From the alternative method the load-line displacement corresponding to a ductile crack extension of 0.5 mm shall be estimated. The additional specimen shall then be loaded to this load-line displacement level, marked, broken open and the ductile crack growth measured. The measured crack extension shall be 0.5 ± 0.25 mm in order for these results, and hence the J_{Ic} value, to be qualified according to this method.

8.7.2 If displacement measurements are made in a plane other than that containing the load-line, the ability to infer load-line displacement shall be demonstrated using the test material under similar test temperatures and conditions. Inferred load-line displacement values shall be accurate to within ± 1 %.

9. Analysis of Results

9.1 *Qualification of Data*—The data shall meet the following requirements to be qualified according to this test method. If the data do not pass these requirements, no fracture toughness measures can be determined in accordance with this test method.

Note 4—This section contains the requirements for qualification that are common for all tests. Additional qualification requirements are given with each type of test in the Annexes as well as requirements for determining whether the fracture toughness parameter developed is insensitive to in-plane dimensions.

9.1.1 All requirements on the test equipment in Section 6 shall be met.

9.1.2 All requirements on machining tolerance and precracking in Section 7 shall be met.

9.1.3 All requirements on fixture alignment, test rate, and temperature stability and accuracy in Section 8 shall be met.

9.1.4 The following crack size requirements shall be met in all stable tests. Unstable tests need only meet the original crack size requirement.

9.1.4.1 *Original Crack Size*—None of the nine physical measurements of initial crack size defined in 8.5.3 shall differ by more than $0.1(b_oB_N)^{1/2}$ from the average a_o.

9.1.4.2 *Final Crack Size*—None of the nine physical measurements of final physical crack size, a_p, defined in 8.5.3 shall differ by more than $0.1(b_oB_N)^{1/2}$ from the average a_p. In subsequent tests, the side-groove configuration may be modified within the requirements of 7.5 to facilitate meeting this requirement.

9.1.5 The following crack size requirements shall be met in all stable tests using the resistance curve procedure of 8.6.

9.1.5.1 *Crack Extension*—None of the nine physical measurements of crack extension shall be less than 50 % of the average crack extension.

9.1.5.2 *Crack Extension Prediction*—The crack extension, $\Delta a_{predicted}$, predicted from elastic compliance (or other method), at the last unloading shall be compared with the measured physical crack extension, Δa_p. The difference between these shall not exceed $0.15 \Delta a_p$ for crack extensions less than $0.2 b_o$, and the difference shall not exceed $0.03 b_o$ thereafter.

9.2 *Fracture Instability*—When the test terminates with fracture instability, evaluate whether the fracture occurred before stable tearing or after stable tearing. The beginning of stable tearing is defined in A6.3 and A7.3. For fracture instability occurring before stable tearing proceed to Annex A6, and Annex A7 to evaluate the toughness values in terms of *K, J,* or CTOD. For fracture instability occurring after stable tearing, proceed to Annex A6, and Annex A7 to evaluate toughness values and then go to 9.3 to evaluate stable tearing.

9.3 *Stable Tearing:*

9.3.1 *Basic Procedure*—When the basic procedure is used, only an initiation toughness can be evaluated. Proceed to Annex A9 and Annex A11 to evaluate initiation toughness values.

9.3.2 *Resistance Curve Procedure*—When the resistance curve procedure is used, refer to Annex A8 and Annex A10 to develop the *R*-curves. Proceed to Annex A9 and Annex A11 to develop initiation values of toughness.

10. Report

10.1 Recommended tables for reporting results are given in Figs. 8 and 9.

10.2 Report the following information for each fracture toughness determination:

10.2.1 Type of test specimen and orientation of test specimen according to Terminology E1823 identification codes,

10.2.2 Material designation (ASTM, AISI, SAE, and so forth), material product form (plate, forging, casting, and so forth), and material yield and tensile strength (at test temperature),

10.2.3 Specimen dimensions (8.2.1), thickness *B* and B_N, and width *W*,

10.2.4 Test temperature (8.2.2), loading rate (8.4.2 and 8.6.2), and type of loading control,

10.2.5 Fatigue precracking conditions (7.4), K_{max}, ΔK range, and fatigue precrack size (average),

10.2.6 Load-displacement record and associated calculations (Section 9),

10.2.7 If the loading rate is other than quasi-static, report the applied *dK/dt*,

10.2.8 Original measured crack size, a_o (8.5), original predicted crack size, a_{oq}, final measured crack size, a_p, final predicted crack extension, $\Delta a_{predicted}$, physical crack extension during test, Δa_p, crack front appearance—straightness and planarity, and fracture appearance,

10.2.9 Qualification of fracture toughness measurement (Annex A4 and Annex A6 – Annex A11), based on size requirements, and based on crack extension, and

10.2.10 Qualified values of fracture toughness, including *R*-curve values.

Basic Test Information
Loading Rate, time to P_m = [min]
Test temperature = [°C]

Crack Size Information
Initial measured crack size, a_o = [mm]
Initial predicted crack size, a_{oq} = [mm]
Final measured crack size, a_f = [mm]
Final Δa_p = [mm]
Final $\Delta a_{predicted}$ = [mm]

Analysis of Results
Fracture type = (Fracture instability or stable tearing)

K Based Fracture
K_{Jlc} = [MPa-m$^{1/2}$]

J Based Fracture
J_c = [kJ/m^2]
J_{lc} = [kJ/m^2]
J_u = [kJ/m^2]

δ Based Results
δ_c^* = [mm]
δ_{lc} = [mm]
δ_c = [mm]
δ_u = [mm]

Final $\Delta a/b$ =
Final J_{max}/σ_{YS} = [mm]

Specimen Information
Type =
Identification =
Orientation =

Basic dimensions
B = [mm]
B_N = [mm]
W = [mm]
h (Notch Height) = [mm]
a_N(Notch Length) = [mm]

Particular dimensions
C(T) H = [mm]
SE(B) S = [mm]
DC(T) D = [mm]

Material
Material designation =
Form =

Tensile Properties
E (Young's modulus) = [MPa]
ν (Poisson's ratio) =
σ_{YS} (Yield Strength) = [MPa]
σ_{TS} (Ultimate Strength) = [MPa]

Precracking Information
Final P_{max} = [N]
Final P_{min} = [N]
P_m = [N]
Final $\Delta K/E$ = [MPa-m$^{1/2}$]
Fatigue temperature = [°C]
Fatigue crack growth information

FIG. 8 Suggested Data Reporting Format

Test Information			Specimen ID:			Date		
Test Record Information			Operator:					
Event	P [N]	v [mm]	a [mm]	Δa [mm]	K [MPa-m$^{1/2}$]	J [kJ/m^2]	δ [mm]	

FIG. 9 Suggested Data Reporting Format

11. Precision and Bias

11.1 *Bias*—There is no accepted "standard" value for any of the fracture toughness criteria employed in this test method. In the absence of such a true value no meaningful statement can be made concerning bias of data.

11.2 *Precision*—The precision of any of the various fracture toughness determinations cited in this test method is a function of the precision and bias of the various measurements of linear dimensions of the specimen and testing fixtures, the precision of the displacement measurement, the bias of the force measurement as well as the bias of the recording devices used to produce the force-displacement record, and the precision of the constructions made on this record. It is not possible to make meaningful statements concerning precision and bias for all these measurements. However, it is possible to derive useful information concerning the precision of fracture toughness measurements in a global sense from interlaboratory test programs. Most of the measures of fracture toughness that can be determined by this procedure have been evaluated by an interlaboratory test program. The J_{Ic} was evaluated in (**9**), the *J-R* curve was evaluated in (**10**), and δ_c was evaluated in a research report.[6] In addition, the overall analysis procedures of this test method were evaluated in an interlaboratory test program. Note that for the evaluation of J_{Ic}, if the slope of the power law regression line, dJ/da, evaluated at the abscissa value Δa_Q is greater than σ_Y, the uncertainty of the J_{Ic} measurement is likely to be much greater than that obtained during the interlaboratory test programs cited. Likewise note that for the evaluation of δ_{Ic}, if the slope of the power law regression line, dδ/da, evaluated at the abscissa value Δa_Q, is greater than 1, the uncertainty of the δ_{Ic} measurement is likely to be much greater than that obtained during the interlaboratory test programs cited.

12. Keywords

12.1 crack initiation; crack-tip opening displacement; CTOD; ductile fracture; elastic-plastic fracture toughness; fracture instability; J-integral; J_{Ic}; K_{Jic}; J_c; δ_c; plane-strain fracture toughness; resistance curve; stable crack growth

ANNEXES

(Mandatory Information)

A1. SPECIAL REQUIREMENTS FOR TESTING SINGLE EDGE BEND SPECIMENS

NOTE A1.1—Annex A1 – Annex A3 cover specimen information.

A1.1 Specimen

A1.1.1 The standard bend specimen is a single edge-notched and fatigue-cracked beam loaded in three-point bending with a support span, S, equal to four times the width, W. The general proportions of the specimen configuration are shown in Fig. A1.1.

A1.1.2 Alternative specimens may have $1 \leq W/B \leq 4$. These specimens shall also have a nominal support span equal to $4W$.

A1.2 Apparatus

A1.2.1 For generally applicable specifications concerning the bend-test fixture and displacement gage see 6.2 and 6.5.1.

A1.3 *Specimen Preparation:*

A1.3.1 For generally applicable specifications concerning specimen configuration and preparation see Section 7.

A1.3.2 All specimens shall be precracked in three-point bending fatigue based upon the force P_m, as follows:

$$P_m = \frac{0.5Bb_o^2\sigma_Y}{S} \qquad (A1.1)$$

See 7.4.5 for fatigue precracking requirements.

A1.4 Calculation

A1.4.1 *Calculation of K*—For the bend specimen at a force $P_{(i)}$, calculate K as follows:

$$K_{(i)} = \left[\frac{P_i S}{(BB_N)^{1/2} W^{3/2}} \right] f(a_i/W) \qquad (A1.2)$$

where:

$$f\left(\frac{a_i}{W} \right) = \qquad (A1.3)$$

$$\frac{3\left(\frac{a_i}{W} \right)^{1/2} \left[1.99 - \left(\frac{a_i}{W} \right)\left(1 - \frac{a_i}{W} \right)\left(2.15 - 3.93\left(\frac{a_i}{W} \right) + 2.7\left(\frac{a_i}{W} \right)^2 \right) \right]}{2\left(1 + 2\frac{a_i}{W} \right)\left(1 - \frac{a_i}{W} \right)^{3/2}}$$

A1.4.2 *Calculation of J:*
For the single edge bend specimen, calculate J as follows:

$$J = J_{el} + J_{pl} \qquad (A1.4)$$

where:

J_{el} = elastic component of J, and
J_{pl} = plastic component of J.

A1.4.2.1 *J Calculations for the Basic Test Method*—At a point corresponding to v and P on the specimen force versus displacement record, calculate the J integral as follows:

$$J = \frac{K^2(1 - v^2)}{E} + J_{pl} \qquad (A1.5)$$

where K is from A1.4.1 with $a = a_o$, and

$$J_{pl} = \frac{\eta_{pl} A_{pl}}{B_N b_o} \qquad (A1.6)$$

where:

A_{pl} = area under force versus displacement record as shown in Fig. A1.2,
η_{pl} = 1.9 if the load-line displacement is used for A_{pl},
= $3.667 - 2.199(a_o/W) + 0.437(a_o/W)^2$ if the crack mouth opening displacement record is used for A_{pl},
B_N = net specimen thickness ($B_N = B$ if no side grooves are present), and
b_o = $W - a_o$.

All basic test method J integral values shall be corrected for crack growth using the following relationship (11):

$$J = J_{e/0} + \frac{J_{p/0}}{1 + \left(\frac{\alpha - 0.5}{\alpha + 0.5} \right)\frac{\Delta a}{b_o}} \qquad (A1.7)$$

with $\alpha = 1$ for SE(B) specimen.

A1.4.2.2 *J Calculations for the Resistance Curve Test Method*—At a point corresponding to $a_{(i)}$, $v_{(i)}$, and $P_{(i)}$ on the specimen force versus displacement record, calculate the J integral as follows:

$$J_{(i)} = \frac{(K_{(i)})^2(1 - v^2)}{E} + J_{pl(i)} \qquad (A1.8)$$
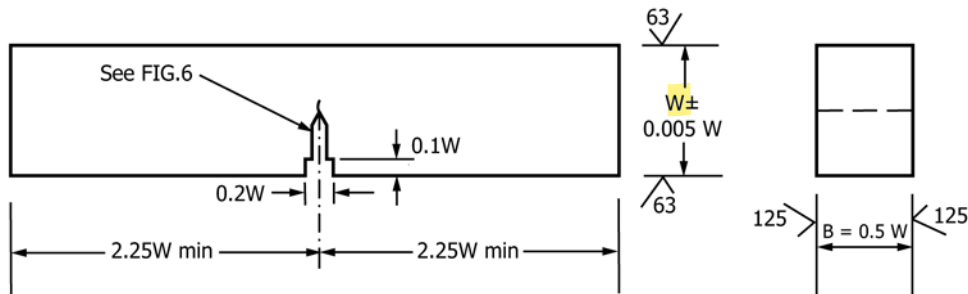
NOTE 1—The two side planes and the two edge planes shall be parallel and perpendicular as applicable to within 0.5°.
NOTE 2—The machined notch shall be perpendicular to specimen length and thickness to within ±2°.

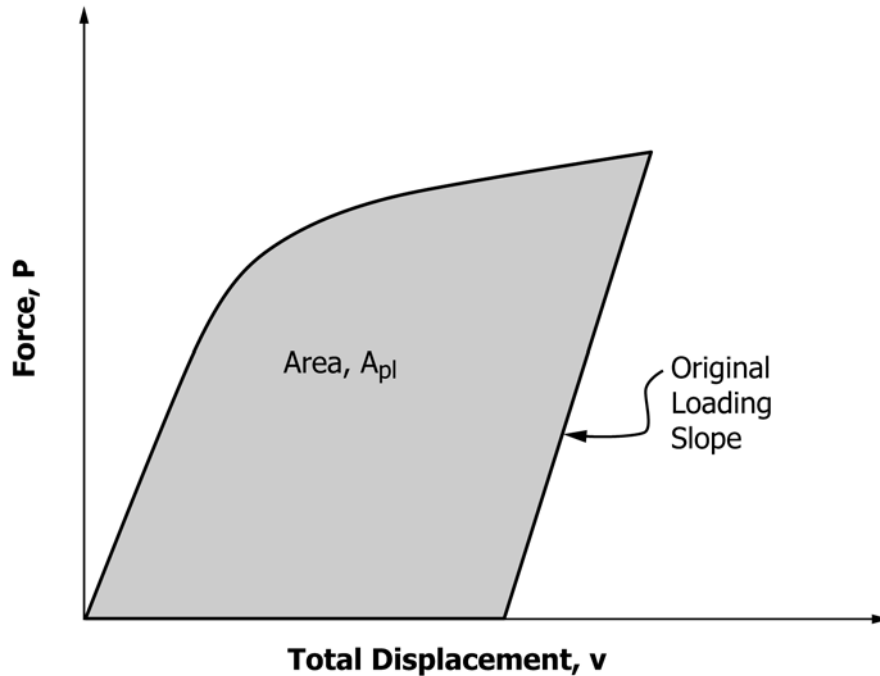**FIG. A1.1 Recommended Single Edge Bend [SE(B)] Specimen**

FIG. A1.2 Definition of Area for *J* Calculation Using the Basic Method

where $K_{(i)}$ is from A1.4.1, and

$$J_{pl(i)} = \left[J_{pl(i-1)} + \left(\frac{\eta_{pl(i-1)}}{b_{(i-1)}} \right) \left(\frac{A_{pl(i)} - A_{pl(i-1)}}{B_N} \right) \right] \times \quad (A1.9)$$

$$\left[1 - \gamma_{pl(i-1)} \left(\frac{a_{(i)} - a_{(i-1)}}{b_{(i-1)}} \right) \right]$$

where:

$\eta_{pl(i-1)}$ = 1.9, and
$\gamma_{pl(i-1)}$ = 0.9

if the load-line displacement is used to measure A_{pl} and,

$$\eta_{pl} = 3.667 - 2.199 \left(\frac{a_{(i-1)}}{W} \right) + 0.437 \left(\frac{a_{(i-1)}}{W} \right)^2$$

and

$$\gamma_{pl} = 0.131 + 2.131 \left(\frac{a_{(i-1)}}{W} \right) - 1.465 \left(\frac{a_{(i-1)}}{W} \right)^2$$

if the crack mouth opening displacement is used to measure A_{pl}.

In Eq A1.9, the quantity $A_{pl(i)} - A_{pl(i-1)}$ is the increment of plastic area under the chosen force versus plastic displacement record between lines of constant plastic displacement at points $i-1$ and i shown in Fig. A1.3. The quantity $J_{pl(i)}$ represents the total crack growth corrected plastic *J* at point *i* and is obtained in two steps by first incrementing the existing $J_{pl(i-1)}$ and then by modifying the total accumulated result to account for the crack growth increment. Accurate evaluation of $J_{pl(i)}$ from the Eq A1.9 relationship requires small and uniform crack growth increments consistent with the suggested elastic compliance spacing of Annex A8 and Annex A10. The quantity $A_{pl(i)}$ can be calculated from the following equation:

$$A_{pl(i)} = A_{pl(i-1)} + \left[P_{(i)} + P_{(i-1)} \right] \left[v_{pl(i)} - v_{pl(i-1)} \right] / 2 \quad (A1.10)$$

where:

$v_{pl(i)}$ = plastic part of the load-line or crack mouth opening displacement = $v_{(i)} - (P_{(i)} C_{(i)})$, and
$C_{(i)}$ = experimental compliance, $(\Delta v / \Delta P)_{(i)}$, corresponding to the current crack size, a_i.

Note A1.2—The point $P_{(i)}$, $v_{(i)}$ is the last data point recorded before the *i*-th unloading begins and before any hold period for stress relaxation as in accordance with 8.6.4.

For test methods that do not evaluate an experimental load-line elastic compliance, the load-line compliance $C_{(i)}$ can be determined from the following equation:

$$C_{(i)} = \frac{1}{EB_e} \left(\frac{S}{W - a_i} \right)^2 \times \quad (A1.11)$$

$$\left[1.193 - 1.98 \left(\frac{a_i}{W} \right) + 4.478 \left(\frac{a_i}{W} \right)^2 - 4.443 \left(\frac{a_i}{W} \right)^3 + 1.739 \left(\frac{a_i}{W} \right)^4 \right]$$

where:

$B_e = B - (B - B_N)^2 / B$

while for the crack mouth opening displacement case:

$$C_{(i)} = \frac{6S}{EWB_e} \left(\frac{a_i}{W} \right) \times \quad (A1.12)$$

$$\left[0.76 - 2.28 \left(\frac{a_i}{W} \right) + 3.87 \left(\frac{a_i}{W} \right)^2 - 2.04 \left(\frac{a_i}{W} \right)^3 + \frac{0.66}{(1 - a_i/W)^2} \right]$$

where:

$B_e = B - (B - B_N)^2 / B$

The compliance estimated using Eq A1.11 or Eq A1.12 should be verified by calibrating against the initial experimental force versus load-line displacement data to assure the integrity of the load-line displacement measurement system.
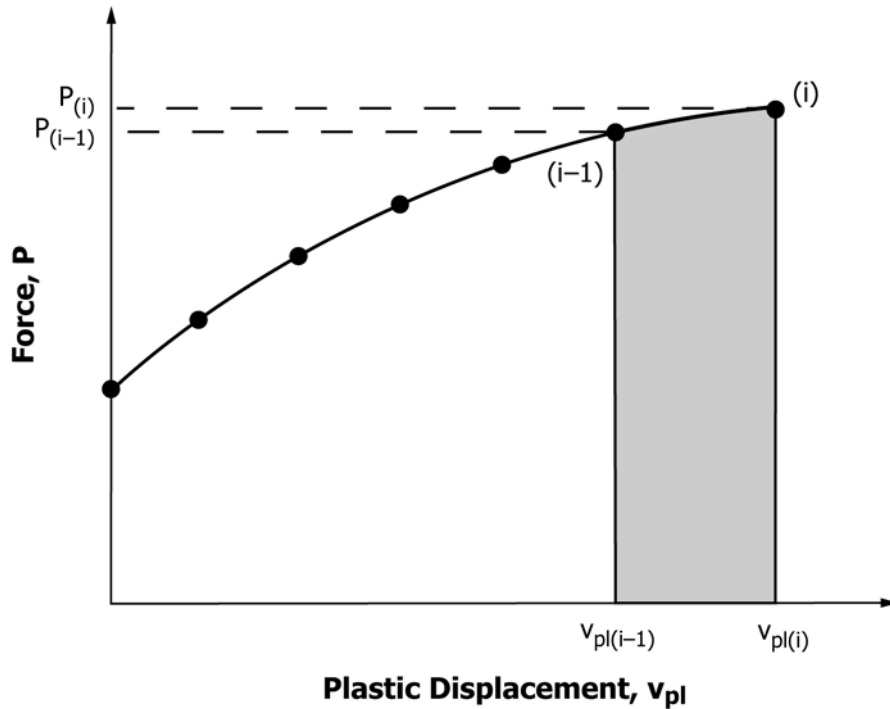
15

FIG. A1.3 Definition of Plastic Area for Resistance Curve
J **Calculation**

A1.4.3 *Calculation of Crack Size*—For a resistance curve test method using an elastic compliance technique on single edge bend specimens with crack mouth opening displacements measured at the notched edge, the crack size is given as follows:

$$\frac{a_i}{W} = [0.999748 - 3.9504\, u + 2.9821\, u^2 - 3.21408\, u^3$$
$$+ 51.51564\, u^4 - 113.031\, u^5] \quad \text{(A1.13)}$$

where:

$$u = \frac{1}{\left[\dfrac{B_e W E C_i}{S/4}\right]^{1/2} + 1} \quad \text{(A1.14)}$$

C_i = $(\Delta v_m/\Delta P)$ on an unloading/reloading sequence,
v_m = crack mouth opening displacement at notched edge,
B_e = $B - (B - B_N)^2/B$.

NOTE A1.3—Crack size on a single edge bend specimen is normally determined from crack mouth opening compliance. It can be determined from load-line compliance if the correct calibration is available.

A1.4.4 Other compliance equations are acceptable if the resulting accuracy is equal to or greater than those described and the accuracy has been verified experimentally.

A1.4.5 *Calculation of CTOD:*

A1.4.5.1 *Calculation of CTOD for the Basic Test Method*—For the basic test method, calculations of CTOD for any point on the force-displacement curve are made from the following expression:

$$\delta = \frac{J}{m\sigma_Y} \quad \text{(A1.15)}$$

where: J is defined in A1.4.2.1 with $a = a_o$, the original crack size, and then crack growth corrected using Annex A16 and:

$$m = A_0 - A_1*\left(\frac{\sigma_{YS}}{\sigma_{TS}}\right) + A_2*\left(\frac{\sigma_{YS}}{\sigma_{TS}}\right)^2 - A_3*\left(\frac{\sigma_{YS}}{\sigma_{TS}}\right)^3 \quad \text{(A1.16)}$$

with :
A_0 = 3.18-0.22 * (a_o/W),
A_1 = 4.32-2.23 * (a_o/W),
A_2 = 4.44-2.29 * (a_o/W), and
A_3 = 2.05-1.06 * (a_o/W).

Calculation of δ requires $\sigma_{YS}/\sigma_{TS} \geq 0.5$.

A1.4.5.2 *Calculations of CTOD for the Resistance Curve Test Method*—For the resistance curve test method, calculations of CTOD for any point on the force-displacement curve are made from the following expression:

$$\delta_i = \frac{J_i}{m_i\sigma_Y} \quad \text{(A1.17)}$$

where J_i is defined in A1.4.2.2 with $a = a_i$, the current crack size and:

$$m = A_0 - A_1*\left(\frac{\sigma_{YS}}{\sigma_{TS}}\right) + A_2*\left(\frac{\sigma_{YS}}{\sigma_{TS}}\right)^2 - A_3*\left(\frac{\sigma_{YS}}{\sigma_{TS}}\right)^3 \quad \text{(A1.18)}$$

with :
A_0 = 3.18-0.22 * (a_i/W),
A_1 = 4.32-2.23 * (a_i/W),
A_2 = 4.44-2.29 * (a_i/W), and
A_3 = 2.05-1.06 * (a_i/W).

Calculation of δ_i requires $\sigma_{YS}/\sigma_{TS} \geq 0.5$.

A2. SPECIAL REQUIREMENTS FOR TESTING COMPACT SPECIMENS

A2.1 Specimen

A2.1.1 The standard compact specimen, *C(T)*, is a single edge-notched and fatigue cracked plate loaded in tension. Two acceptable specimen geometries are shown in Fig. A2.1.

A2.1.2 Alternative specimens may have $2 \leq W/B \leq 4$ but with no change in other proportions.

A2.2 Apparatus

A2.2.1 For generally applicable specifications concerning the loading clevis and displacement gage, see 6.2 and 6.5.2.

A2.3 Specimen Preparation

A2.3.1 For generally applicable specifications concerning specimen size and preparation, see Section 7.

A2.3.2 All specimens shall be precracked in fatigue at a force value based upon the force P_m as follows:

$$P_m = \frac{0.4 B b_o^2 \sigma_Y}{2W + a_o} \tag{A2.1}$$

See Section 7 for fatigue precracking requirements.

Notes:
1. Tolerance on all dimensions ±0.013W
2. Pin shall be sized so that maximum clearance with hole is 0.02W

Notes:
1. Tolerance on all dimensions ±0.013W
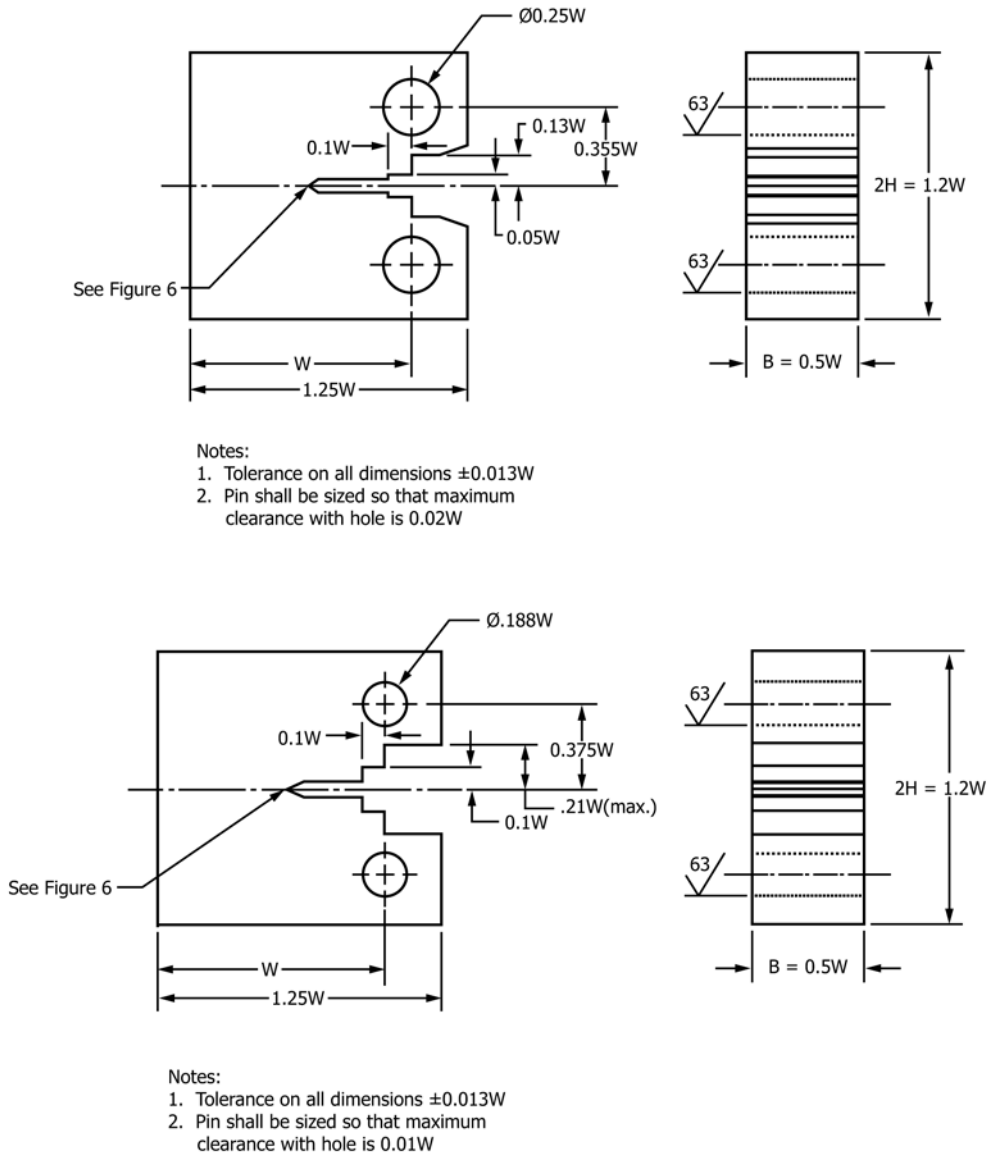2. Pin shall be sized so that maximum clearance with hole is 0.01W

FIG. A2.1 Two Compact Specimen Designs That Have Been Used Successfully for Fracture Toughness Testing

17

A2.4 Calculation

A2.4.1 *Calculation of K*—For the compact specimen at a force $P_{(i)}$, calculate K as follows:

$$K_{(i)} = \frac{P_{(i)}}{(BB_N W)^{1/2}} f\left(\frac{a_i}{W}\right) \quad \text{(A2.2)}$$

with:

$$f\left(\frac{a_i}{W}\right) = \quad \text{(A2.3)}$$

$$\frac{\left\{\left(2+\frac{a_i}{W}\right)\left[0.886+4.64\left(\frac{a_i}{W}\right) - 13.32\left(\frac{a_i}{W}\right)^2 + 14.72\left(\frac{a_i}{W}\right)^3 - 5.6\left(\frac{a_i}{W}\right)^4\right]\right\}}{\left(1-\frac{a_i}{W}\right)^{3/2}}$$

A2.4.2 *Calculation of J*—For the compact specimen calculate J as follows:

$$J = J_{el} + J_{pl} \quad \text{(A2.4)}$$

where:

J_{el} = elastic component of J, and
J_{pl} = plastic component of J.

A2.4.2.1 *J Calculations for the Basic Test Method*—For the compact specimen at a point corresponding to ν, P on the specimen force versus load-line displacement record, calculate as follows:

$$J = \frac{K^2(1-\nu^2)}{E} + J_{pl} \quad \text{(A2.5)}$$

where:
K is from A2.4.1 with $a = a_o$, and

$$J_{pl} = \frac{\eta_{pl} A_{pl}}{B_N b_o} \quad \text{(A2.6)}$$

where:

A_{pl} = area shown in Fig. A1.2,
B_N = net specimen thickness ($B_N = B$ if no side grooves are present),
b_o = uncracked ligament, ($W - a_o$), and
η_{pl} = $2 + 0.522 b_o/W$.

All basic test method J integral values shall be corrected for crack growth using the following relationship (**11**):

$$J = J_{e/0} + \frac{J_{p/0}}{1+\left(\dfrac{\alpha - 0.5}{\alpha + 0.5}\right)\dfrac{\Delta a}{b_o}} \quad \text{(A2.7)}$$

with α = 0.9 for the C(T) specimen.

A2.4.2.2 *J Calculation for the Resistance Curve Test Method*—For the C(T) specimen at a point corresponding $a_{(i)}$, $\nu_{(i)}$, and $P_{(i)}$ on the specimen force versus load-line displacement record calculate as follows:

$$J_{(i)} = \frac{(K_{(i)})^2(1-\nu^2)}{E} + J_{pl(i)} \quad \text{(A2.8)}$$

where $K_{(i)}$ is from A2.4.1, and:

$$J_{pl(i)} = \quad \text{(A2.9)}$$

$$\left[J_{pl(i-1)} + \left(\frac{\eta_{pl(i-1)}}{b_{(i-1)}}\right)\frac{A_{pl(i)} - A_{pl(i-1)}}{B_N}\right]\left[1 - \gamma_{(i-1)}\left(\frac{a_{(i)} - a_{(i-1)}}{b_{(i-1)}}\right)\right]$$

where:

$\eta_{pl(i-1)}$ = $2.0 + 0.522\, b_{(i-1)}/W$, and
$\gamma_{(i-1)}$ = $1.0 + 0.76\, b_{(i-1)}/W$.

In Eq A2.9, the quantity $A_{pl(i)} - A_{pl(i-1)}$ is the increment of plastic area under the force versus plastic load-line displacement record between lines of constant displacement at points $i-1$ and i shown in Fig. A1.3. The quantity $J_{pl(i)}$ represents the total crack growth corrected plastic J at point i and is obtained in two steps by first incrementing the existing $J_{pl(i-1)}$ and then by modifying the total accumulated result to account for the crack growth increment. Accurate evaluation of $J_{pl(i)}$ from the above relationship requires small and uniform crack growth increments consistent with the suggested elastic compliance spacing of Annex A8 and Annex A10. The quantity $A_{pl(i)}$ can be calculated from the following equation:

$$A_{pl(i)} = A_{pl(i-1)} + \frac{[P_{(i)} + P_{(i-1)}][\nu_{pl(i)} - \nu_{pl(i-1)}]}{2} \quad \text{(A2.10)}$$

where:

$\nu_{pl(i)}$ = plastic part of the load-line displacement,
$\nu_i - P_{(i)}C_{LL(i)}$, and
$C_{LL(i)}$ = experimental compliance, $(\Delta\nu/\Delta P)_i$, corresponding to the current crack size, a_i.

NOTE A2.1—The point $P_{(i)}$, $\nu_{(i)}$ is the last data point recorded before the i-th unloading begins and before any hold period for stress relaxation as in accordance with 8.6.4.

For test methods that do not evaluate an experimental elastic compliance, $C_{LL(i)}$ can be determined from the following equation:

$$C_{LL(i)} = \frac{1}{EB_e}\left(\frac{W+a_i}{W-a_i}\right)^2\left[2.1630 + 12.219\left(\frac{a_i}{W}\right) - 20.065\left(\frac{a_i}{W}\right)^2\right.$$
$$\left. - 0.9925\left(\frac{a_i}{W}\right)^3 + 20.609\left(\frac{a_i}{W}\right)^4 - 9.9314\left(\frac{a_i}{W}\right)^5\right] \quad \text{(A2.11)}$$

where:

$$B_e = B - \frac{(B-B_N)^2}{B} \quad \text{(A2.12)}$$

The load-line compliance estimated using Eq A2.11 should be verified by calibrating against the initial experimental compliance to assure the integrity of the load-line displacement measurement system.

In an elastic compliance test, the rotation corrected compliance, $C_{c(i)}$, described in A2.4.5 shall be used instead of $C_{LL(i)}$ in Eq A2.11.

A2.4.3 *Calculation of Crack Size*—For a single specimen test method using an elastic compliance technique on the compact specimen with crack opening displacements measured on the load-line, the crack size is given as follows:

$$a_i/W = 1.000196 - 4.06319u + 11.242u^2 - 106.043u^3 + 464.335u^4$$
$$- 650.677u^5 \quad \text{(A2.13)}$$

where:

$$u = \frac{1}{[B_e E C_{c(i)}]^{1/2}+1} \quad \text{(A2.14)}$$

18

Eqr{tki j v'd{ "CUVO "Koyyi"cmftki j vu'tgugtxgf +='Hk'Tcp"4: "374: -25'I O V'4244
Fqy pmqcf gf Irtlkp ygf"d{
Rtkpegvqp"Wplkxgtuk{ "*Rtkpegvqp"Wplkxgtuk{+'rwtuwcpv'vq'Nkegpug'Ci tggo gpv0P q'hwtvj gt'tgr tqf wevkqpu'cwj qtk|gf0

$C_{c(i)}$ = specimen load-line crack opening elastic compliance ($\Delta v/\Delta P$) on an unloading/reloading sequence corrected for rotation (see A2.4.5),

B_e = $B - (B - B_N)^2/B$.

A2.4.4 The calculation of crack size values for $C(T)$ specimens is a two-step procedure. First, values of uncorrected crack size a_i are obtained from measured values of load-line compliance C_i using Eq A2.13 and A2.14. Uncorrected crack size values are then used to calculate the corresponding values of the radius of rotation of the crack centerline, R_i, as follows:

$$R_i = \frac{W + a_i}{2} \qquad (A2.15)$$

A2.4.5 To account for crack opening displacement in $C(T)$ specimens, the crack size estimation shall be corrected for rotation. Compliance is corrected as follows:

$$C_{c(i)} = \frac{C_i}{\left(\dfrac{H^*}{R_i}\sin\theta_i - \cos\theta_i\right)\left(\dfrac{D}{R_i}\sin\theta_i - \cos\theta_i\right)} \qquad (A2.16)$$

FIG. A2.2 Elastic Compliance Correction for Specimen Rotation

where (Fig. A2.2):

C_i = measured specimen elastic compliance, $\Delta v_m/\Delta P_m$, (at the load-line),

$C_{c(i)}$ = corrected specimen elastic compliance, $\Delta v_c/\Delta P_c$ (at the load-line),

H^* = initial half-span of the load points (center of the pin holes),

R_i = radius of rotation of the crack centerline, $(W + a)/2$, where a is the updated crack size,

D = one half of the initial distance between the displacement measurement points,

θ = angle of rotation of a rigid body element about the unbroken midsection line, or

$$\theta_i = \arcsin\left(\frac{D + \dfrac{v_{m(i)}}{2}}{\sqrt{D^2 + R_i^2}}\right) - \arctan\left(\frac{D}{R_i}\right), \text{ and} \qquad (A2.17)$$

$v_{m(i)}$ = total measured load-line displacement at the beginning of the i-th unloading/reloading cycle,

v_c = total corrected load-line displacement at the beginning of the i-th unloading/reloading cycle.

A2.4.6 Other compliance equations are acceptable if the resulting accuracy is equal to or greater than those described and the accuracy has been verified experimentally.

A2.4.7 *Calculation of CTOD:*

A2.4.7.1 *Calculation of CTOD for the Basic Test Method*—For the basic test method, calculations of CTOD for any point on the force-displacement curve are made from the following expression:

$$\delta = \frac{J}{m\sigma_Y} \qquad (A2.18)$$

where J is defined in A2.4.2.1 with a = a_o, the original crack size, and then crack growth corrected using Annex A16 and:

$$m = A_0 - A_1*\left(\frac{\sigma_{YS}}{\sigma_{TS}}\right) + A_2*\left(\frac{\sigma_{YS}}{\sigma_{TS}}\right)^2 - A_3*\left(\frac{\sigma_{YS}}{\sigma_{TS}}\right)^3 \qquad (A2.19)$$

with: A_0=3.62, A_1 = 4.21, A_2=4.33, and A_3=2.00. Calculation of δ requires $\sigma_{YS}/\sigma_{TS} \geq 0.5$.

A2.4.7.2 *Calculation of CTOD for the Resistance Curve Test Method*—For the resistance curve test method, calculations of CTOD for any point on the force-displacement curve are made from the following expression:

$$\delta_i = \frac{J_i}{m\sigma_Y} \qquad (A2.20)$$

where J is defined in A2.4.2.2 with a = a_i, the current crack size, and,

$$m = A_0 - A_1*\left(\frac{\sigma_{YS}}{\sigma_{TS}}\right) + A_2*\left(\frac{\sigma_{YS}}{\sigma_{TS}}\right)^2 - A_3*\left(\frac{\sigma_{YS}}{\sigma_{TS}}\right)^3 \qquad (A2.21)$$

with: A_0=3.62, A_1 = 4.21, A_2=4.33, and A_3=2.00. Calculation of δ_i requires $\sigma_{YS}/\sigma_{TS} \geq 0.5$.
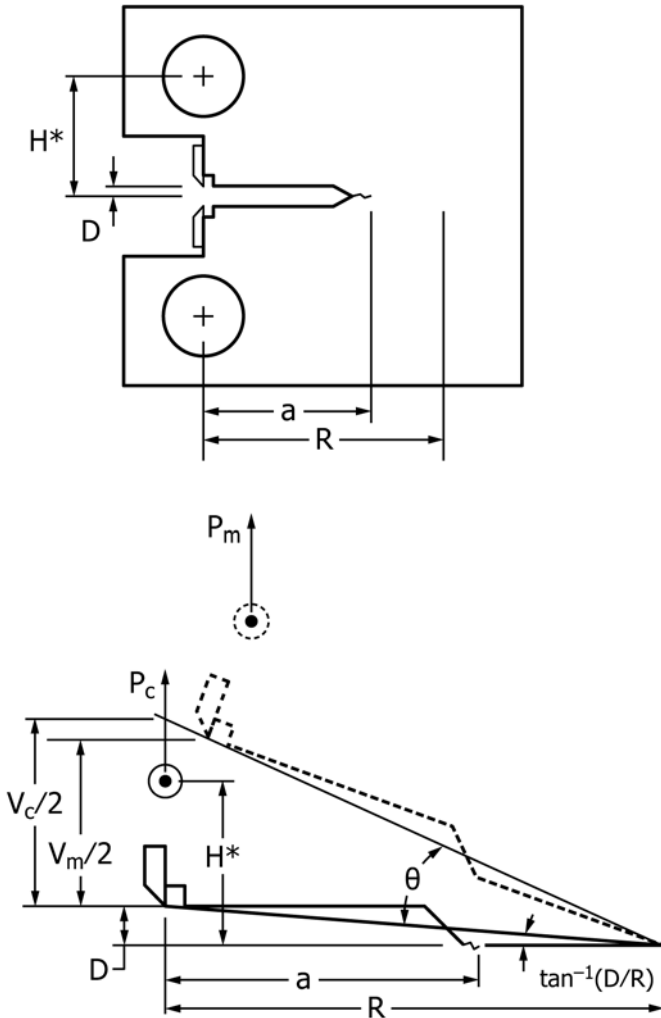
A3. SPECIAL REQUIREMENTS FOR TESTING DISK-SHAPED COMPACT SPECIMENS

A3.1 Specimen

A3.1.1 The standard disk-shaped compact specimen, DC(T), is a single edge-notched and fatigue cracked plate loaded in tension. The specimen geometry which has been used successfully is shown in Fig. A3.1.

A3.1.2 Alternative specimens may have $2 \leq W/B \leq 4$ but with no change in other proportions.

A3.2 Apparatus

A3.2.1 For generally applicable specifications concerning the loading clevis and displacement gage see 6.2 and 6.5.2.

A3.3 Specimen Preparation

A3.3.1 For generally applicable specifications concerning specimen size and preparation, see Section 7.

A3.3.2 All specimens shall be precracked in fatigue at a force value based upon the force P_m as follows:

$$P_m = \frac{0.4 B b_o^2 \sigma_Y}{2W + a_o} \qquad (A3.1)$$

See 7.4 for precracking requirements.

A3.4 Procedure

A3.4.1 *Measurement*— The analysis assumes the specimen was machined from a circular blank, and, therefore, measure-ments of circularity as well as width, W; crack size, a; and thicknesses, B and B_N, shall be made. Measure the dimensions B_N and B to the nearest 0.05 mm (0.002 in.) or 0.5 %, whichever is larger.

A3.4.1.1 The specimen blank shall be checked for circular-ity before specimen machining. Measure the diameter at eight equally spaced points around the circumference of the speci-men blank. One of these measurements shall lie in the intended notch plane. Average these readings to obtain the diameter, D. If any measurement differs from the average diameter, D, by more than 5 %, machine the blank to the required circularity. Otherwise, $D = 1.35\ W$.

A3.4.1.2 Measure the width, W, and the crack size, a, from the plane of the centerline of the loading holes (the notched edge is a convenient reference line but the distance from the centerline of the holes to the notched edge must be subtracted to determine W and a). Measure the width, W, to the nearest 0.05 mm (0.002 in.) or 0.5 %, whichever is larger.

A3.5 Calculation

A3.5.1 *Calculation of K*—For the DC(T) specimen at a force $P_{(i)}$, calculate K as follows:

$$K_{(i)} = \frac{P_{(i)}}{(BB_N W)^{1/2}} f(a_i/W) \qquad (A3.2)$$

where:
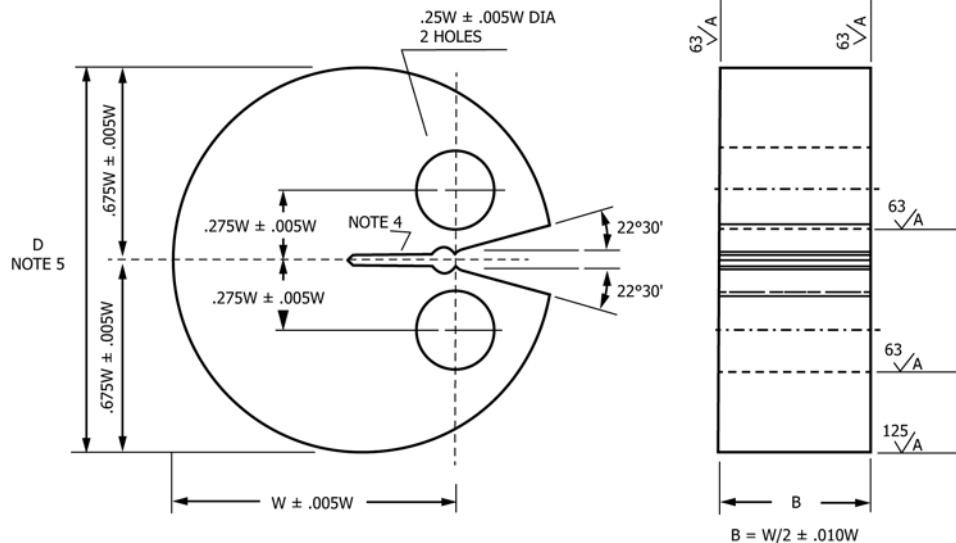
NOTE 1—All surfaces shall be perpendicular and parallel as applicable within 0.002 W TIR.

NOTE 2—The intersection of the crack starter notch tips on each surface of the specimen shall be equally distant within 0.005W from the centerline of the loading holes.

NOTE 3—Integral or attached knife edges for clip gage attachment to the crack mouth may be used.

NOTE 4—For starter-notch and fatigue-crack configuration see Fig. 7.

NOTE 5—Required circularity measurements shall be made at eight equally spaced points around the circumference. One of these points shall be the notch plane. Average the readings to obtain the radius. All values shall be within 5 % of the average.

FIG. A3.1 Disk-Shaped Compact Specimen, DC(T), Standard Proportions and Dimensions

$$f\left(\frac{a_i}{W}\right) = \qquad (A3.3)$$

$$\frac{\left\{\left(2+\frac{a_i}{W}\right)\left[0.76+4.8\left(\frac{a_i}{W}\right)-11.58\left(\frac{a_i}{W}\right)^2+11.43\left(\frac{a_i}{W}\right)^3-4.08\left(\frac{a_i}{W}\right)^4\right]\right\}}{\left(1-\frac{a_i}{W}\right)^{3/2}}$$

A3.5.2 *Calculation of J*—For the DC(T) specimen, calculate J as follows:

$$J = J_{el}+J_{pl} \qquad (A3.4)$$

where:

J_{el} = elastic component of *J*, and
J_{pl} = plastic component of *J*.

A3.5.2.1 *J Calculation for the Basic Test Method*—For the DC(T) specimen at a point corresponding to $v_{(i)}$, $P_{(i)}$ on the specimen force versus load-line displacement record, calculate as follows:

$$J = \frac{K^2(1-v^2)}{E}+J_{pl} \qquad (A3.5)$$

where *K* is from A3.5.1 with $a = a_o$, and

$$J_{pl} = \frac{\eta_{pl}A_{pl}}{B_N b_o} \qquad (A3.6)$$

where:

A_{pl} = area shown in Fig. A1.2,
B_N = net specimen thickness ($B_N = B$ if no side grooves are present),
b_o = uncracked ligament, ($W - a_o$), and
η_{pl} = $2 + 0.522 b_o/W$.

All basic test method *J* integral values shall be corrected for crack growth using the following relationship (**11**):

$$J = J_{e/0}+\frac{J_{p/0}}{1+\left(\frac{\alpha-0.5}{\alpha+0.5}\right)\frac{\Delta a}{b_o}} \qquad (A3.7)$$

with $\alpha = 0.9$ for the DC(T) specimen.

A3.5.2.2 *J Calculation for the Resistance Curve Test Method*—For the DC(T) specimen at a point corresponding to a_i, v_i, and P_i on the specimen force versus load-line displacement record, calculate as follows:

$$J_{(i)} = \frac{(K_{(i)})^2(1-v^2)}{E}+J_{pl(i)} \qquad (A3.8)$$

where $K_{(i)}$ is from A3.5.1 and:

$$J_{pl(i)} = \qquad (A3.9)$$

$$\left[J_{pl(i-1)}+\left(\frac{\eta_{(i-1)}}{b_{(i-1)}}\right)\frac{A_{pl(i)}-A_{pl(i-1)}}{B_N}\right]\left[1-\gamma_{(i-1)}\frac{a_{(i)}-a_{(i-1)}}{b_{(i-1)}}\right]$$

where:

$\eta_{(i-1)}$ = $2.0 + 0.522\, b_{(i-1)}/W$, and
$\gamma_{(i-1)}$ = $1.0 + 0.76\, b_{(i-1)}/W$.

In the preceding equation, the quantity $A_{pl(i)} - A_{pl(i-1)}$ is the increment of plastic area under the force versus load-line

displacement record between lines of constant displacement at points $i-1$ and i shown in Fig. A1.3. The quantity $J_{pl(i)}$ represents the total crack growth corrected plastic *J* at point i and is obtained in two steps by first incrementing the existing $J_{pl(i-1)}$ and then by modifying the total accumulated result to account for the crack growth increment. Accurate evaluation of $J_{pl(i)}$ from the preceding relationship requires small and uniform crack growth increments consistent with the suggested elastic compliance spacing of Annex A8 and Annex A10. The quantity $A_{pl(i)}$ can be calculated from the following equation:

$$A_{pl(i)} = A_{pl(i-1)}+\frac{\left[P_{(i)}+P_{(i-1)}\right]\left[v_{pl(i)}-v_{pl(i-1)}\right]}{2} \qquad (A3.10)$$

where :

$v_{pl(i)}$ = plastic part of the load-line displacement, $v_i - P_{(i)}C_{LL(i)}$, and
$C_{LL(i)}$ = experimental compliance, $(\Delta v/\Delta P)_i$, corresponding to the current crack size, a_i.

For test methods that do not evaluate an experimental elastic compliance, $C_{LL(i)}$ can be determined from the following equation:

$$C_{LL(i)} = \frac{1}{EB_e}\left(\frac{1+\frac{a_{(i)}}{W}}{1-\frac{a_{(i)}}{W}}\right)^2 \times \qquad (A3.11)$$

$$\left[2.0462+9.6496\left(\frac{a_{(i)}}{W}\right)-13.7346\left(\frac{a_{(i)}}{W}\right)^2+6.1748\left(\frac{a_{(i)}}{W}\right)^3\right]$$

where:

B_e = $B - (B - B_N)^2/B$.

NOTE A3.1—The point $P_{(i)}$, $v_{(i)}$ is the last data point recorded before the *i*-th unloading begins and before any hold period for stress relaxation as in accordance with 8.6.4.

The compliance estimated using Eq A3.11 should be verified by calibrating against the initial experimental compliance to assure the integrity of the load-line displacement measurement system.

In an elastic compliance test, the rotation corrected compliance, $C_c(i)$, described in A3.5.5 shall be used instead of $C_{LL(i)}$ given above.

A3.5.3 *Calculation of Crack Size*—For a single-specimen test method using an elastic compliance technique on DC(T) specimens with crack opening displacements measured at the load-line, the crack size is given as follows:

$$\frac{a_{(i)}}{W} = 0.998193 - 3.88087u + 0.187106u^2 + 20.3714u^3 \qquad (A3.12)$$

$$- 45.2125u^4 + 44.5270u^5$$

where:

$$u = \frac{1}{\left[(B_e EC_{c(i)})^{1/2}+1\right]} \qquad (A3.13)$$

where:

$C_{c(i)}$ = specimen crack opening compliance ($\Delta v/\Delta P$) on an unloading/reloading sequence, corrected for rotation (see A3.5.5),

B_e = $B - (B - B_N)^2/B$.

A3.5.4 The calculation of crack size values for the *DC(T)* specimens is a two-step procedure. First, values of uncorrected crack size a_i are obtained from measured values of load-line compliance C_i using Eq A3.12 and Eq A3.13. Uncorrected crack size values are then used to calculate the corresponding values of the radius of rotation of the crack centerline, R_i, as follows:

$$R_i = \frac{W + a_i}{2} \quad \text{(A3.14)}$$

A3.5.5 To account for crack opening displacement in *DC(T)* specimens, the crack size estimation shall be corrected for rotation. Compliance shall be corrected as follows:

$$C_{c(i)} = \frac{C_i}{\left(\dfrac{H^*}{R_i}\sin\theta_i - \cos\theta_i\right)\left(\dfrac{D}{R_i}\sin\theta_i - \cos\theta_i\right)} \quad \text{(A3.15)}$$

where:

R_i = Radius of rotation of the crack centerline, $(W + a)/2$, where a is the updated crack size,

C_i = measured specimen elastic compliance, $\Delta v_m/\Delta P_m$ (at the load-line),

$C_{c(i)}$ = corrected specimen elastic compliance, $\Delta v_c/\Delta P_c$ (at the load-line)

H^* = initial half-span of the load points (center of the pin holes),

D = one half of the initial distance between the displacement measurement points,

θ = angle of rotation of a rigid body element about the unbroken midsection line, or

$$\theta_i = \arcsin\left[\frac{D + \dfrac{v_{m(i)}}{2}}{\sqrt{D^2 + R_i^2}}\right] - \arctan\left(\frac{D}{R_i}\right), \text{ and}$$

$v_{m(i)}$ = total measured load-line displacement, at the beginning of the *i*-th unloading/reloading cycle.

v_c = total corrected load-line displacement at the beginning of the *i*-th unloading/reloading cycle.

A3.5.6 Other compliance equations are acceptable if the resulting accuracy is equal to or greater than those described and the accuracy has been verified experimentally.

A3.5.7 *Calculation of CTOD:*

A3.5.7.1 *Calculation of CTOD for the Basic Test Method*—For the basic test method calculations of CTOD for any point on the force-displacement curve are made from the following expression:

$$\delta = \frac{J}{m\sigma_Y} \quad \text{(A3.16)}$$

where J is defined in A3.5.2.1 with a = a_o, the original crack size and then crack growth corrected using Annex A16 and:

$$m = A_0 - A_1 * \left(\frac{\sigma_{YS}}{\sigma_{TS}}\right) + A_2 * \left(\frac{\sigma_{YS}}{\sigma_{TS}}\right)^2 - A_3 * \left(\frac{\sigma_{YS}}{\sigma_{TS}}\right)^3 \quad \text{(A3.17)}$$

with: A_0=3.62, A_1 = 4.21, A=4.33, and A_3=2.00. Calculation of δ requires $\sigma_{YS}/\sigma_{TS} \geq 0.5$.

A3.5.7.2 *Calculation of CTOD for the Resistance Curve Test Method*—For the resistance curve test method, calculations of CTOD for any point on the force-displacement curve are made from the following expression:

$$\delta = \frac{J_i}{m\sigma_Y} \quad \text{(A3.18)}$$

where J is defined in A3.5.2.2 with a = a_i, the current crack size and,

$$m = A_0 - A_1 * \left(\frac{\sigma_{YS}}{\sigma_{TS}}\right) + A_2 * \left(\frac{\sigma_{YS}}{\sigma_{TS}}\right)^2 - A_3 * \left(\frac{\sigma_{YS}}{\sigma_{TS}}\right)^3 \quad \text{(A3.19)}$$

with: A_0=3.62, A_1 = 4.21, A_2=4.33, and A_3=2.00. Calculation of δ requires $\sigma_{YS}/\sigma_{TS} \geq 0.5$.

A4. METHODS FOR EVALUATING INSTABILITY AND POP-IN

A4.1 *Assessment of Force/Clip Gage Displacement Records*—The applied force-displacement record obtained from a fracture test on a notched specimen will usually be one of the four types shown in Fig. A4.1.

A4.1.1 In the case of a smooth continuous record in which the applied force rises with increasing displacement up to the onset of unstable brittle crack extension or pop-in, and where no significant slow stable crack growth has occurred (see 3.2 and Fig. A4.1a and Fig. A4.1b), the critical CTOD, δ_c, shall be determined from the force and plastic component of clip gage displacement, v_p, corresponding to the points P_c and v_c.

A4.1.2 In the event that significant slow stable crack extension precedes either unstable brittle crack extension or pop-in, or a maximum force plateau occurs, the force-displacement curves will be of the types shown in Fig. A4.1c, Fig. A4.1d, respectively. These figures illustrate the values of *P* and v to be used in the calculation of δ_u.

A4.1.3 If the pop-in is attributed to an arrested unstable brittle crack extension in the plane of the fatigue precrack, the result must be considered as a characteristic of the material tested.

NOTE A4.1—Splits and delaminations can result in pop-ins with no

22

arrested brittle crack extension in the plane of the fatigue precrack.

For this test method, pop-in crack extension in the plane of the fatigue precrack can be assessed by a specific change in compliance. The following procedure may be used to assess the significance of small pop-ins (see Fig. A4.1b and Fig. A4.1d). Referring to Figs. A4.1 and A4.2, measure the values of P_c and v_c or P_u and v_u from the test record at points corresponding to: (a) the earliest significant pop-in fracture, that is, for which $F > 0.05$ and (b) fracture, when pop-ins prior to fracture may be ignored, that is, for which $F < 0.05$ as follows:

$$F = 1 - \frac{v_1}{P_1} \cdot \left(\frac{P_n - y_n}{v_n + x_n} \right) \qquad (A4.1)$$

where:

F = factor representing the accumulated increase in compliance and crack size due to all stable crack extensions, or pop-ins, or both, prior to and including the nth pop-in, and

n = sequential number (see Fig. A4.2) of the last of the particular series of pop-ins being assessed.

NOTE A4.2—When only one pop-in occurs, $n = 1$. When multiple pop-ins occur it may be necessary to make successive assessments of F with $n = 1, 2, 3,$ or more.

v_1 = elastic displacement at pop-in No. 1 (see Fig. A4.2),
P_n = force at the nth pop-in, and
v_n = elastic displacement at the nth pop-in.

NOTE A4.3—v_n may be determined graphically or analytically (see Fig. A4.2).

y_n = force drop at the nth pop-in, and
x_n = displacement increase at the nth pop-in

NOTE A4.4—Although an individual pop-in may be ignored on the basis of these criteria, this does not necessarily mean that the lower bound of fracture toughness has been measured. For instance, in an inhomogeneous material such as a weld, a small pop-in may be recorded because of fortuitous positioning of the fatigue precrack tip. Thus, a slightly different fatigue precrack position may give a larger pop-in, which could not be ignored. In such circumstances the specimens should be sectioned after testing, and examined metallographically to ensure that the crack tips have sampled the weld or base metal region of interest (12).

A4.1.4 The initial compliance C_1 shall be determined by constructing the tangent OA to the initial portion of the force-clip gage displacement curve as shown in Fig. A4.3. The initial compliance C_1 is the inverse of the slope of the tangent line OA:
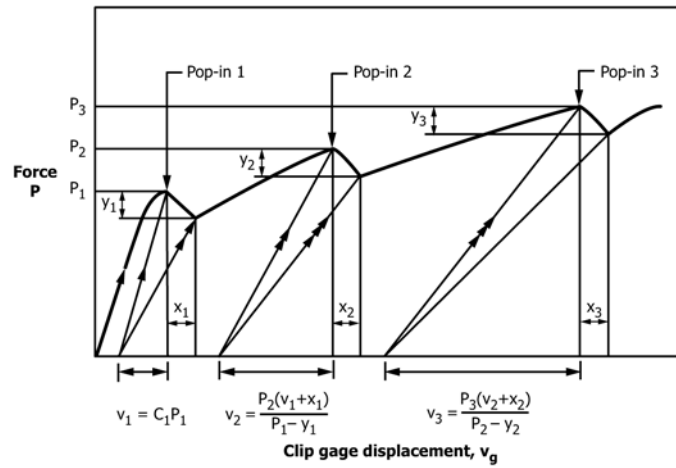
$$C_1 = \frac{\Delta v_g}{\Delta P} \qquad (A4.2)$$
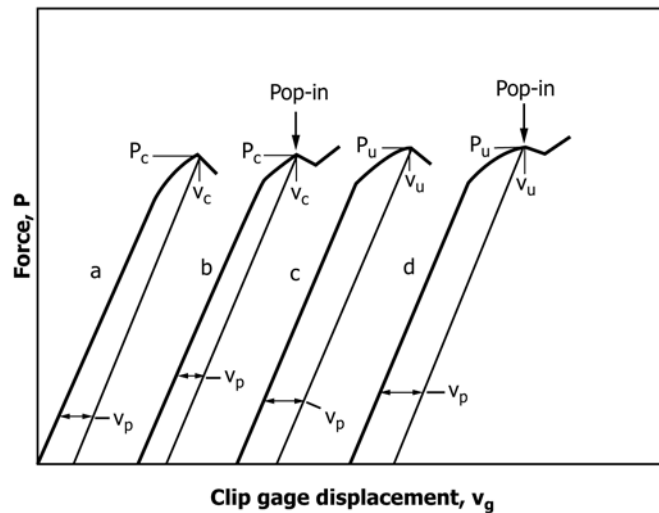
NOTE 1—Construction lines drawn parallel to the elastic loading slope to give v_p, the plastic component of total displacement, v_g.
NOTE 2—In curves b and d, the behavior after pop-in is a function of machine/specimen compliance, instrument response, and so forth..

FIG. A4.1 Types of Force versus Clip Gage Displacement Records

NOTE 1—C_1 is the initial compliance.
NOTE 2—The pop-ins have been exaggerated for clarity.
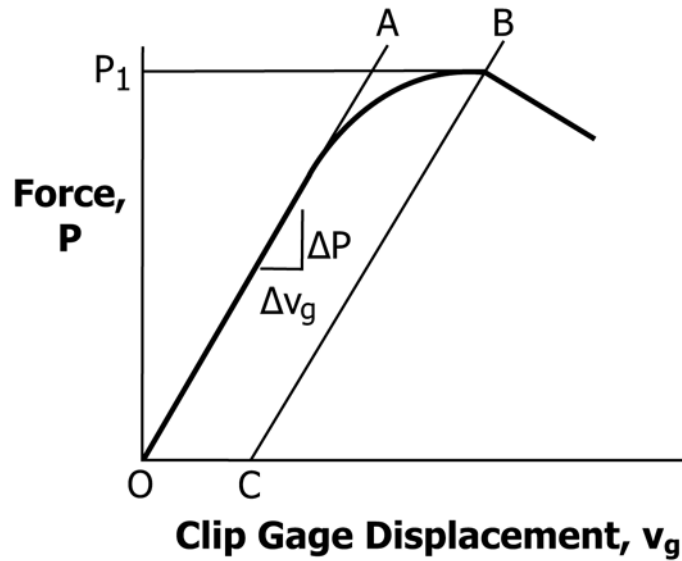**FIG. A4.2 Significance of Pop-In**

FIG. A4.3 Determination of Initial Compliance

A5. METHOD FOR K_{IC} DETERMINATION

A5.1 This annex has been removed from the standard. See Test Method E399.

24

A6. FRACTURE INSTABILITY TOUGHNESS DETERMINATION USING J

A6.1 This annex describes the method for characterizing fracture toughness values based on J, J_c, or J_u, for a fracture instability and the associated requirements for qualifying the data according to this test method. Data meeting all of the qualification requirements of 9.1 and those of this annex result in qualified values of J_c or J_u. Data meeting the size requirement result in a value of J_c that is insensitive to the in-plane dimensions of the specimen.

A6.2 *Fracture Instability Before Stable Tearing*—When fracture occurs before stable tearing, a single-point toughness value may be obtained labeled J_c.

A6.2.1 J is calculated at the final point of instability, using the J formulas for the basic method including the crack growth correction in Annex A16. This point is labeled J_{Qc}, a provisional J_c value.

A6.2.2 *Qualification of J_{Qc} as J_c*—$J_{Qc} = J_c$, a measure of fracture toughness at instability without significant stable crack extension that is independent of in-plane dimensions, provided the following two conditions are both met: (1) B, $b_o \geq 100$ J_{Qc}/σ_Y, and (2) crack extension $\Delta a_p < 0.2$ mm $+ J_{Qc}/2\sigma_Y$. Note that even if these conditions are met, J_c may be dependent on thickness (length of crack front).

A6.3 *Fracture Instability After Stable Tearing*—When fracture occurs after stable tearing crack extension $\Delta a_p > 0.2$ mm (0.008 in.) $+ J_{Qc}/2\sigma_Y$, a single-point fracture toughness value may be obtained, labeled J_{Qu}. In addition, part of an R-curve may be developed or the final point may be used in the evaluation of an initiation toughness value J_{Ic} (these are described in Annex A8 – Annex A11).

A6.3.1 J is calculated at the final point where instability occurs using the J formulas for the basic method including the crack growth correction of Annex A16. This point is a J_u value.

A6.3.2 *Qualification of J_{Qu} as J_u*—$J_{Qu} = J_u$ if crack extension $\Delta a_p \geq 0.2$ mm (0.008 in.) $+ J_{Qu}/2\sigma_Y$.

A6.4 *Significance of J_c and J_u*—Values of J_{Qc} that meet the size criteria are labeled J_c and are considered to be insensitive to the in-plane dimensions of the specimen. For ferritic steel specimens that have failed unstably by cleavage in the ductile to brittle transition, the analysis procedure of Test Method E1921 is recommended. Values of J_{Qc} that do not meet validity remain J_{Qc} and may be size-dependent. J_u is not considered to be a size-insensitive property and therefore is not subject to a size criterion. It is a characteristic of the material and specimen geometry and size. It signifies that at the test temperature the material is not completely ductile and can sustain only limited R-curve behavior.

A7. FRACTURE INSTABILITY TOUGHNESS DETERMINATION USING CTOD (δ)

A7.1 This annex describes the method for characterizing fracture toughness values based on δ, δ_c, or δ_u for a fracture instability and the associated requirements for qualifying the data according to this test method. Data meeting all of the qualification requirements of 9.1 and those in this annex result in qualified values of δ_c or δ_u. Data meeting the size requirement result in a value of δ_c^* that is insensitive to in-plane dimensions of the specimen.

A7.2 *Fracture Instability Before Stable Tearing*—When fracture occurs before stable tearing, a single-point toughness value may be obtained labeled δ_c, the force P_c and the clip gage displacement υ_c, for δ_c are indicated in Fig. 1.

A7.2.1 δ is calculated at the final point, instability, using the δ formulas from Annex A1 – Annex A3. This point is labeled δ_{Qc}, a provisional δ_c value.

A7.2.2 *Qualification of δ_{Qc} as δ_c^**, a fracture toughness value that is insensitive to the in-plane dimensions of the specimen, if the following two conditions are met: (1) B, $b_o \geq 300$ δ_{Qc}, and (2) crack extension $\Delta a_p < 0.2$ mm (0.008 in.) $+ \delta_{Qc}/1.4$.

Data that fail to meet the size criterion based on B or b_o, but still meet the restriction on crack extension, are labeled δ_c.

A7.3 *Fracture Instability After Stable Tearing*—When fracture occurs after stable tearing, crack extension $\Delta a_p \geq 0.2$ mm (0.008 in.) $+ \delta_{Qc}/1.4$, a single-point fracture toughness value may be obtained, labeled δ_u. In addition, part of an R-curve may be developed or the final point may be used in the evaluation of an initiation toughness value (these are described in Annex A8 – Annex A11).

A7.3.1 δ is calculated at the final point where instability occurs, using the δ formulas for the basic method. This point is labeled δ_{Qu}, a provisional δ_u value.

A7.3.2 *Qualification of δ_{Qu} as δ_u*—$\delta_{Qu} = \delta_u$, if crack extension, $\Delta a_p > 0.2$ mm (0.008 in.) $+ \delta_{Qu}/1.4$.

A7.3.3 *Significance of δ_c and δ_u*—Values of δ_{Qc} that meet the qualification requirements are labeled δ_c^* and are considered to be insensitive to the in-plane dimensions of the specimen. Values of δ_{Qc} that do not meet the size requirement are labeled δ_c and may be size-dependent. δ_u is not considered

25

to be a size-insensitive property and, therefore, is not subject to a size criterion. It is a characteristic of the material and specimen geometry and size. It signifies that at the test temperature the material is not completely ductile and can sustain only limited *R*-curve behavior.

A8. *J-R* CURVE DETERMINATION

Note A8.1—Annex A8 – Annex A11 cover methods for evaluating toughness for stable tearing.

A8.1 This method describes a single-specimen technique for determining the *J-R* curve of metallic materials. The *J-R* curve consists of a plot of *J* versus crack extension in the region of *J* controlled growth. The *J-R* curve is qualified provided that the criteria of 9.1 and A8.3 are satisfied.

A8.2 *J Calculation:*

A8.2.1 *J* can be calculated at any point on the force versus load-line displacement record using the equations suggested in the calculation section of Annex A1 – Annex A3 for the different specimen geometries.

A8.2.2 If a resistance curve method is used, the values of crack size are calculated using the compliance equations described in Annex A1 – Annex A3 (or an alternative method for measuring crack size). The rotation correction shall be applied to account for geometry changes due to deformation for the compact, C(T), and disk-shaped compact, DC(T), specimens.

A8.2.3 If an elastic compliance method is used, the unload/reload sequences should be spaced with the displacement interval not to exceed $0.01b_o$, the average being about $0.005b_o$. The use of larger increments between unloadings will lead to less accurate *J-R* curves although the result will be conservative. If an initiation value of toughness is being evaluated, more unload/reload sequences may be necessary in the early region of the *J-R* curve.

A8.3 *Measurement Capacity of Specimen:*

A8.3.1 The maximum *J*-integral capacity for a specimen is given by the smaller of the following:

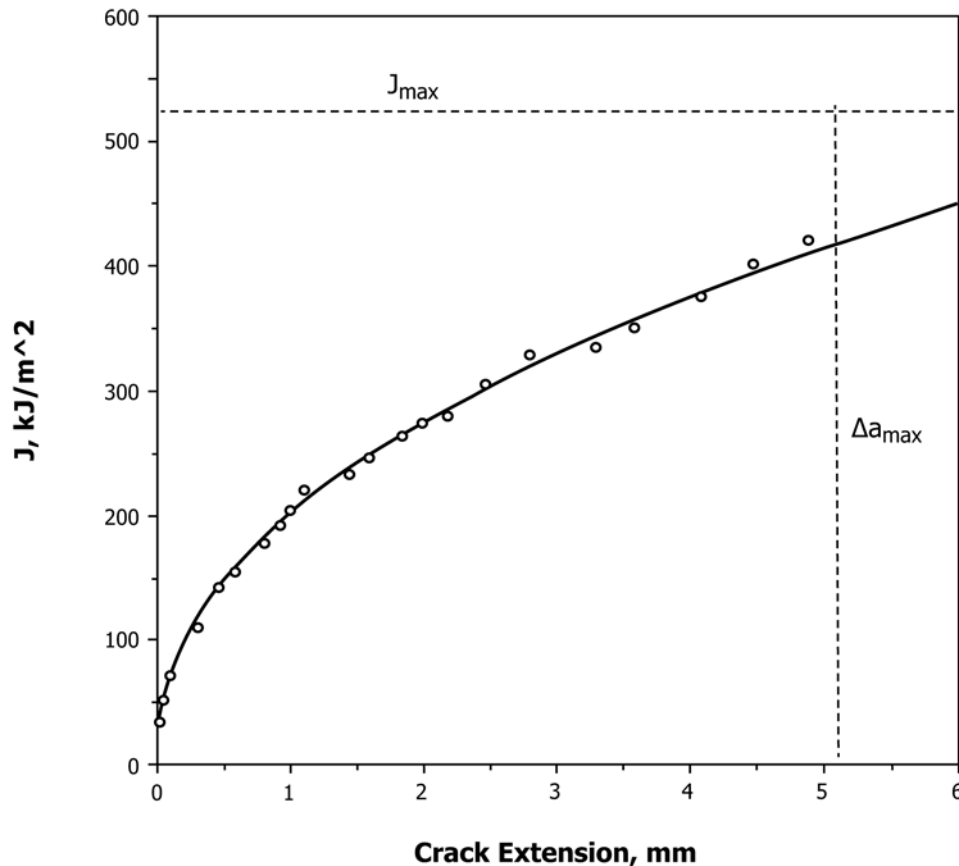$$J_{max} = b_o \sigma_Y / 10, \text{ or}$$

FIG. A8.1 Typical *J-R* Curve

$$J_{max} = B\sigma_Y/10.$$

A8.3.2 The maximum crack extension capacity for a specimen is given by the following:

$$\Delta a_{max} = 0.25\, b_o$$

A8.4 *Constructing the J-R Curve:*

A8.4.1 The *J*-integral values and the corresponding crack extension values must be plotted as shown in Fig. A8.1. If an elastic compliance method is used, shift the *J-R* curve according to the procedure described in A9.3. The *J-R* curve is defined as the data in a region bounded by the coordinate axes and the J_{max} and Δa_{max} limits given in A8.3.1 and A8.3.2.

A9. J_{Ic} and K_{JIc} EVALUATION

A9.1 *Significance*—The property J_{Ic} determined by this method characterizes the toughness of a material near the onset of crack extension from a preexisting fatigue crack. The J_{Ic} value marks the beginning stage of material crack growth resistance development, the full extent of which is covered in Annex A8. J_{Ic} is qualified provided that the criteria of 9.1 and A9.9 and A9.10 are satisfied.

A9.2 *J Calculation*:

A9.2.1 Calculations of the *J* integral are made using the equations in Annex A1 – Annex A3.

A9.2.2 A collection of standard data sets, E1820/1–DS1(2016)-E1820/9–DS9(2020), is available for verifying computer algorithms developed to implement the calculations to evaluate J_{Ic}. See 2.2.

A9.3 *Corrections and Adjustments to Data:*

A9.3.1 If the basic method is used, calculate crack growth corrected *J* values using the procedure of Annex A16.

A9.3.2 If an elastic compliance method is used, a correction is applied to the estimated Δa_i data values to obtain an improved a_{oq}. This correction is intended to obtain the best value of a_{oq}, based on the initial set of crack size estimates, a_i, data. For data generated using the basic procedure of 8.4, no adjustments to the crack size and crack extension data are necessary. To evaluate J_{Ic} using data from the basic procedure, proceed to A9.6.

A9.3.3 *Adjustment of a_{oq}*—The value of J_Q is very dependent on the a_{oq} used to calculate the Δa_i quantities. The value obtained for a_{oq} in 8.6.3.1 might not be the correct value and the following adjustment procedure is required.

A9.3.3.1 Identify all J_i and a_i points that were determined before the specimen reached the maximum force for the test. Use this data set of points to calculate a revised a_{oq} from the following equation:

$$a = a_{oq} + \frac{J}{2\sigma_Y} + BJ^2 + CJ^3 \qquad (A9.1)$$

The coefficients of this equation shall be found using a least squares fit procedure, see Appendix X1.

A9.3.3.2 If the number of points used in A9.3.3.1 to determine a_{oq} is less than 8 or of these 8 there are less than 3 between 0.4 J_Q and J_Q or the correlation coefficient of this fit is less than 0.96, the data set is not adequate to evaluate any toughness measures in accordance with this test method.

A9.4 If the optically measured crack size, a_o, differs from a_{oq} by more than the larger of $0.01W$ or 0.5mm, the data set is not adequate according to this test method.

A9.5 Evaluate the final J_i values using the adjusted a_{oq} of A9.3.3 and the equations of the applicable Annex A1, Annex A2, or Annex A3.

A9.6 *Calculation of an Interim J_Q:*

A9.6.1 *Basic Procedure*—For each specimen, calculate Δa as follows:

$$\Delta a = a_p - a_o \qquad (A9.2)$$

Resistance Curve Procedure—For each a_i value, calculate a corresponding Δa_i as follows:

$$\Delta a_i = a_i - a_{0q} \qquad (A9.3)$$

Plot *J* versus Δa as shown in Fig. A9.1. Determine a construction line in accordance with the following equation:

$$J = 2\sigma_Y\Delta a \qquad (A9.4)$$

A9.6.2 Plot the construction line, then draw an exclusion line parallel to the construction line intersecting the abscissa at 0.15 mm (0.006 in.). Draw a second exclusion line parallel to the construction line intersecting the abscissa at 1.5 mm (0.06 in.). Plot all $J - \Delta a$ data points that fall inside the area enclosed by these two parallel lines and capped by $J_{limit} = b_o\sigma_Y/7.5$.

A9.6.3 Plot a line parallel to the construction and exclusion lines at an offset value of 0.2 mm (0.008 in.).

A9.6.4 At least one $J–\Delta a$ point shall lie between the 0.15-mm (0.006-in.) exclusion line and a parallel line with an offset of 0.5 mm (0.02 in.) from the construction line as shown in Fig. A9.2. At least one $J−\Delta a$ point shall lie between this 0.5-mm offset line and the 1.5-mm (0.06-in.) exclusion line. Acceptable data are shown in Fig. A9.2. The other $J−\Delta a$ points can be anywhere inside the region of qualified data.

A9.6.5 J_{Ic} is determined by fitting a power law to selected data that fall in the region defined in A9.6.2.

$$J = C_1\left(\frac{\Delta a}{k}\right)^{c_2} \qquad (A9.5)$$

To select the $(\Delta a, J)$ data points to be used in determination of the power law coefficients, C_1 and C_2, start with the last point that falls within the limits defined in A9.6.2 (designate the index of this point as n). Working back toward the start of the test one unload/reload at a time, find the first point that falls

FIG. A9.1 Definition of Construction Lines for Data Qualification

FIG. A9.2 Definition of Regions for Data Qualification

to the left of the 0.15 mm exclusion line (designate the index of this point as m). Perform a power law regression analysis using the method of least squares using all data points between indices m+1 and n. The power law is linearized for regression analysis in the following form::

$$\ln J = \ln C_1 + C_2 \ln\left(\frac{\Delta a}{k}\right) \qquad (A9.6)$$

where k = 1.0 mm or 0.0394 in. Use only the data which conform to the requirements stated in the previous sections. Draw the regression line as illustrated in Fig. A9.1.

NOTE A9.1—This data selection procedure avoids the situation where

backup or other anomalies at the start of the test cause a point with low J to fall to the right of the 0.15 mm exclusion line, thereby either causing C_2 > 1 or providing an unreasonably low determination of J_Q.

A9.6.6 The intersection of the regression line of A9.6.5 with the 0.2-mm offset line defines J_Q and Δa_Q. To determine this intersection the following procedure is recommended.

A9.6.6.1 As a starting point estimate an interim $J_{Q(1)} = J_{Q(i)}$ value from the data plot of Fig. A9.1.

A9.6.6.2 Evaluate $\Delta a_{(i)}$ from the following:

$$\Delta a_{(i)} = \frac{J_{Q(i)}}{2\sigma_Y} + 0.2 \text{ mm (0.008 in.)} \qquad (A9.7)$$

A9.6.6.3 Evaluate an interim $J_{Q(i+1)}$ from the following power law relationship:

$$J_{Q(i+1)} = C_1 \left(\frac{\Delta a_{(i)}}{k}\right)^{C_2} \qquad (A9.8)$$

where k = 1.0 mm or 0.0394 in.

A9.6.6.4 Increment i and return to A9.6.6.2 and A9.6.6.3 to get $\Delta a_{(i)}$ and interim $J_{Q(i+1)}$ until the interim J_Q values converge to within ±2 %.

A9.6.6.5 Project the intercepts of the power law curve with the 0.15-mm (0.006-in.) and the 1.5-mm (0.06-in.) exclusion lines vertically down to the abscissa. This indicates Δa_{min} and Δa_{limit}, respectively. Eliminate all data points that do not fall between Δa_{min} and Δa_{limit} as shown in Fig. A9.1. Also eliminate all data points which lie above the limiting J capacity where $J_{limit} = b_o\sigma_Y / 7.5$. The region of qualified data is shown in Fig. A9.2.

A9.6.6.6 At least five data points must remain between Δa_{min}, Δa_{limit}, and J_{limit}. Data point spacing must meet the requirements of A9.6.4. If these data points are different from

28

Eqr{tki j v'd{ "CUVO "Ipvi"%crń'tki j w'tgugtxgf +"Hk'Icp"4: "374: -25'I O V"4244
F qy prqcf gf Ir tkpygf "d{
Rtkpegvqp"Wpkxgtuk{"Rtkpegvqp"Wpkxgtuk{+'r wtuwcpv'\q 'Nkegpug"Ci tggo gpv0P q'hwtvj gt 'tgrtqf wevkqpu'cwj qtk\gf 0

those used in A9.6.6 to evaluate J_Q, obtain a new value of J_Q based only on qualified data.

A9.7 If the specimen fails by instability or the onset of cleavage without a J-Δa point exceeding the 0.5 mm offset line, an alternative data set can be used to obtain J_Q. In this case at least 4 data points shall be in Region A of Fig. A9.2 and at least one of these points shall fall between the 0.2 mm (0.008 in.) offset line and the 0.5 mm (0.02 in.) offset line. The data available is fit with the same power law procedure of A9.6.6.1 – A9.6.6.4 and J_Q is evaluated at the intersection of the linear regression line of A9.6.5 and the 0.2 mm offset line.

Note A9.2—In the case of ductile instability, more stable tests can be achieved by stiffening the test machine, generally by reducing the length of the load train, especially by removing any unnecessary alignment fixtures or threaded connections, or both. If the test machine is servo controlled, controlling using the CMOD gage signal rather than the stroke signal can also improve the stability of the test.

A9.8 If the specimen fails unstably without a J-Δa data point beyond the 0.2 mm offset line of Fig. A9.2, the maximum J value measured is evaluated using Annex A6. Additionally, for all specimens that do not fail by cleavage instability, the J value measured at the last unloading can be taken as J_Q and shall meet only the requirements of A9.10.1 and A9.10.2 to be qualified as J_{Ic}.

A9.8.1 For ferritic steel specimens that have failed unstably by cleavage in the ductile to brittle transition, the analysis procedure of Test Method E1921 is recommended.

A9.9 *Qualification of Data*—The data shall satisfy the requirements of 9.1 and all of the following requirements to be qualified according to this test method. If the data do not pass these requirements no fracture toughness values can be determined according to this test method.

A9.9.1 The power coefficient C_2 of A9.6.5 shall be less than 1.0.

A9.9.2 For the *Resistance Curve Procedure* the following additional requirements must be satisfied:

A9.9.2.1 If an elastic compliance method is used, a_{oq} shall not differ from a_o by more than the larger of $0.01W$ or 0.5 mm.

A9.9.2.2 The number of data available to calculate a_{oq} shall be ≥ 8; the number of data between $0.4J_Q$ and J_Q shall be ≥ 3; and the correlation coefficient of the least squares fit of A9.3.3.1 shall be greater than 0.96.

A9.10 *Qualification of J_Q as J_{Ic}*—$J_Q = J_{Ic}$, a size-independent value of fracture toughness, if:

A9.10.1 Thickness, $B > 10\ J_Q\ /\ \sigma_Y$,

A9.10.2 Initial ligament, $b_o > 10\ J_Q\ /\ \sigma_Y$,

A9.11 *Evaluation of K_{JIc}*—Calculate $K_{JIc} = \sqrt{(E'J_{Ic})}$ using $E' = E/(1-\nu^2)$ and the qualified J_{Ic} of A9.10.

A10. METHOD FOR δ-*R* CURVE DETERMINATION

A10.1 This annex describes a single-specimen technique for determining the δ-*R* curve of metallic materials. The δ-*R* curve consists of a plot of δ versus crack extension. To measure the δ-*R* curve the resistance curve procedure of 8.6 must be used. The δ-*R* curve is qualified provided that the criteria of 9.1 and A10.3 are satisfied.

A10.2 *δ Calculation:*

A10.2.1 δ can be evaluated at any point along the force versus load-line displacement record using the equations suggested in the calculation section of Annex A1 – Annex A3 for the different specimen geometries.

A10.2.2 The values of crack size are calculated using compliance equations described in Annex A1 – Annex A3. The rotation correction shall be applied to account for geometry changes due to deformation for the compact, C(T), and disk-shaped compact, DC(T), specimens.

A10.2.3 The unload/reload sequences should be spaced with the displacement interval less than 0.01 *W*, the average being about 0.005 *W*. If an initiation value of toughness is being evaluated, more unload/reload sequences may be necessary in the early region of the δ-*R* Curve.

A10.3 *Measurement Capacity of a Specimen:*

A10.3.1 The maximum δ capacity for a specimen is given as follows:

$$\delta_{max} = b_o/10m$$

where *m* is defined in Annex A1 – Annex A3 for the different specimen geometries.

A10.3.2 The maximum crack extension capacity for a specimen is given as follows:

$$\Delta a_{max} = 0.25\ b_o.$$

A10.4 *Constructing the δ-R Curve:*

A10.4.1 The δ values and the corresponding crack extension values must be plotted as shown in Fig. A10.1. A δ-*R* curve is established by smoothly fitting the data points in the region bounded by the coordinate axes and the δ_{max} and Δa_{max} limits.
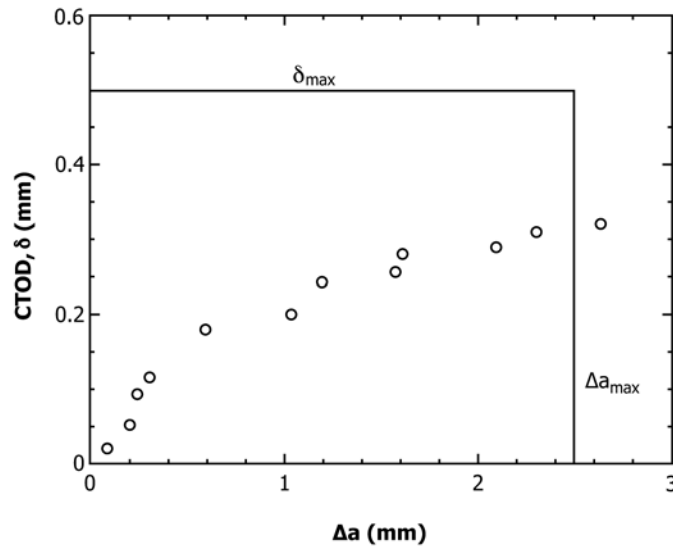
FIG. A10.1 Typical δ-*R* Curve

A11. METHOD FOR δ_{Ic} DETERMINATION

A11.1 *Significance*—The value of CTOD, δ_{Ic}, determined by this method characterizes the fracture toughness of materials near the onset of stable crack extension from a preexisting fatigue crack. δ_{Ic} is qualified provided that the criteria of 9.1 and A11.9 and A11.10 are satisfied.

A11.2 *δ Calculation*—Calculations of δ are made using the equations in Annex A1 – Annex A3.

A11.3 *Corrections and Adjustments to Data:*

A11.3.1 A correction is applied to the estimated a_i data values to obtain an improved a_{oq}. This correction is intended to obtain the best value of a_{oq}, based on the initial set of crack size estimates, a_i, data. For data generated using the basic procedure of 8.4, no adjustments to the data are necessary. To evaluate δ_{Ic} using data from the basic procedure, proceed to A11.6.

A11.3.2 *Adjustment of a_{oq}*—The value of δ_Q is very dependent on the a_{oq} used to calculate the Δa_i quantities. The value obtained for a_{oq} in 8.6.3.1 might not be the correct value, and the following adjustment procedure is required.

A11.3.2.1 Identify all δ_i and a_i points that were determined before the specimen reached the maximum force for the test. Use this data set of points to calculate a revised a_{oq} from the following equation:

$$a = a_{oq} + \frac{\delta}{1.4} + B\delta^2 + C\delta^3 \qquad (A11.1)$$

The coefficients of this equation shall be found using a least squares fit procedure, see Appendix X1.

A11.3.2.2 If the number of points used in A11.3.2.1 to calculate a_{oq} is less than 8, or of these 8 there are less than 3 between $0.4\delta_Q$ and δ_Q, or the correlation coefficient of this fit

is < 0.96, the data set is not adequate to evaluate any toughness measures in accordance with this method.

A11.4 If the optically measured crack size, a_o, differs from a_{oq} by more than the larger of 0.01 W or 0.5 mm, the data set is not adequate in accordance with this method.

A11.5 Evaluate the final δ_i values using the adjusted a_{oq} of A11.3.2.1 and the equations of the applicable Annex A1, Annex A2, or Annex A3.

A11.6 *Calculation of an Interim δ_Q:*

A11.6.1 *Basic Procedure*—for each specimen, calculate Δa as follows:

$$\Delta a = a_p - a_o \qquad (A11.2)$$

Resistance Curve Procedure—for each a_i value, calculate a corresponding Δa_i as follows:

$$\Delta a_i = a_i - a_{0q} \qquad (A11.3)$$

Plot δ versus Δa as shown in Fig. A11.1. Draw a construction line in accordance with the following equation:

$$\delta = 1.4\,\Delta a \qquad (A11.4)$$

A11.6.2 Plot the construction line. Draw an exclusion line parallel to the construction line intersecting the abscissa at 0.15 mm (0.006 in.) as shown in Fig. A11.1. Draw a second exclusion line intersecting the abscissa at 1.5 mm (0.06 in.). Plot all δ-Δa_p data points that fall inside the area enclosed by these two parallel lines and capped by $\delta_{limit} = b_o /7.5m$, where m is defined in Annex A1 – Annex A3 for the different specimen geometries.

A11.6.3 One δ-Δa_p point must lie between the 0.15-mm (0.006-in.) exclusion line and a parallel line with an offset of
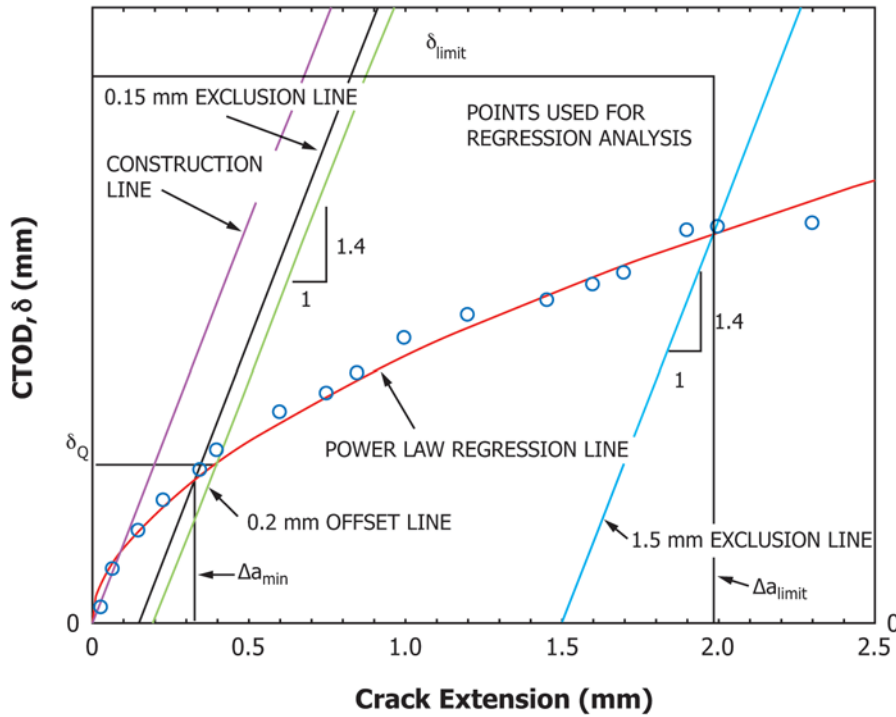
30

Eqr{tki j v'd{ 'CUVO "kpvi%cm'tki j u't gugtxgf +="Hk'Lcp"4: '374: '25'T O V'4244
Fqy pmqcf gf lr tlkpvgf 'd{
Rtkpegvqp'Wpkxgtuku{ "'Rtkpegvqp'Wpkxgtuku{+'r wtuvcpv'q'Nkegpug'Ci tggo gpv0P q 'hwtvj gt 'tgrtqf wevkqpu'cwj qtk{gf 0

FIG. A11.1 Definition of Construction Lines for Data Qualification

0.5 mm (0.02 in.) from the construction line. One δ-Δa_p point must lie between a line parallel to the construction line at an offset of 0.5 mm (0.020 in.) and the 1.5-mm exclusion line. Acceptable data are shown in Fig. A11.2 with at least one point in Region A and at least one point in Region B. The other δ-Δa_p points can be placed anywhere inside the region of qualified data.

A11.6.4 Plot a line parallel to the construction line and exclusion lines at an offset value of 0.2 mm (0.008 in.).

A11.6.5 To establish a crack initiation measurement point under dominant slow-stable crack growth, a power law curve fitting procedure shall be used. This has the following form:

FIG. A11.2 Definition of Regions for Data Qualification

$$\delta_Q = C_1 \left(\frac{\Delta a}{k} \right)^{C_2} \tag{A11.5}$$

where $k = 1$ mm (or 0.0394 in.) depending upon units used. This power law can be determined by using a method of least squares to determine a linear regression line of the following form:

$$\ln\delta = \ln C_1 + C_2 \ln\left(\frac{\Delta a}{k} \right) \tag{A11.6}$$

Use only the data that conform to the criteria stated in the previous sections. Plot the regression line as illustrated in Fig. A11.1.

A11.6.6 The intersection of the regression line of A11.6.4 with the offset line of A11.6.5 defines δ_Q and Δa_Q. To determine this intersection the following procedure is recommended:

A11.6.6.1 Estimate a $\delta_{Q(1)}$ value from the data plot of Fig. A11.1.

A11.6.6.2 Evaluate $\Delta a_{p(1)}$ from the following:

$$\Delta a_{p(1)} = \frac{\delta_{Q(1)}}{1.4} + 0.2 \text{ mm } (0.008 \text{ in.}) \tag{A11.7}$$

A11.6.6.3 Evaluate

$$\delta_{Q(1)} = C_1 \left(\frac{\Delta a_{p(1)}}{k} \right)^{C_2} \tag{A11.8}$$

A11.6.6.4 Return to A11.6.2 and A11.6.6.3 to get $\Delta a_{(i)}$ and $\delta_{Q(i+1)}$ until the δ_Q values converge to within 2 %.

A11.6.6.5 Project the intercepts of the power law curve with the 0.15-mm (0.006-in.) and the 1.5-mm (0.06-in.) exclusion lines vertically down to the abscissa. This indicates Δa_{min} and Δa_{limit}, respectively. Eliminate all data points that do not fall
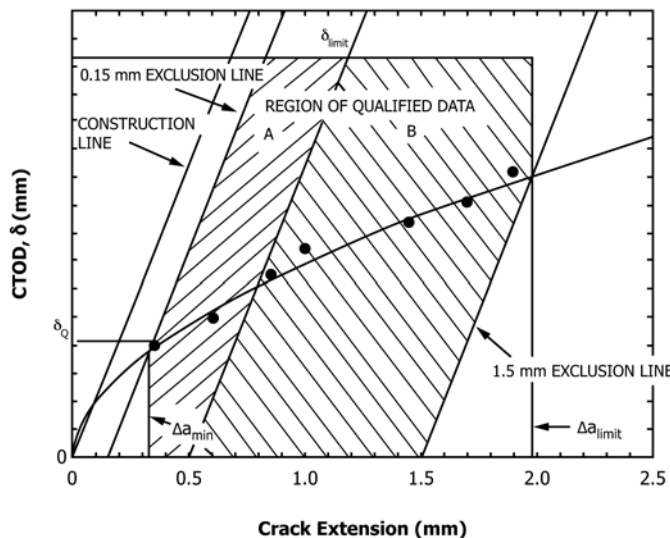
between Δa_{min} and Δa_{limit} as shown in Fig. A11.1. Also eliminate all data points which lie above the limiting δ capacity where $\delta_{limit} = b_o/7.5m$, where m is defined in Annex A1 through Annex A3 for the different specimen geometries.

A11.6.6.6 At least five data points must remain between Δa_{min}, Δa_{limit}, and δ_{limit}. Data point spacing must meet the requirements of A11.6.3. If these data points are different from those used in A11.6.6 to evaluate δ_Q, obtain a new value of δ_Q based only on qualified data.

A11.7 If the specimen fails by instability or the onset of cleavage without a δ-Δa point exceeding the 0.5 mm offset line, an alternative data set can be used to obtain δ_Q. In this case at least 4 data points shall be in Region A of Fig. A11.2 and at least one of these points shall fall between the 0.2 mm (0.008 in.) offset line and the 0.5 mm (0.02 in.) offset line. The data available is fit with the same power law procedure of A11.6.6.1 – A11.6.6.4 and δ_Q is evaluated at the intersection of the linear regression line of A11.6.5 and the 0.2 mm offset line.

NOTE A11.1—In the case of ductile instability, more stable tests can be achieved by stiffening the test machine, generally by reducing the length of the load train, especially by removing any unnecessary alignment fixtures or threaded connections, or both. If the test machine is servo controlled, controlling using the CMOD gage signal rather than the stroke signal can also improve the stability of the test.

A11.8 If the specimen fails unstably without a δ-Δa data point beyond the 0.2 mm offset line of Fig. A11.2, the maximum δ value measured is evaluated using Annex A7. Additionally, for specimens that do not fail by cleavage instability, the δ value measured at the last unloading can be taken as δ_Q and shall meet only the requirements of A11.9.1 to be qualified as δ_{Ic}.

A11.8.1 For ferritic steel specimens that have failed unstably by cleavage in the ductile to brittle transition, the analysis procedure of Test Method E1921 is recommended.

A11.9 *Qualification of Data*—The data shall satisfy the requirements of 9.1 and all of the following requirements to be qualified according to this method. If the data do not pass these requirements, no fracture toughness values can be determined according to this method.

A11.9.1 The power coefficient C_2 of A11.6.5 shall be less than 1.0.

A11.9.2 For the *Resistance Curve Procedure* the following additional requirements must be satisfied:

A11.9.2.1 a_{oq} shall not differ from a_o by more than the greater of $0.01W$ or 0.5 mm.

A11.9.2.2 The number of data available to calculate a_{oq} shall be ≥ 8; the number of data between $0.4\delta_Q$ and δ_Q shall be ≥ 3; and the correlation coefficient of the least squares fit of A11.6.5 shall be greater than 0.96.

A11.10 *Qualification of δ_Q as δ_{Ic}:*

$\delta_Q = \delta_{Ic}$, a size-independent value of fracture toughness, if:

A11.10.1 The initial ligament, $b_o \geq 10m\delta_Q$,

where m is defined in Annex A1 through Annex A3 for the different specimen geometries.

A12. COMMON EXPRESSIONS

NOTE A12.1—Annex A12 covers miscellaneous information.

A12.1 *Stress-Intensity Factor:*

A12.1.1 The elastic stress intensity factor for a specimen is expressed as follows:

$$K = \frac{Pf(a/W)}{(BB_N W)^{1/2}} \qquad (A12.1)$$

where:

$$f\left(\frac{a}{W}\right) = \left(\frac{\xi}{\zeta}\right)\left[C_0 + C_1\left(\frac{a}{W}\right) + C_2\left(\frac{a}{W}\right)^2 + C_3\left(\frac{a}{W}\right)^3 + C_4\left(\frac{a}{W}\right)^4\right]$$

A12.1.2 The parameters for $f(a/W)$ are listed in Table A12.1.

A12.2 *Compliance from Crack Size:*

TABLE A12.1 Parameters for Stress-Intensity Factors

	Specimens		
	SE(B)	C(T)	DC(T)
ξ	$3(S/W)(a/W)^{1/2}$	$2 + a/W$	$2 + a/W$
ζ	$2(1 + 2a/W)(1 - a/W)^{3/2}$	$(1 - a/W)^{3/2}$	$(1 - a/W)^{3/2}$
C_0	1.99	0.886	0.76
C_1	−2.15	4.64	4.8
C_2	6.08	−13.32	−11.58
C_3	−6.63	14.72	11.43
C_4	2.7	−5.6	−4.08
Limits	$0 \leq a/W \leq 1$	$0.2 \leq a/W \leq 1$	$0.2 \leq a/W \leq 1$
	$S/W = 4$	$H/W = 0.6$	$D/W = 1.35$
Refs	(13)	(13, 14)	(15)

TABLE A12.2 Parameters for Compliance Expressions

Specimen	SE(B)	C(T)	DC(T)
Location	v_{LL}	v_{LL}	v_{LL}
Y	$\dfrac{S}{(W-a)}$	$\dfrac{(W+a)}{(W-a)}$	$\dfrac{(W+a)}{(W-a)}$
A_0	1.193	2.163	2.0462
A_1	−1.980	12.219	9.6496
A_2	4.478	−20.065	−13.7346
A_3	−4.433	−0.9925	6.1748
A_4	1.739	20.609	0
A_5	0	−9.9314	0
Limits	$0 \leq a/W \leq 1$	$0.2 \leq a/W \leq$ 0.975	$0.2 \leq a/W \leq$ 0.8
Refs	(16)	(17)	(18)

A12.2.1 Compliance, C, of a specimen is expressed as a function of crack size as follows:

$$C = \frac{v}{P} = \qquad (A12.2)$$

$$\frac{Y^2}{B_e E}\left[A_0 + A_1\left(\frac{a}{W}\right) + A_2\left(\frac{a}{W}\right)^2 + A_3\left(\frac{a}{W}\right)^3 + A_4\left(\frac{a}{W}\right)^4 + A_5\left(\frac{a}{W}\right)^5\right]$$

A12.2.2 $B_e = B - (B - B_N)^2/B$ for all cases and the other parameters for compliance are listed in Table A12.2.

A13. METHOD FOR RAPID LOADING K_{IC} DETERMINATION

A13.1 This annex has been removed from the standard. See Test Method E399.

A14. SPECIAL REQUIREMENTS FOR RAPID-LOAD J-INTEGRAL FRACTURE TOUGHNESS TESTING[7]

A14.1 Scope

A14.1.1 This annex covers the determination of the rate dependent $J_{Ic}(t)$ and the J-integral versus crack growth resistance curve (J-$R(t)$ curve) for metallic materials under conditions where the loading rate exceeds that allowed for conventional (static) testing, see 8.4.2.

A14.1.2 *This international standard was developed in accordance with internationally recognized principles on standardization established in the Decision on Principles for the Development of International Standards, Guides and Recommendations issued by the World Trade Organization Technical Barriers to Trade (TBT) Committee.*

A14.2 Summary of Requirements

A14.2.1 Special requirements are necessary for J-integral fracture toughness testing of metallic materials at loading rates exceeding those of conventional (static) testing. Standard fracture toughness test specimens are prepared as described in this method, tested under rapid-load or drop weight conditions,

and a J-$R(t)$ curve is calculated. From this J-$R(t)$ curve a $J_Q(t)$ can be evaluated using Section 9 of this method. If unstable fracture intervenes, a $J_{Qc}(t)$ can be evaluated at the onset of unstable behavior as in the static case.

A14.2.1.1 Force, load-line displacement, and time are recorded for each test. The force versus displacement curve resulting from each test is analyzed to ensure that the initial portion of the curve is sufficiently well defined that an unambiguous curve can be determined from the $J(t)$ versus crack size $(a(t))$ data. In addition, a minimum test time is calculated from the specimen stiffness and effective mass that sets a maximum allowed test rate for the material and geometry being tested. At times less than the minimum test time a significant kinetic energy component is present in the specimen relative to the internal energy, and the static J integral equations presented in this method are not accurate. Evaluation of a $J_Q(t)$ or $J_{Qc}(t)$ at a time less than the minimum test time is not allowed by this method.

A14.2.1.2 Evaluation of the J-$R(t)$ curve requires estimation of crack extension as a function of load-line displacement or time using the normalization method of Annex A15. An elastic compliance method cannot be used. A multiple specimen method can be used to evaluate $J_Q(t)$ from a series of tests, which can be corrected using Annex A16 and assembled into a

---

[7] This test method is an Annex to ASTM E1820. It is under the jurisdiction of ASTM Committee E08 on Fatigue and Fracture and is the direct responsibility of Subcommittee E08.08 on Elastic-Plastic and Fracture Mechanics Technology.

J-R(t) curve. The *J-R(t)* curve is valid if it meets the requirements of this method.

A14.2.1.3 All of the criteria for the static J_{Ic}, J_c, and *J-R* curve evaluations apply to the rapid load *J* integral fracture toughness test. The rapid load *J* integral resistance curve is denoted *J-R(t)*, the stable initiation property $J_{Ic}(t)$, and the unstable initiation property by $J_c(t)$, where the time to reach the instant corresponding to J_Q in milliseconds is indicated in the brackets.

A14.3 Terminology

A14.3.1 *Definitions:*

A14.3.1.1 The definitions given in Terminology E1823 are applicable to this annex.

A14.3.1.2 The definitions given in Section 3 of this method are applicable.

A14.3.1.3 *Rapid Load*—In *J* integral fracture testing, any loading rate such that the time taken to reach P_m (see 7.4.4) is less than 0.1 minutes.

A14.3.1.4 *Minimum Test Time, $t_w(t)$*—In *J* integral fracture testing, the minimum time to the rate dependent $J_Q(t)$ or $J_{Qc}(t)$ accepted by this method (19). Test times less than t_w will lead to inaccurate *J* integral results since large kinetic energy components will be present. In this method:

$$t_w = \frac{2\,\pi}{\sqrt{k_s/M_{eff}}} \qquad (A14.1)$$

where:

k_s = specimen load-line stiffness, (N/m),
M_{eff} = effective mass of the specimen, taken here to be half of the specimen mass (kg).

A14.3.1.5 *Test Time, $t_Q(t)[T]$*—In *J* integral fracture testing, the observed time to the rate dependent $J_Q(t)$.

A14.3.1.6 *$J_c(t)[FL^{-1}]$*—In *J* integral fracture testing, the rate dependent *J* integral at the onset of fracture instability prior to the onset of significant stable tearing crack extension, see 3.2.12, as defined in this annex.

A14.3.1.7 *$J_{Qc}(t)[FL^{-1}]$*—In *J* integral fracture testing, the provisional rate dependent *J* integral at the onset of fracture instability prior to the onset of significant stable tearing crack extension, as defined in this annex.

A14.3.1.8 *$J_u(t)[FL^{-1}]$*—In *J* integral testing, the rate dependent *J* integral at the onset of fracture instability after significant stable tearing crack extension, see 3.2.13, as defined in this annex.

A14.3.1.9 *$J_{Ic}(t)[FL^{-1}]$*—In *J* integral testing, the rate dependent *J* integral at the onset of stable crack extension as defined in this annex.

A14.3.1.10 *$J_Q(t)[FL^{-1}]$*—In *J* integral fracture toughness testing, the provisional, rate dependent, *J* integral at the onset of stable crack extension as defined in this annex.

A14.3.1.11 *dJ/dt [$FL^{-1}T^{-1}$]*—In *J* integral fracture testing, the rate of change of the *J* integral per unit time. Two loading rate quantities are defined in this method, $(dJ/dt)_I$ measured before $J_Q(t)$, and $(dJ/dt)_T$ measured after $J_Q(t)$, as defined by this annex.

A14.4 Significance and Use

A14.4.1 The significance of the static *J-R* curve, J_{Ic}, and J_c properties applies also to the case of rapid loading. The *J* integral fracture toughness of certain metallic materials is sensitive to the loading rate and to the temperature of test. The *J-R(t)* curve and $J_{Ic}(t)$ properties are usually elevated by higher test rates while $J_c(t)$ can be dramatically lowered by higher test rates.

A14.5 Apparatus

A14.5.1 *Loading*—Two types of high rate loading systems are anticipated. Servohydraulic machines with high flow rate servovalves and high capacity accumulators, or alternatively, drop weight impact machines can be used. On-specimen force measurements are recommended for high rate tests. Remote force cells or other transducers can be used for high rate tests if the requirements of this annex are met. Strain gage bridges are recommended for on-specimen force measurement, as shown in Figs. A14.1 and A14.2. For each specimen type, four gages are connected to construct a four-arm bridge and calibrated statically before the rapid load test (see A14.5.4). Strain gages with grid patterns of approximately 0.25B are recommended. For SE(B) specimens, gages should be positioned on the specimen mid-plane at the specimen span quarterpoints. For C(T) specimens, the gages should be positioned on the specimen upper and lower surfaces near the specimen mid-plane with the gage edge at least 0.1W behind the initial crack, a_o.

A14.5.2 *Servohydraulic Testing Fixtures*—The fixtures used for static fracture toughness tests generally require some modification for rapid load tests. Slack grip fixtures are often necessary to reduce the applied force oscillation and to allow the actuator to accelerate before force is applied to the specimen. Soft metal absorbers are generally used in drop tower tests to reduce the inertial shock caused by the impact of the test machine striker on the specimen surface.

Both initial and final crack sizes are required by the normalization method of *J-R(t)* curve development of Annex A15. The high rate test must be stopped abruptly to obtain a limited specimen deformation and a crack extension increment satisfying the requirement of A15.1.1. Rigid stop block fixtures can be used to obtain the abrupt stop. In some cases a ramp and hold or square wave command signal can be used to obtain limited specimen deformation for the specimen test.

A14.5.3 *Drop Tower Testing Fixtures*—Special fixtures are necessary for drop tower testing according to this standard. Recommended fixtures for SE(B) and C(T) specimens are shown in Figs. A14.3 and A14.4, respectively (20). Stop block fixtures are required to obtain a limited extent of stable crack growth for *J-R(t)* curve development. Soft metal absorbers are recommended to reduce the initial shock resulting from the impact of the drop tower striker on the specimen surface. A high frequency load-line displacement transducer and signal conditioner is required for drop tower tests.

A14.5.4 *Force Transducers*—If remote force transducers are used, they shall meet the requirements of Practice E4. Requirements on the measured initial specimen stiffness and on
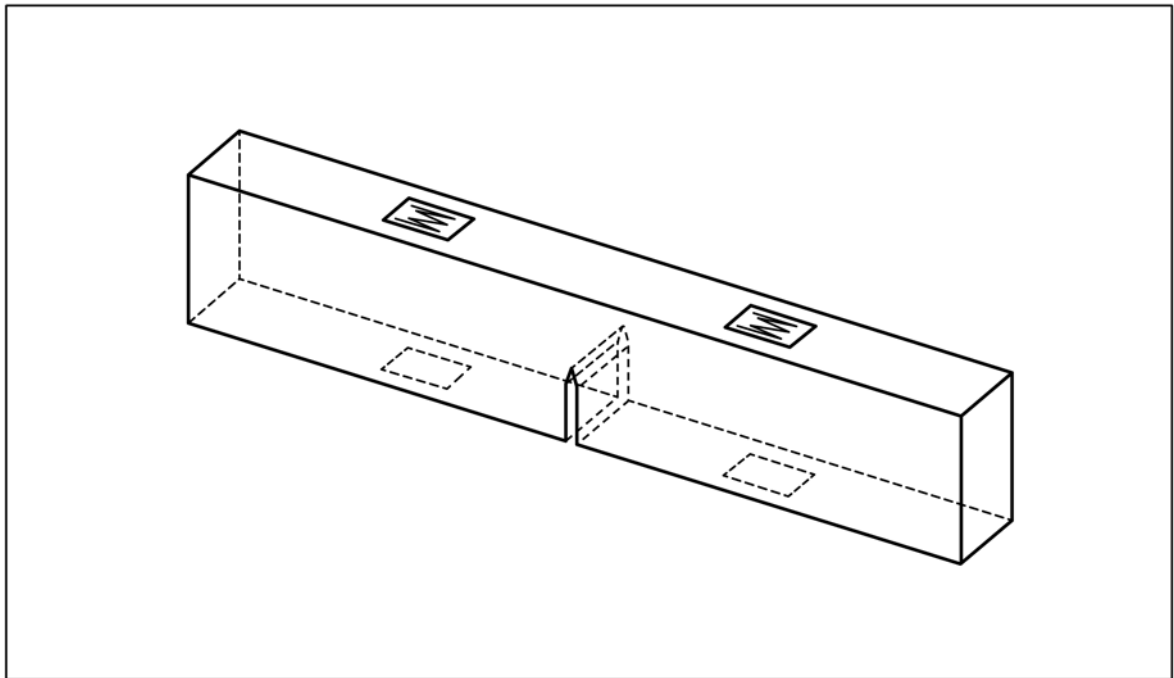
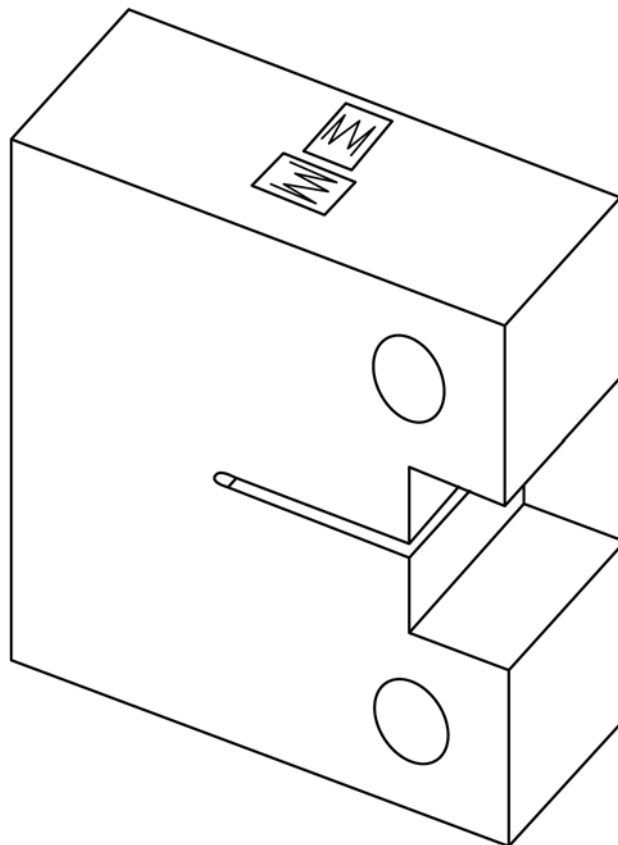FIG. A14.1 Strain Gages Mounted on SE(B) Specimen for Measurement of Transmitted Force

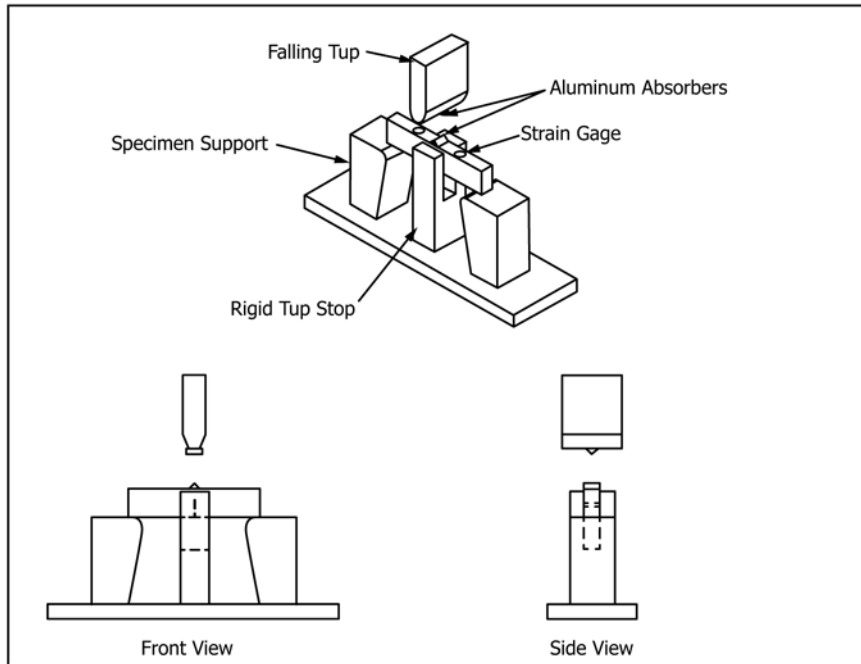FIG. A14.2 Strain Gages Mounted on C(T) Specimen for Measurement of Transmitted Force

35

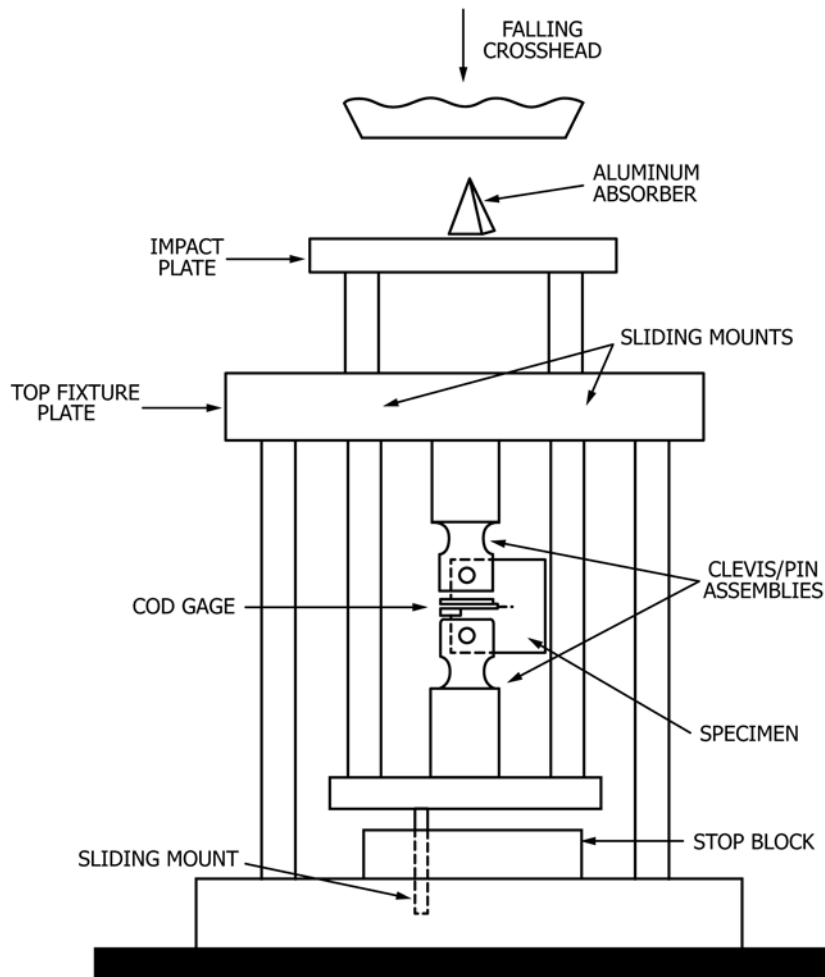**FIG. A14.3 Test Fixture for Drop Tower SE(B) Specimens**

FIG. A14.4 Test Fixtures for Drop Tower C(T) Specimens

the force and displacement signal smoothness are presented in A14.7.4. Static calibration of the on-specimen strain gage bridge should be done over a force range from 20 to 100 % of the final precracking force. At least five force calibration values shall be used, spaced evenly over this interval, and at least two repeat data sets are required. The applied force shall exceed ¼ of the calibrated range of the reference force cell used. The on-specimen, transmitted force measuring system shall be accurate to within 2 % of the final precracking force over the calibration range.

A14.5.5 *Displacement Transducers*—The transducer shall have response characteristics that allow it to follow the motion of the specimen while not introducing excessive mechanical noise into the measured displacement.

A14.5.5.1 Cantilever beam displacement gages such as those used in static fracture toughness testing may be suitable for rapid-load testing (see 6.2). The cantilever beam displacement gage described in Annex A1 of Test Method E399 has been used successfully at loading times (t_Q) slightly less than 1 ms.

A14.5.5.2 Gap measuring transducers that use either capacitance or optical means to measure displacement have also been used successfully in rapid-load testing (20). These transducers have the advantage that they can be rigidly attached to the specimen, and the vibration characteristics of the transducer generally do not affect the measured displacement. The disadvantages are that the output may be non-linear, and the signal conditioners used with these transducers are often the limiting component in frequency response of the displacement measurement system. Capacitive transducers have been designed to fit in the notch of the C(T) specimen as shown in Fig. A14.5. Fiber-optic transducers have been used to measure load-line displacement of SE(B) specimens. If the load-line displacement is measured relative to the test fixture, care must be taken to account for the effects of fixture compliance and brinnelling on the measured displacement, as discussed in 8.3.1.1.

A14.5.6 *Signal Conditioners*—The user is referred to Guide E1942 for a detailed discussion of requirements for data acquisitions systems. The signal conditioner must have sufficient bandwidth to capture the transducer signal without introducing distortion.

A14.5.6.1 Signal conditioners shall have a frequency bandwidth in excess of $10/t_Q$ for the force signal and $2/t_Q$ for the displacement signal(s). The more stringent requirement on the force signal is necessary to obtain an accurate measurement of the elastic component of the J integral near crack initiation. No "phase shifting" of transducer signals is allowed by this method. The bandwidth required to accurately capture a signal of that frequency will depend on the type of low-pass filter in the signal conditioner, and the tolerable error. If a low-pass filter is present in the measurement system it should not introduce more than 0.5 % measurement error, see Guide E1942.

A14.5.7 *Data Sampling*—The user is referred to Guide E1942 for a detailed discussion of requirements for data acquisitions systems. The rate at which an analog signal is sampled to create a digital signal shall be high enough to ensure that the peak value is accurately captured. The rate of data acquisition shall result in the time per data set being less than $t_Q/50$.

A14.6 Procedure

A14.6.1 Follow the procedure of Sections 7 and 8 to prepare and test specimens. The following items are additional steps necessary for high rate testing.
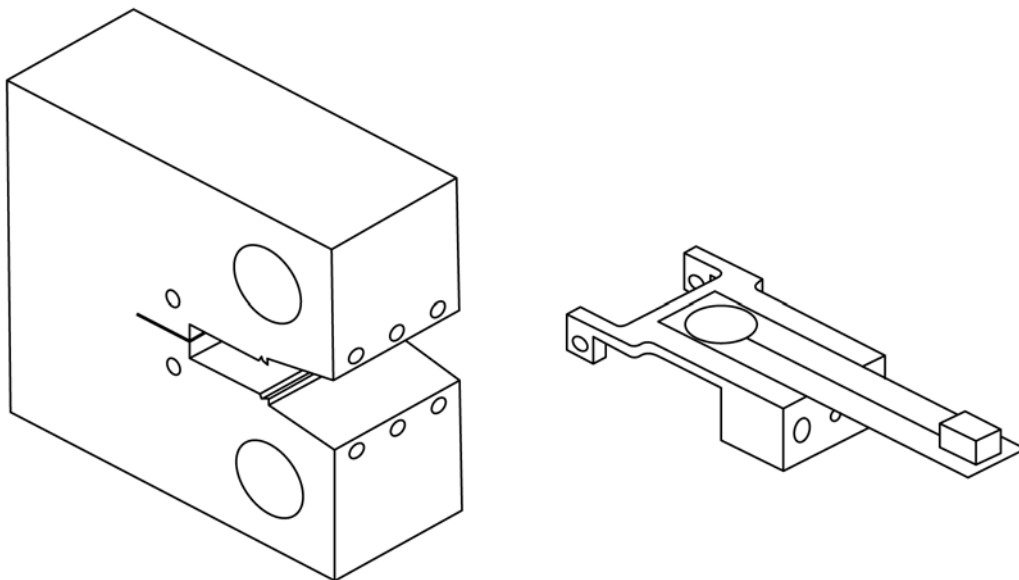

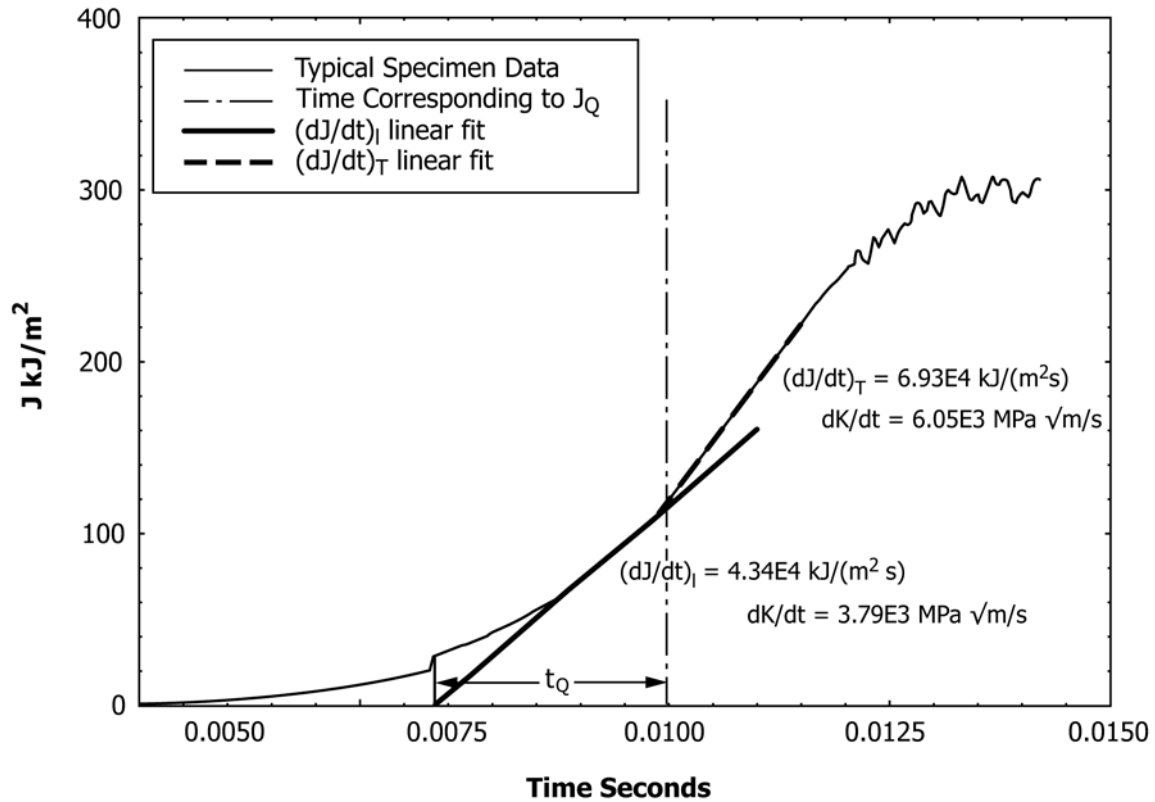FIG. A14.5 High Rate Capacitance COD gage and C(T) Specimen with Attachment Holes

FIG. A14.6 Evaluation of t_Q and the Test Rates $(dJ/dt)_I$ and $(dJ/dt)_T$

A14.6.2 Calculate t_w, the minimum test time from Eq A14.1. The loading rate is optional but the time to reach $J_Q(t)$ or $J_{Qc}(t)$ shall be not less than t_w.

A14.6.3 For each test, force and load-line displacement are required as functions of time. Additional crack opening displacement data, electric potential data, or both, can be acquired as well if desired.

A14.6.4 Install and align the specimen in the test fixtures, establish the test temperature, conduct the test at the desired test rate, collect and store the data required. Remove the test specimen from the fixture and mark the extent of the ductile crack growth according to 8.5.3, break the specimen open according to 8.5.4 to expose the fracture surface, and measure the initial crack size a_o, and the final crack size a_f according to 8.5.4.

A14.6.5 If the specimen is characterized by ductile upper shelf behavior, the normalization method of Annex A15 can be used to develop the J-R(t) curve for the test specimen. A multi-specimen method can also be used with J evaluated using the basic method relationships corrected for crack extension using Annex A16. Using Section 9, calculate J_Q (the tentative J_{Ic}) and the corresponding force P_Q and time t_Q. If a ductile instability occurs so that the final stable crack size a_f cannot be determined, the normalization method cannot be used to develop the J-R(t) curve or the corresponding J_Q for this test specimen.

A14.6.5.1 The dynamic yield strength and dynamic ultimate tensile strength at the relevant strain rate are required for the evaluation of J_Q. An approximate equivalent strain rate to be used for dynamic tensile testing shall be obtained from (21, 22)

$$\dot{\varepsilon} = \frac{2\sigma_{YS}}{t_Q E} \qquad (A14.2)$$

where σ_{YS} and E are values corresponding to quasistatic strain rates and evaluated at the temperature of the fracture toughness test and t_Q is the time to fracture from A14.6.

A14.6.5.2 If a pop-in is present, refer to Annex A4 to assess its significance. If the pop-in is significant, $J_c(t)$ or $J_u(t)$ values corresponding to the point of onset can be calculated using Annex A6. If fracture instability occurs without significant ductile crack extension, $J_c(t)$ or $J_u(t)$ values corresponding to the point of onset can be calculated as defined in Annex A6. If fracture instability follows significant ductile crack extension, the J-R(t) and $J_{Ic}(t)$ can be determined providing that a_f is distinguishable. The validity of the J-R(t) curve and $J_{Ic}(t)$ are subject to the requirements of Annex A8 and Annex A9, and Section 9.

A14.7 Qualification of the Data

A14.7.1 Test equipment, specimen geometries, specimen fixture alignment, and measured data must meet all requirements of Sections 6 – 9, except as specifically replaced in A14.5. Additional requirements specified here are necessary for high rate testing.

A14.7.2 All of the test equipment requirements of A14.5 shall be met.

38

A14.7.3 Plot the *J* integral versus the time as shown in Fig. A14.6. If fracture instability occurs, calculate *J* based on a_o using the basic analysis procedure and plot the data up to and including $J_{Qc}(t)$ or $J_{Qu}(t)$. Use a linear regression analysis to evaluate $(dJ/dt)_I$ as shown in the example of Fig. A14.5 using the data from $0.5J_Q(t)$ to $J_Q(t)$, from $0.5J_{Qc}(t)$ to $J_{Qc}(t)$, or from $0.5 J_{Qu}(t)$ to $J_{Qu}(t)$, as the case may be. Extrapolate this line to the abscissa to evaluate the quantity t_Q, as shown in Fig. A14.6.

A14.7.3.1 A second loading rate, $(dJ/dt)_T$, is defined as the slope of the *J* versus time data beyond maximum force, as shown in Fig. A14.6, over the range from J_Q to $J_Q + 0.5(J_{max} - J_Q)$ or the end of test, if fracture instability occurs.

A14.7.4 Plot force versus load-line displacement for the time interval $0 \leq t \leq t_Q$, as shown schematically in Fig. A14.7. Use a linear regression analysis to evaluate the initial specimen stiffness k_s using data over the range from 20 % to 50 % of the maximum force measured in the test. Plot this best fit line on the figure, and also plot two parallel lines of the same slope with the *y*-intercept offset by ± 10 % of P_{max} as shown in Fig. A14.7. Locate the final crossover Δ_{LL}^F.

A14.7.4.1 For this data set to be qualified according to this method, the compliance, $1/k_s$, shall agree with the predictions of Eq A2.11 for the C(T) specimen and Eq A1.11 for the SE(B) specimen within ± 10 %. Additionally, the measured force displacement data in the region between $0.3\Delta_{LL}^F$ and $0.8\Delta_{LL}^F$ should remain within the bounds of the parallel lines constructed on Fig. A14.7. If these requirements are not met, slack grips or impact absorbers must be added or modified or the test rate reduced to obtain a smoother data set that can be qualified according to this method.

A14.7.5 If $t_Q < t_w$, the test data are not qualified according to this method. A slower loading rate must be used, or the specimen geometry changed to decrease t_w for the test to be qualified according to this method.

A14.7.6 If the normalization method of Annex A15 is used to obtain J_{Ic}, the *J* resistance curve, or both, at least one confirmatory specimen must be tested at the same test rate and under the same test conditions. From the normalization method the load-line displacement corresponding to a ductile crack extension of 0.5 mm shall be estimated. The additional specimen shall then be loaded to this load-line displacement level, marked, broken open and the ductile crack growth measured. The measured crack extension shall be 0.5 ± 0.25 mm in order for these results to be qualified according to this method.

A14.8 Qualifying the High Rate Results

A14.8.1 All qualification requirements of 9.1, Annex A6, Annex A8, Annex A9, and A14.7 must be met to qualify the *J-R(t)* curve, $J_Q(t)$ as $J_{Ic}(t)$, or $J_{Qc}(t)$ as $J_c(t)$ according to this method. If the normalization method of Annex A15 is used, the additional requirements of this annex shall also be met.

A14.8.2 The maximum crack extension capacity for a specimen to qualify the *J-R(t)* curve is given by the following:

$$\Delta a_{max} = 0.15b_o \qquad (A14.3)$$

A14.9 Report

A14.9.1 The report shall include all the items of Section 10 as well as the following:

A14.9.1.1 The minimum test time, t_w, according to A14.6.2.

A14.9.1.2 The P_Q and t_Q, corresponding to the calculated $J_Q(t)$ or $J_{Qc}(t)$.

A14.9.1.3 The $(dJ/dt)_I$, $(dJ/dt)_T$ values, or both.

A14.9.1.4 If $J_{Ic}(t)$ is being reported, the final crack extension obtained on the confirmatory specimen of A14.7.6 shall be reported.
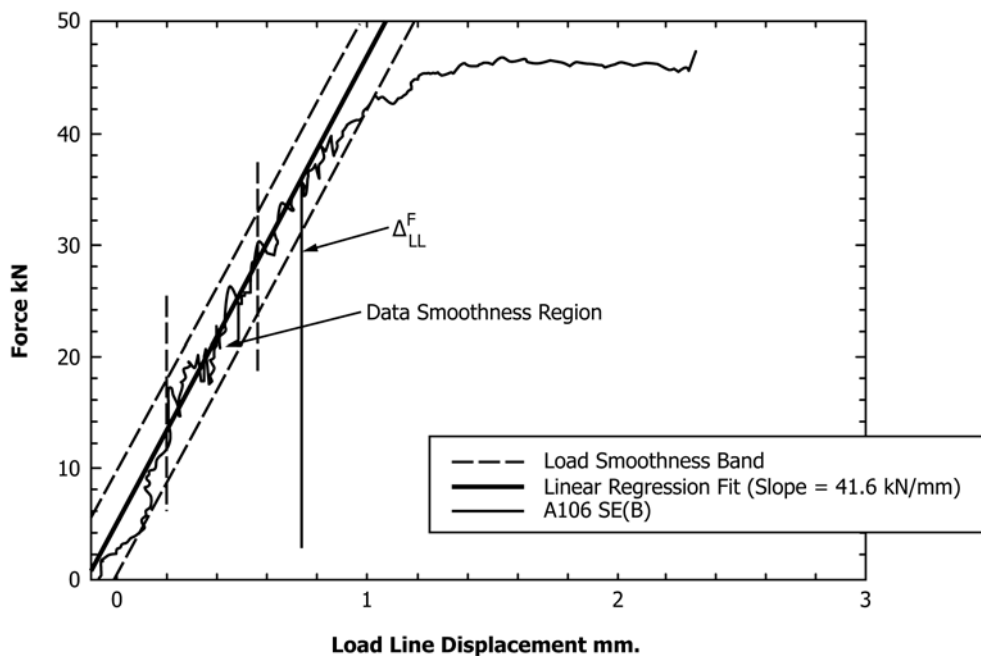

FIG. A14.7 Force Smoothness Verification Schematic

A14.10 Precision and Bias

A14.10.1 *Precision*—The precision of *J* versus crack growth is a function of material variability, the precision of the various measurements of linear dimensions of the specimen and testing fixtures, precision of the displacement measurement, precision of the force measurement, as well as the precision of the recording devices used to produce the force displacement record used to calculate *J* and crack size. For the test rates allowed by this annex, if the procedures outlined in this annex are followed, the force and load-line displacement can be measured with an precision comparable with that of the static loading as described in the main body. If the normaliza-

tion function method of Annex A15 is used, the crack size and crack extension information must be inferred from initial and final crack size measurements. The requirement for the additional specimen to be tested near to the point of crack initiation has been added to validate the $J_{Ic}(t)$ measurement. A round robin used to evaluate the overall test procedures of this method is reported in (23).

A14.10.2 *Bias*—There is no accepted "standard" value for measures of elastic-plastic fracture toughness of any material. In absence of such a true value, any statement concerning bias is not meaningful.

A15. NORMALIZATION DATA REDUCTION TECHNIQUE

A15.1 Scope

A15.1.1 The normalization technique can be used in some cases to obtain a *J-R* curve directly from a force displacement record taken together with initial and final crack size measurements taken from the specimen fracture surface. Additional restrictions are applied (see A15.3) which limit the applicability of this method. The normalization technique is described more fully in Herrera and Landes (24) and Landes, et al. (25), Lee (26), and Joyce (23). The normalization technique is most valuable for cases where high loading rates are used, or where high temperatures or aggressive environments are being used. In these, and other situations, unloading compliance methods are impractical. The normalization method can be used for statically loaded specimens if the requirements of this section are met. The normalization method is not applicable for low toughness materials tested in large specimen sizes where large amounts of crack extension can occur without measurable plastic force line displacement.

A15.1.2 *This international standard was developed in accordance with internationally recognized principles on standardization established in the Decision on Principles for the Development of International Standards, Guides and Recommendations issued by the World Trade Organization Technical Barriers to Trade (TBT) Committee.*

A15.2 Analysis

A15.2.1 The starting point for this analysis is a force versus load point displacement record like that shown in Fig. A15.1. Also required are initial and final physical crack sizes optically measured from the fracture surface. This procedure is applicable only to Test Method E1820 standard specimen geometries with $0.45 \le a_o/W \le 0.70$ and cannot be used if the final physical crack extension exceeds the lesser of 4 mm or 15 % of the initial uncracked ligament. Open source software that can be used to perform the analysis described in this annex is discussed in (27)

A15.2.2 Each force value P_i up to, but not including, the maximum force P_{max}, is normalized using:

$$P_{Ni} = \frac{P_i}{WB\left(\frac{W - a_{bi}}{W}\right)^{\eta_{pl}}} \tag{A15.1}$$

where a_{bi} is the blunting corrected crack size at the ith data point given by:

$$a_{bi} = a_o + \frac{J_i}{2\,\sigma_Y} \tag{A15.2}$$

with J_i calculated from:

$$J_i = \frac{K_i^2\,(1 - v^2)}{E} + J_{pli} \tag{A15.3}$$

where K_i and J_{pli} are calculated as in Annex A1 and Annex A2 for each specimen type using the crack size a_o.

A15.2.3 Each corresponding load-line displacement is normalized to give a normalized plastic displacement:

$$v'_{pli} = \frac{v_{pli}}{W} = \frac{v_i - P_i\,C_i}{W} \tag{A15.4}$$

where C_i is the specimen elastic load-line compliance based on the crack size a_{bi}, which can be calculated for each specimen type using the equations of Annex A1 and Annex A2.

A15.2.4 The final measured crack size shall correspond to a crack extension of not more than 4 mm or 15 % of the initial uncracked ligament, whichever is less. If this crack extension is exceeded, this specimen cannot be analyzed according to this annex.

A15.2.5 The final force displacement pair shall be normalized using the same equations as above except that the final measured crack size, a_f, is used. Typical normalized data are shown in Fig. A15.2.

A15.2.6 A line should be drawn from the final force displacement pair tangent to the remaining data as shown in Fig. A15.2. Data to the right of this tangent point shall be excluded from the normalization function fit. Data with $v_{pli}/W \le 0.001$ shall also be excluded from the normalization function fit.
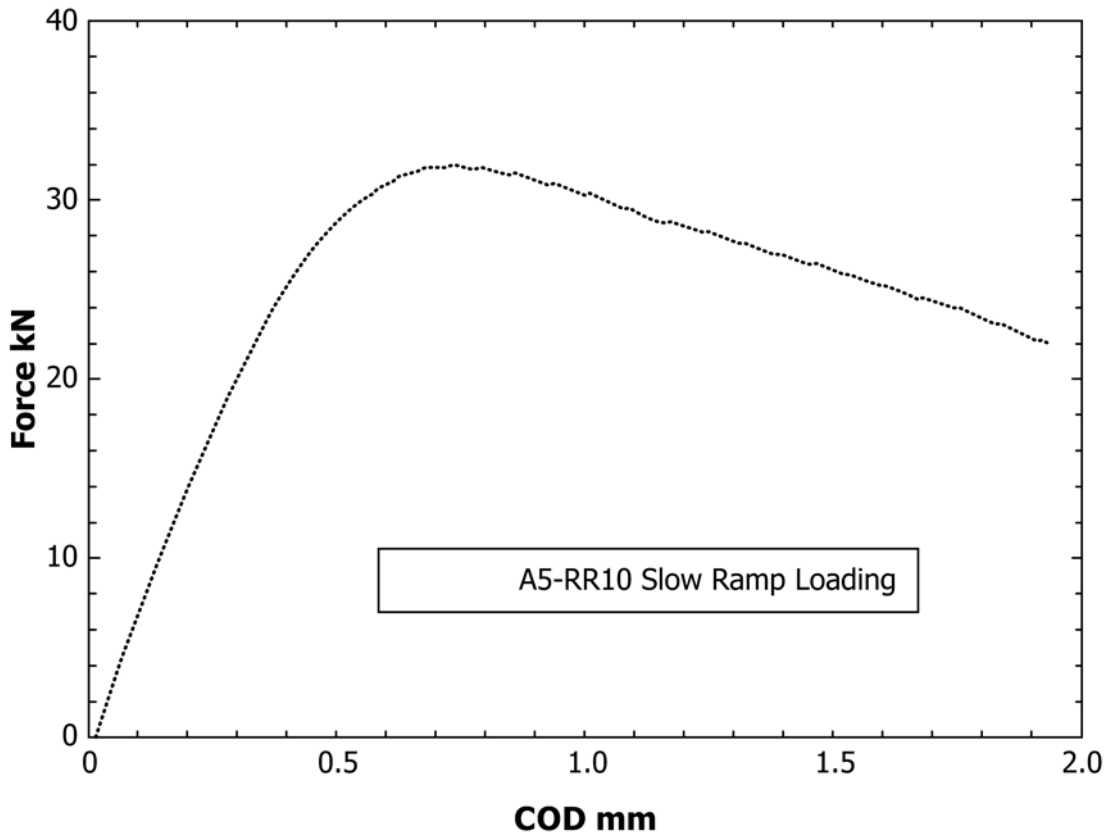
FIG. A15.1 Typical Force versus Displacement Curve

A15.2.7 If at least ten data pairs conform with A15.2.6, the data of Fig. A15.2 can be fit with the following required analytical normalization function:

$$P_N = \frac{a + b \, v'_{pl} + c \, v'^2_{pl}}{d + v'_{pl}} \qquad (A15.5)$$

where *a, b, c,* and *d* are fitting coefficients. This function can be fitted to the data of Fig. A15.1 using standard curve fitting packages available as part of computer spreadsheet programs or separately. An example fit for the data of Fig. A15.2 is shown in Fig. A15.3. The normalization function shall fit all the data pairs described above (including the final pair) with a maximum deviation less than 1 % of the P_N at the final point. Data should be evenly spaced between $v_{pli}/W = 0.001$ and the tangency point. If less than ten data pairs are available for this fit, including the final measured data pair, this method cannot be used.

A15.2.8 An iterative procedure is now used to force P_{Ni}, v_{pli}/W, a_i data to lie on Eq A15.5. This involves adjusting the crack size of each data set to get the normalized force and displacement pair defined in A15.2.2 and A15.2.3 to fall on the function defined in Eq A15.5. To do so, start at the first data point with $v_{pli}/W \geq 0.002$, normalize the force and displacement using the initial measured crack size a_o, and compare the normalized force with the result of the normalization function of A15.2.7. Adjust the crack size until the measured P_{Ni} and the functional value of P_N are within ±0.1 %. Each subsequent data set is treated similarly. If each step is started with the crack size resulting from the previous data set, only small, positive

adjustments of crack size are necessary, and the process of obtaining the crack sizes corresponding to each data set is relatively rapid.
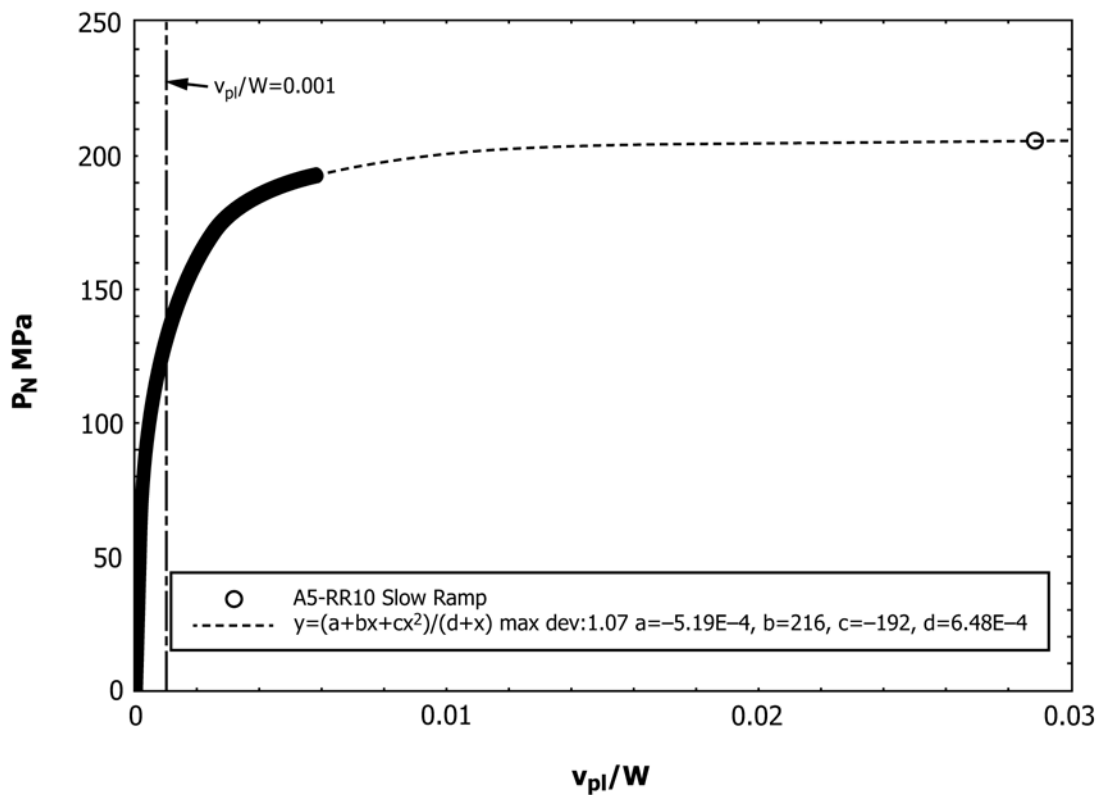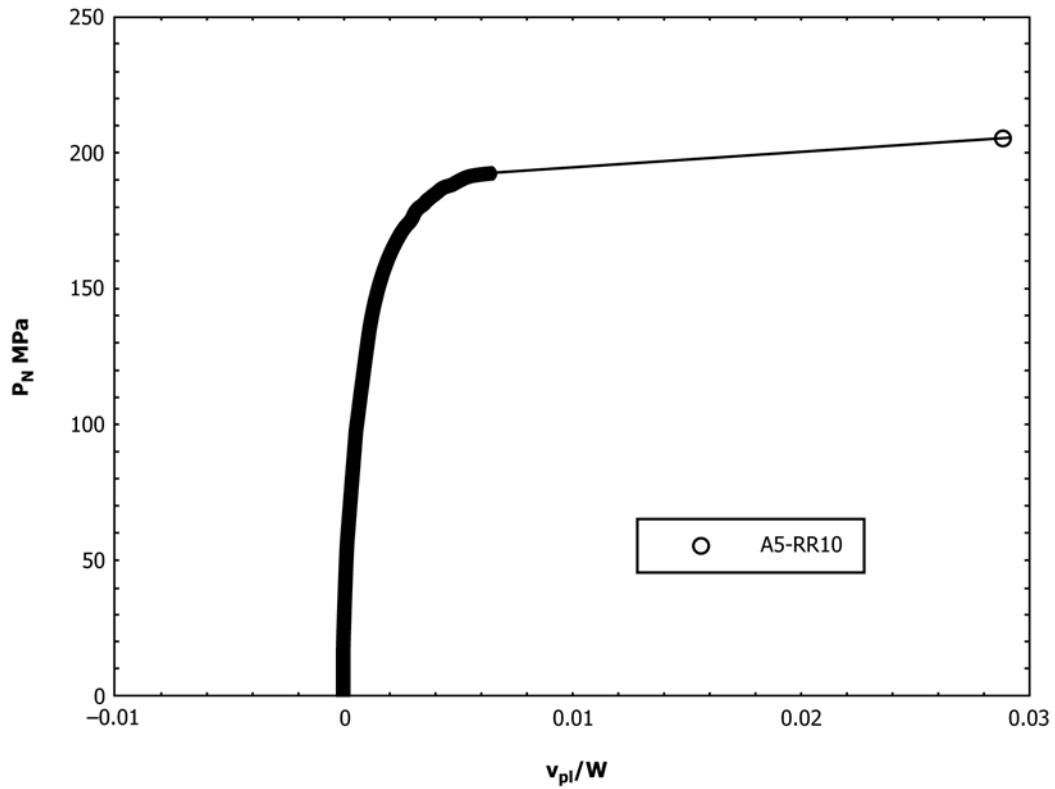
A15.2.8.1 The data of Fig. A15.1, normalized and adjusted to fit the normalization function of Fig. A15.3, is shown in Fig. A15.4.

A15.2.9 Since force, load-line displacement, and crack size estimates are now available at each data point, the standard equations of Annex A1 and Annex A2 are used to evaluate the *J* integral at each data point, resulting in a *J-R* curve as shown in Fig. A15.5. A J_{Ic} value can now be evaluated from this *J-R* curve using the method of Section Annex A9.

A15.3 Additional Requirements

A15.3.1 Requirements presented in 9.1, Annex A8, and Annex A9 shall be met to qualify a *J-R* curve or a J_{Ic} value obtained by the normalization method. Additional requirements specific to the use of the normalization method are presented below.

A15.3.2 If the normalization method is used to obtain J_{Ic}, at least one additional, confirmatory specimen shall be tested at the same test rate and under the same test conditions. From the normalization method the load-line displacement corresponding to a ductile crack extension of 0.5 mm shall be estimated. The additional specimen shall then be loaded to this load-line displacement level, marked, broken open and the ductile crack growth measured. The measured crack extension shall be 0.5 ±

FIG. A15.2 Normalized Force versus Displacement Curve Showing Points up to Maximum Force and the Final Data Point

FIG. A15.3 The Normalization Function Shown Fitted to the Normalization Data
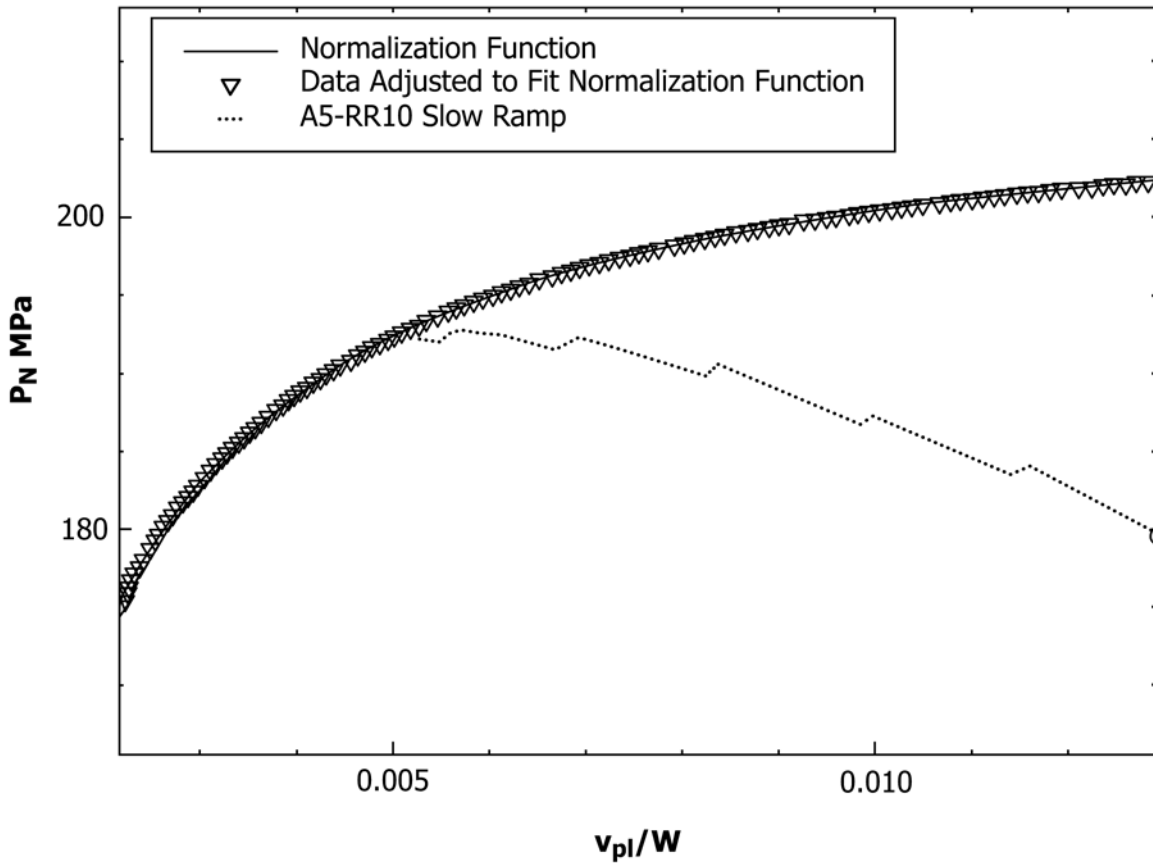
FIG. A15.4 Data is Adjusted, Defining the Crack Size Necessary to Place All Points on the Analytical Normalization Function
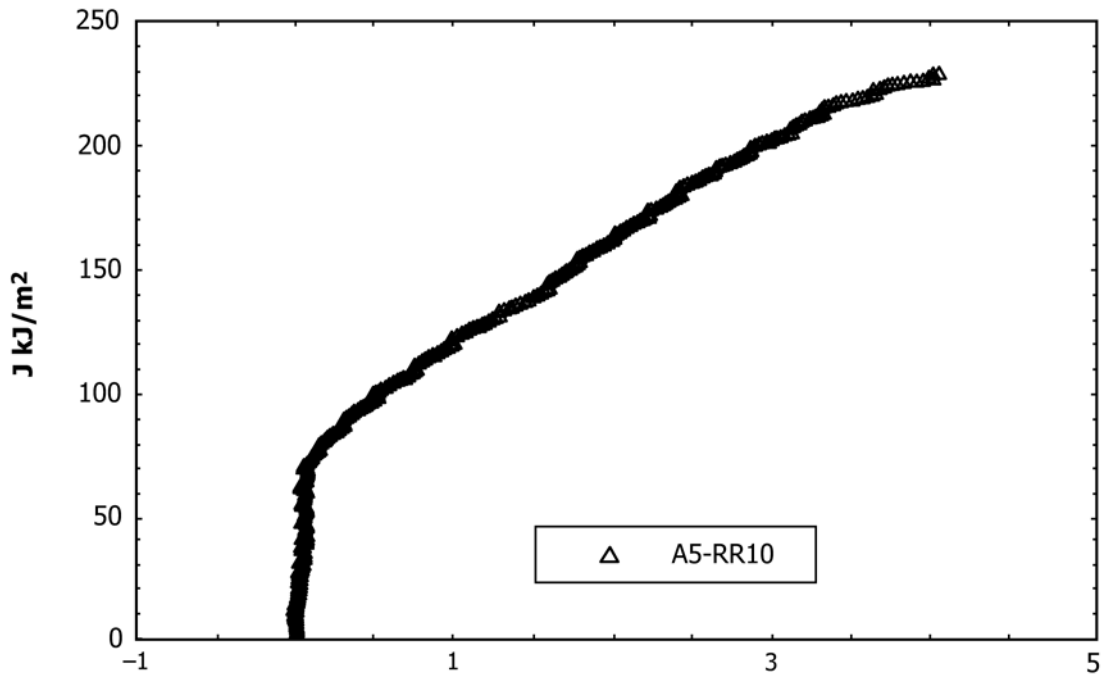(Only a portion of the data is shown for clarity)

FIG. A15.5 The Resulting *J-R* Curve for this Specimen

0.25 mm in order for these results, and hence the J_{Ic} value, to be qualified according to this method.

A15.4 Report

A15.4.1 Section 10 describes the reporting requirements for this method. If the normalization method is used, the following additional items shall be reported.

A15.4.2 If the normalization function is used the coefficients of the fit shall be reported as well as the maximum deviation of the fit and the number of data used.

A15.4.3 If J_{Ic} is reported, the accuracy of the confirmatory specimen of A15.3.2 shall be reported.

A15.5 Precision and Bias

A15.5.1 *Precision*—The precision of the *J* resistance curve is a function of material variability, the precision of the various measurements of linear dimensions of the specimen and testing fixtures, precision of the displacement measurement, precision of the force measurement, as well as the precision of the recording devices used to produce the force displacement record used to calculate *J* and crack size. For the test rates allowed by this annex, if the procedures outlined in this annex

are followed, the crack size throughout the fracture toughness test can be measured with a precision comparable with that of the unloading compliance procedure described in the main body. A round robin describing the use of the normalization procedure on rapidly loaded SE(B) and C(T) specimens is presented in (**23**). A requirement for the testing of a confirmatory specimen tested near the point of stable crack initiation is present to validate the J_{Ic} measurement.

A15.5.2 *Bias*—Crack sizes generally vary through the thickness of fracture toughness specimens. A nine point average procedure based on optical measurements obtained from the post-test fracture surface is generally used to give a reportable crack size. Different measurements would be obtained using more or less measurement points. Alternative crack sizes can be estimated using compliance methods, which obtain different average crack size estimates for irregular crack front shapes. Stringent crack front straightness requirements are present in this standard to minimize differences caused by these effects. The normalization method acts to interpolate between optically measured crack average lengths measured at the start and end of the stable resistance curve fracture toughness test. This method has been demonstrated in (**23**) to give results consistent with those obtained by unloading compliance procedures.

A16. EVALUATION OF CRACK GROWTH CORRECTED *J*-INTEGRAL VALUES

A16.1 This annex had been removed from the standard. Crack growth correction of *J*-integral values is addressed in Annex A1–Annex A3.

A17. FRACTURE TOUGHNESS TESTS AT IMPACT LOADING RATES USING PRECRACKED CHARPY-TYPE SPECIMENS

A17.1 Scope

A17.1.1 This Annex specifies requirements for performing and evaluating instrumented impact tests on precracked Charpy-type specimens using a fracture mechanics approach. Minimum requirements are given for measurement and recording equipment such that similar sensitivity and comparable measurements are achieved. Dynamic fracture mechanics properties determined are comparable to conventional large-scale fracture mechanics results when the validity criteria of Annex A8 – Annex A11 and Annex A14 are met. However, because of the small absolute size of the Charpy specimen, this is often not the case. Nevertheless, the values obtained can be used in research and development of materials, in quality control and service evaluation and to establish the relative variation of properties with test temperature and loading rate measured on precracked Charpy-type specimens.

A17.2 Principle

A17.2.1 This Annex prescribes impact bend tests which are performed on fatigue precracked Charpy-type specimens to obtain dynamic fracture mechanics properties of materials. This Annex extends the procedure for V-notch impact bend tests in accordance with Test Methods E23, and may be used for evaluation of the Master Curve in accordance with Test Method E1921. Instrumented testing machines are required in order to utilize this Annex, together with ancillary instrumentation and recording equipment in accordance with Test Method E2298. The characteristic fracture toughness parameters depend on material response reflected in the force/time diagrams described in Table A17.1 and Fig. A17.1. Note that only Type I diagrams can be linearly fit up to fracture.

NOTE A17.1—The symbol used in these Test Methods for force is *P*, while Test Method E2298 uses *F*. Therefore the parameters P_{max}, P_{bf}, P_{gy}

TABLE A17.1 Fracture Toughness Properties to be Determined

Material response/fracture behavior	Corresponding diagram type (See Fig. A17.1)	J-R curve	Characteristic Parameters
Linear-elastic	I	...	J_{cdX}, $K_{Jcd,X}$
Elastic-plastic, unstable fracture with $\Delta a < 0.2$ mm	II	...	$J_{cd,X}$ (B)
Elastic-plastic, unstable fracture with 0.2 mm $\leq \Delta a \leq 0.15$ ($W–a_o$)	II	...	$J_{ud,X}$ (B, Δa)
Elastic-plastic, unstable fracture with $\Delta a \geq 0.15$ ($W–a_o$)	III	J_d $-\Delta a$	$J_{Qd,X}$ or $J_{lcd,X}$
Elastic plastic; no unstable fracture	IV	J_d $-\Delta a$	$J_{Qd,X}$ or $J_{lcd,X}$

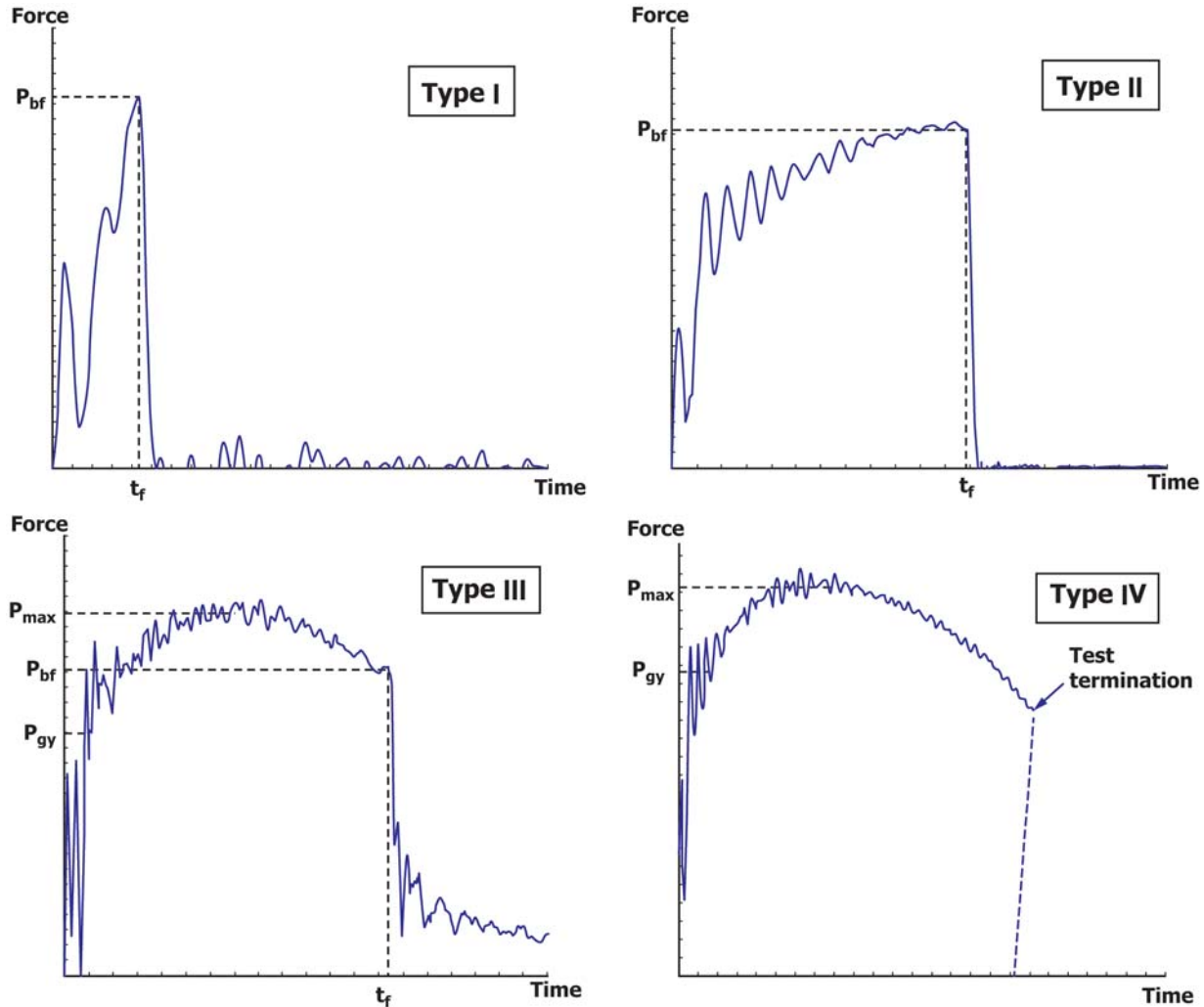**FIG. A17.1 Typical Force-time Diagrams (Schematic)**

used in the following sections correspond to the E2298 parameters F_m, F_{bf}, F_{gy}.

A17.3 Specimen Size, Configuration, and Preparation

A17.3.1 Specimens shall be prepared in accordance with the dimensions of the type A Charpy impact specimens of Test Methods E23, with or without the 2.0 mm V-notch, followed by fatigue precracking.

A17.3.2 Fatigue precracking shall be conducted in accordance with 7.4.

A17.3.3 Specimens are fatigue precracked to produce an initial crack size a_o in the range $0.45 < a_o/W < 0.70$.

A17.3.4 Side-grooving of the specimens in accordance with 7.5 is recommended.

A17.4 Apparatus

A17.4.1 The preferred testing apparatus is the instrumented Charpy pendulum impact testing machine according to Test Method E2298, modified to have a variable pendulum release position.

A17.4.2 Other pendulum machines may be used, with either fixed anvil/moving striker or fixed striker/moving anvil, and fixed or moving test specimen. The pendulum release position

for such machines is normally variable, and the striker or anvils are normally instrumented to provide force/time or force/displacement records.

A17.4.3 Falling weight testing machines, which may be spring assisted, are allowed. The striker is normally instrumented to provide force/time or force/time and force/displacement records.

A17.4.4 Other testing machines which comply with the calibration and other requirements of Test Method E2298 are not excluded.

A17.4.5 *Requirements on Absorbed Energy*—The reliability of instrumented force values on which these tests are based depends on the quality of the acquisition system and the calibration of the instrumented striker. The calibration of the striker shall be performed in accordance with Test Method E2298. Additionally, for each test in which the entire force signal has been recorded (that is, until the force returns to the baseline), one of the following requirements shall be met:

(a) the difference between KV and W_t shall be within ± 15 % of KV or ± 1 J, whichever is larger, or

(b) the difference between KV and W_t shall not exceed ± 25 % or ± 2 J, whichever is larger.

For every test that fulfills requirement (b), but not (a), force values may be adjusted using an iterative procedure until the equivalence $KV = W_t$ is achieved (28). If the difference between KV and W_t exceeds ± 25 % of KV or ± 2 J, whichever is larger, the test shall be discarded and the user shall check and if necessary repeat the instrumented striker calibration. If recording of the entire force signal for an individual test is not achieved (for example due to the specimen being ejected from the machine without being fully broken), the user shall demonstrate conformance of the testing system using at least five specimens of the same test series, for which the entire force signal has been recorded, that fulfil one of the above requirements. Otherwise, conformance shall be demonstrated by testing at least five additional non-precracked or precracked Charpy specimens, and showing that in all cases the difference between KV and W_t is within ± 15 % of KV or ± 1 J, whichever is larger. If this requirement is not met but the difference between KV and W_t does not exceed ± 25 % of KV or ± 2 J, the force adjustment described above shall be applied.

NOTE A17.2—From a theoretical point of view, KV is expected to be slightly higher than W_t, the difference being due to vibrational energy losses and other smaller contributions such as secondary impacts between striker and specimen. For more insight on the difference between KV and W_t, see reference (29).

A17.5 Test Procedures and Measurements

A17.5.1 Tests are performed in a manner similar to the standard Charpy impact test of Test Methods E23 and the instrumented impact test of Test Method E2298, especially with regard to the pendulum hammer and the handling of pre-cooled or pre-heated specimens.

A17.5.2 *Data recording*—The force/displacement diagram is recorded according to Test Method E2298, from which the key data values P_{max}, P_{bf}, W_m, and W_t are determined. In addition to the procedures of Test Method E2298, the following

procedures are provided concerning impact velocity, available energy and time to fracture. These data form the basis for evaluation of toughness parameters according to A17.6 – A17.9.

A17.5.2.1 *Impact velocity and available energy*—This standard applies to any impact velocity v_0, provided the time to fracture fulfills the requirements of A17.5.2.2. Impact velocities for pendulum or falling weight testing machines can be varied by adjusting the striker release height. The impact velocity v_0 for a pendulum machine can be determined as follows: set the pointer to the end-of-scale position as in a conventional Charpy test in accordance with Test Methods E23, release the pendulum from the appropriately reduced height, with no specimen in place. Read the energy KV_0 (in J) indicated by the pointer on the analogue scale. From this, the corresponding impact velocity is calculated as:

$$v_o = v_{os} \sqrt{\frac{MC - KV_0}{MC}} \qquad (A17.1)$$

where v_{os} is the maximum pendulum velocity corresponding to MC, the full pendulum capacity. A reduced velocity (1 to 2 m/s) can be advantageous, especially for brittle materials, since it reduces the effect of oscillations by lowering their relative amplitude and by increasing their number within the fracture time t_f (see A17.5.2.2).

A17.5.2.2 *Time to Fracture*—When the time t_f to initiate unstable fracture is less than the minimum test time t_w of A14.3.1.4, the instant of crack initiation is not detectable in the force signal with adequate accuracy because of oscillations (see Fig. A17.1, Type I), and fracture toughness cannot be evaluated using this test method.

A17.5.3 *Recording Apparatus*—Refer to Section 7 of Test Method E2298.

A17.5.4 *Execution of the Test*—Refer to Section 9 of Test Method E2298.

A17.5.5 *Evaluation of the Force-Displacement Curve*—Refer to Section 11 of Test Method E2298.

A17.5.6 *Calculation of fracture parameters*— The value of J-integral at unstable fracture, J_{cd} (force-time diagrams Type I and II in Fig. A17.1) or J_{ud} (force-time diagram of Type III in Fig. A17.1), or at test termination, J_d (force-time diagram of Type IV in Fig. A17.1) shall be calculated using the appropriate formulas Eq A1.4-A1.6 for the Basic Test Method. In particular, the specimen elastic compliance C_0 is required to evaluate the plastic component of the area under the force-displacement curve (Fig. A1.2). This can be obtained using the following theoretical expression:

$$C_{0,th} = C_S + C_M \qquad (A17.2)$$

where C_S is the specimen compliance calculated using Eq A1.11 and C_M is the impact machine compliance. This latter can be measured with unnotched specimens using one of the methods described in (30). Alternatively, if C_M is not available, C_0 can be estimated as the reciprocal of the initial elastic slope ($C_{0,exp}$), by fitting force-displacement data between the second oscillation (that is, discarding the first inertia peak) and the onset of general yielding. If both $C_{0,exp}$ and $C_{0,th}$ are available, $C_{0,th}$ shall be used and the difference between the two values shall be within ± 15 %. Values of

stress intensity factor shall be obtained from the corresponding J-integral values using:

$$K_{Jd} = \sqrt{\frac{EJ_d}{1 - v^2}} \qquad (A17.3)$$

Calculated K_{Jd} values at the onset of cleavage fracture, K_{Jcd}, can be used to calculate the reference temperature, T_0, in accordance with Test Method E1921, provided all relevant requirements are met.

A17.5.7 *Crack Size Measurements*—Original crack size and final physical crack size shall be measured in accordance with 8.5.

A17.5.8 *Multiple Specimen Tests*—To determine dynamic J-R curves by multi-specimen techniques, the fracture process is interrupted over a range of stable crack extension values, that are combined to obtain a single J-R curve. This procedure is described in A17.7.

A17.5.9 *Single Specimen Tests*—It is also possible to estimate dynamic J-R curves from an individual specimen using the Normalization Data Reduction technique, as described in A17.8.

A17.6 Analysis of Results

A17.6.1 *Fracture Behavior*—The adequacy of fracture toughness parameters depends on the fracture behavior of the test specimen as reflected in the force-displacement diagrams described in Table A17.1. Therefore the measured force displacement or force-time diagram shall be assigned to one of the diagram types shown in Fig. A17.1, using the indications provided in Table A17.1.

A17.6.2 *Unstable Fracture*—In the case of unstable fracture as in Fig. A17.1 (Types I or II), the applicable evaluation method depends on the oscillations superimposed on the force signal. If time to fracture is more than the minimum test time of A14.3.1.4, fracture toughness shall be evaluated according to the quasi-static approach of Annex A6 and Annex A7. Impact velocity may be reduced in order for the time to fracture to fulfil the requirements of A14.3.1.4 and A17.5.2.

A17.6.3 *Stable Crack Extension*—In the case of stable crack extension as in Fig. A17.1 (Types III or IV), either multi specimen or single-specimen techniques described in A17.7 and A17.8, respectively, are to be used to determine the J R curve. The determination of characteristic fracture toughness values from dynamic J-R curves is described in A17.9.

A17.6.4 *Loading Rate*— As indicated in Table A17.1, fracture toughness values shall be stated with the corresponding loading rate added in parentheses. The latter may be estimated as follows:
Type I:

$$\dot{K} = \frac{K_{Jcd}}{t_f} \qquad (A17.4)$$

Types I and II:

$$\dot{j} = \frac{J_{cd}}{t_f} \qquad (A17.5)$$

or

$$\dot{j} = \frac{J_{ud}}{t_f}$$

Types III and IV:

$$\dot{j} = \frac{P_{max} \cdot v_o}{B_N \cdot (W - a_o)} \cdot \eta_{pl}\left(\frac{a_o}{W}\right) \qquad (A17.6)$$

In alternative to Eq A17.6, the procedures given in A14.7.3 and A14.7.3.1 can also be used for calculating $(dJ/dt)_I$ and $(dJ/dt)_T$ respectively. For practical purposes, the loading rate shall be indicated using its order of magnitude (for example, the stress intensity factor corresponding to a loading rate of 4×10^5 MPa√m/s shall be indicated as K_{Jcd5}).

A17.6.5 *Dynamic Tensile Properties*— The dynamic yield and ultimate tensile stresses at the relevant strain rate may be required for certain evaluation procedures and validity checks. An approximate equivalent strain rate for the fracture mechanics test, which can be used for dynamic tensile testing, may be calculated from (**21, 22**):

$$\dot{\varepsilon} = 2 \frac{\sigma_{YS}}{\bar{t} \cdot E} \qquad (A17.7)$$

where: σ_{YS} and E are values corresponding to quasistatic strain rates (that is, conforming to the requirements of Test Methods E8/E8M) and evaluated at the temperature of the fracture mechanics test; $\bar{t}$ is the time to fracture in the case of small scale yielding (Type I in Fig. A17.1), or the time interval of the initial linear part of the force-time record in the case of distinct elastic-plastic material behavior (Types II-IV in Fig. A17.1). Eq A17.7 provides a general estimate of strain rate values associated with fracture in the test specimen.

A17.7 Determination of J-R curves at Impact Loading Rates by Multiple Specimen Methods

A17.7.1 The following methods make it possible to determine fracture toughness parameters in those cases where stable crack extension occurs, Fig. A17.1 (Types III and IV). The multi-specimen procedure involves loading a series of nominally identical specimens to selected displacement levels, resulting in corresponding amounts of stable crack extension. Each specimen tested provides one point on the resistance curve. The requirements and procedures of Annex A8-Annex A11 concerning number and spacing of data points shall be fulfilled.

A17.7.2 *Low-blow Test*—This test procedure is intended to limit the impact energy W_0 of the pendulum hammer or drop weight so that it is sufficient to produce a certain stable crack extension, but not sufficient to fully break the specimen. By selecting different energy levels in a series of tests on nominally identical specimens, a series of different crack extensions Δa_i are produced. From the corresponding J-values, J-Δa curves are constructed.

NOTE A17.3—An alternative method is the Stop Block approach, whereby the hammer swing is arrested by using stop blocks, thus avoiding complete fracture of the specimen.

A17.7.2.1 The following procedure is recommended:
(1) Prepare 7 – 10 specimens to nominally the same initial crack length a_0.
(2) Perform a full blow instrumented impact bending test on one of the specimens. Evaluate the energy at maximum

47

Eqr{tki j v'd{ ''CUVO ''Kpvt"cmt'tki j vu''tgugtxgf +'Hhk"Lcp''4: '37:4: '25'T O V'4244
Fqy ptqcf gf Irtlkpvgf''d{
Rtlkpegvqp''Wplkxgtuku{ ''Rtlkpegvqp''Wplkxgtuku{ +'r wtuwcpv'q'Nkegpug'Ci tggo gpv0P q''hwtvj gt'tgrtqf wevkqpu'cwj qtk|gf0

force and the total fracture energy, W_m and W_t, in accordance with Test Method E2298.

(3) Determine the energy spacing as $\Delta W_0 = 2W_m/N$, where N is the number of available specimens.

(4) Perform an impact test by setting the release position of the pendulum hammer, or the height of the drop weight, such that $W_0 = 2W_m/N$. Avoid a second impact between the striker and the test specimen.

(5) Repeat the test on the remaining specimens, increasing the impact energy W_0 by the amount $\Delta W_0 = 2W_m/N$ at each test.

(6) In order to mark the crack extension, post-test fatigue cycling or heat tinting may be used.

(7) Break all specimens open after testing. Care is to be taken to minimize post-test specimen deformation. Cooling ferritic steels may help to ensure brittle behavior during specimen opening.

(8) Measure a_0 and $\Delta a_p = \Delta a_i$ (where "i" is the test index, with $1 \leq i \leq N\text{-}1$) in accordance with 8.5.

(9) Calculate J_i according to A1.4.2.1.

(10) Plot the resulting N-1 pairs of values ($J_i, \Delta a_i$) in a J-Δa diagram and determine the J-R curve according to Annex A8 and $J_{Qd,X}$ (a provisional value of $J_{Icd,X}$) according to Annex A9.

A17.7.2.2 The differences in impact velocity and loading rate between the various tests are small enough to have a negligible influence on the results and can be ignored, provided velocity and loading rate do not vary by more than a factor 3 between the minimum and maximum values.

A17.7.3 *Cleavage J-R curve Method*—This test method can only be used for steels that exhibit a brittle-ductile transition. The test temperature is varied within the ductile-to-brittle transition zone so that stable crack extensions of varying lengths Δa_p are obtained from tests terminated by cleavage fracture. J_{ud} values calculated according to A1.4.2 and the corresponding Δa_p represent points on the cleavage J-Δa curve which can be analyzed in accordance with Annex A8 and Annex A9. Differences between the temperatures of the various resistance points can be neglected, provided they don't exceed 50°C. The requirements of Annex A8 and Annex A9 shall be satisfied in order to obtain a valid J-R curve. Details of this method are given in (31).

A17.7.4 The user is warned that results obtained using the Low-blow or Stop Block methods, in which the loading rate is progressively reduced down to zero, may differ from results obtained using tests leading to specimen fracture, such as the Cleavage J-R curve method.

A17.8 J-R Curve Determination by Single Specimen Methods

A17.8.1 The Normalization Data Reduction (NDR) technique can be applied to a Low-blow test performed in accordance with A17.7.1, provided the measured crack extension does not exceed 15 % of the initial uncracked ligament. The provisions of Annex A15 apply, including the additional requirements of A15.3. A study published in (32) shows that for two steels and two test temperatures, NDR single-specimen results are in good agreement with multiple specimen data generated using the Low-blow technique.

A17.9 Determination of Fracture Toughness Near the Onset of Stable Crack Extension

A17.9.1 From J-R curves determined according to A17.7 or A17.8, fracture toughness values near the onset of stable crack extension can be determined in conformance to Annex A9. Specimen qualification in accordance with Annex A9 requirements will be difficult to achieve if the specimen undergoes significant plasticity during crack extension because of the relatively small size of the specimen. In this case, values of J_{Qd} cannot be regarded as material properties independent of specimen size and their use in safety assessments may result in non conservative results. Nevertheless, these values can be used for research and development of materials, in quality control and service evaluation and to establish the variation of properties with test temperature.

A17.9.2 The construction line for J_Q calculation shall have the following expression, see also Eq A9.4:

$$J = 2\sigma_{Yd}\Delta a \;, \qquad (A17.8)$$

where σ_{Yd}, the dynamic effective yield strength, is calculated using the following relationship (33):

$$\sigma_{Yd} = \frac{2.58 P_Y W}{B(W - a_0)^2} \;, \qquad (A17.9)$$

where P_Y is the average between the force at general yield, P_{gy}, and the maximum force P_{max}, determined from the force/displacement diagram in accordance with Test Method E2298.

Note A17.4—For side-grooved specimens, $B = B_N$.

A17.10 Report

A17.10.1 In addition to the information listed in Section 10 of the main body, the test report shall include the following.

A17.10.2 Identification and type of testing apparatus.

A17.10.3 Striker impact velocity v_o (A17.5.3).

A17.10.4 Nominal energy of the striker at velocity v_o.

A17.10.5 Absorbed energy KV according to Test Method E2298.

A17.10.6 Calibration of the instrumented striker.

A17.10.7 Details of force adjustment in accordance with A17.4.5, if applicable.

A17.10.8 Specimen elastic compliance (theoretical or experimental, or both) and, if available, machine compliance.

A17.10.9 Time to fracture or time at test termination, as appropriate.

A17.10.10 Fracture parameters determined as:

(1) value of K_{Jcd} obtained, if applicable,

(2) value of $\dot{K}$ obtained, if applicable (only order of magnitude),

(3) value of J obtained, if applicable,

(4) value of $\dot{J}$ obtained, if applicable (only order of magnitude),

(5) type of force-time diagram, with reference to Fig. A17.1, Types I – IV,

(6) for diagrams of Types III or IV, final crack extension, and

(7) a copy of the test record.

A17.10.11 In case of *J*-R curve determination, values of J and Δa in tabular form and values of $J_{Qd,X}$ or $J_{Icd,X}$ obtained.

A17.10.12 Dynamic tensile properties used, if applicable.

A18. GUIDELINES FOR THE USE OF DIRECT CURRENT ELECTRIC POTENTIAL DIFFERENCE METHODS FOR THE DETERMINATION OF CRACK SIZE

A18.1 Applications

A18.1.1 Electric Potential Difference (EPD) procedures for crack size determination are applicable to metallic materials in a wide range of testing environments. The Direct Current EPD (DCEPD) single-specimen technique relies on simple calibration functions for standard specimen geometries, and can yield a higher density of data points to define a *J-R* curve than typically achievable using elastic compliance procedures. Specimen geometries for fracture toughness testing explicitly covered in this annex are the compact, C(T), specimen and the single-edge bend, SE(B), specimen.

A18.2 Principles

A18.2.1 Inferring crack extension from electric potential difference measurements relies on the principle that the electric field in a cracked specimen with a current flowing through it is a function of specimen geometry, and in particular of the crack size. For a constant current flow, the electric potential difference across the crack plane will increase with increasing crack size due to modification of the electric field and associated perturbation of the current streamlines. The change in DCEPD can be related to crack size through a suitable calibration relationship. DCEPD may be used for both specimen preparation (fatigue precracking) and testing (crack initiation and stable crack propagation).

A18.3 Basic Methods

A18.3.1 Both direct current (DC) and alternating current (AC) techniques have been used to measure crack size in laboratory specimens. However, this annex only addresses DC techniques since these are more commonly used than AC methods.

A18.3.2 In the DC method, a constant current is passed through the specimen resulting in a potential difference across the crack plane. The plasticity associated with elastic-plastic fracture of ductile materials can increase the measured electric potential due to a combination of material resistivity and geometric changes that are unrelated to crack extension. These changes shall be properly accounted for in order to determine crack extension in ductile materials.

A18.3.3 Changes in the specimen or instrumentation may also result in proportional changes in the measured voltage. For example, a 1 °C change in specimen temperature can result in a noticeable change in the DCEPD signal due to the change in the material's electric resistivity. Also, some materials exhibit time-dependent resistivity changes while at elevated temperatures **(34)**. Moreover, system-level drift occurs when the

response of system components such as amplifiers, relays, data-acquisition devices, or power supplies change over time. These phenomena can all produce apparent crack size changes that introduce errors between the predicted and actual crack size. One way to compensate for these effects is to normalize DCEPD measurements using additional voltage measurements taken at a reference location. The reference location may be either on the test specimen or on an additional specimen of the same material in the same environment, and powered by the same electric current source as the test specimen. If the reference measurements are taken on an additional specimen, this specimen may be fatigue precracked or blunt-notched. If the reference measurements are taken directly on the test specimen, the location must be chosen so that the reference voltage is not affected by crack propagation and plastic deformation. Since all material and instrument variations are also included in the reference measurements, this normalization process will eliminate them. The reference voltage should be of the same order of magnitude as the primary DCEPD measurements to avoid introducing excessive noise in the measurement signal.

Note A18.1—The effects of material and instrument variation are often not as critical to toughness testing as to tests which require a longer duration, such as fatigue crack growth rate tests.

A18.3.4 The DCEPD method can be applied using equipment found in most testing laboratories, as shown in Fig. A18.1. A computerized system for control and acquisition is strongly recommended. High-gain, low-noise amplification (typically 30 to 40 dB power gain) may be used to increase the measured EPD data (typically on the order of 100 µV or less at the specimen) up to voltage levels that are readily recorded with digital data acquisition instrumentation. Since the test loading rate must take into account both the response time of the measurement system and the voltage resolution, the provisions of this annex only apply to quasi-static tests in accordance with 8.4.2.

A18.3.5 The DCEPD method is susceptible to thermoelectric effects **(35)** which produce potentials in addition to those due to the sample electric field. These can be a substantial fraction of the total measured voltage. Since the thermoelectric effects are present even without the input current, it is possible to account for them by subtracting voltage measurements taken with the current off from the measurements made with the current on. An alternative method (Reversing DCEPD, or RDCEPD) corrects for the thermoelectric effects by taking voltage measurements while reversing the direction of current flow. Positive measurements of DCEPD are taken, followed by
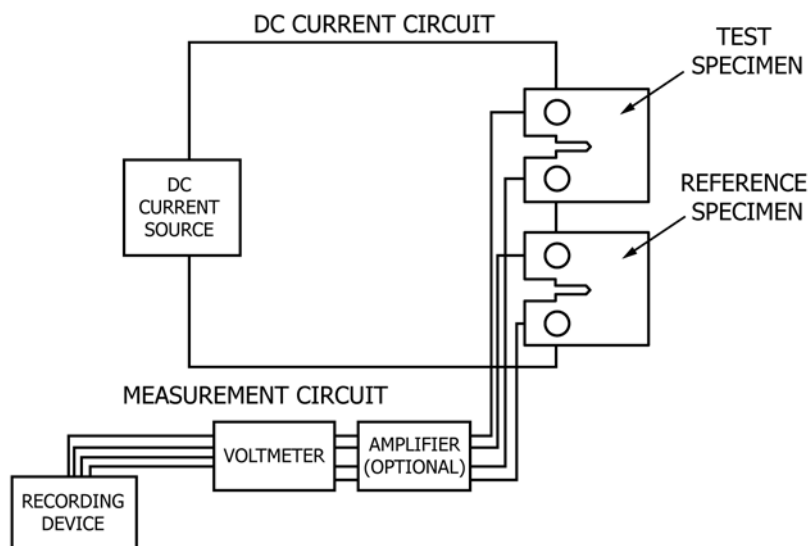
49

FIG. A18.1 Schematic Diagram of a DCEPD System with Reference Specimen

reversing the current flow direction and then taking negative DCEPD measurements. The corrected DCEPD signal is given by one-half of the difference between positive and negative potential readings. This procedure is repeated for each measurement (**36, 37**).

NOTE A18.2—When using the RDCEPD method, appropriate consideration should be given to specific features, such as settling time after current reversal and averaging of multiple voltage readings. The specific conditions to be chosen should account for the characteristic of the equipment used, see also refs. (**36, 37**).

A18.4 Current Generating Equipment

A18.4.1 Any suitable constant current supply may be used which has sufficient short- and long-term stability. The current shall be stable to one part in 10^3. For optimum conditions, the relative stability of the power supply should be equal to the effective resolution of the voltage measurement system; that is, if the voltage measurement system can effectively resolve one part in 10^3 of the output voltage from the specimen (including electric noise, inherent inaccuracies such as nonlinearity, and so forth), then the power supply should be stable to one part in 10^3.

A18.5 Voltage Measurement Equipment

A18.5.1 Voltage measurements shall be made with any equipment that has sufficient resolution, accuracy, and stability characteristics. The DCEPD method requires equipment capable of measuring small changes in DC voltage (for example, 0.05 µV to 0.5 µV) with relatively low DC signal to AC RMS noise ratios. Although there are a variety of ways to implement the voltage measurement system, three commonly used systems are: amplifier/autographic recorder, amplifier/microcomputer analog-to-digital converter, and digital voltmeter/microcomputer. The use of analog or digital filtering, or both to reduce measurement noise is recommended.

A18.5.2 Autographic recorders are commonly available with suitable sensitivity and can be used to record the output voltage directly from the specimen. A preamplifier can be used

to boost the direct voltage output from the specimen before recording. Another common technique uses a preamplifier to boost the direct output from the specimen to a level that can be digitized using a conventional analog-to-digital (A/D) converter and microcomputer. A third method makes use of a digital voltmeter with a digital output capability. The advantage of this type of system is that all the sensitive analog circuits are contained within a single instrument.

A18.6 Gripping Considerations

A18.6.1 The DCEPD method for crack size determination relies on a current of constant magnitude passing through the specimen when the voltage is measured. During such potential measurements, it is essential that no portion of the applied current be shunted in a parallel circuit through the test machine. Shunting of current through the test machine, the test fixtures or the clip gage will cause under-prediction in the crack size measurements. If current shunting is suspected, it is recommended that the specimen be electrically insulated from the test fixture. Leaving one contact point between the specimen and the test machine may be required to interrupt current shunting while maintaining a ground connection to the specimen, in order to avoid a floating ground.

NOTE A18.3—One common practice to ensure that there are no current shunting paths through the test cell is to measure the voltage across the crack before and after the specimen is mounted in the fixture. The two measurements will be equal if there are no appreciable current paths other than through the test specimen. Alternative current paths are more likely while force is applied to the test specimen as this can improve the electric contact between the specimen and the test frame.

NOTE A18.4—To electrically insulate the specimen from the test fixture, a thin layer of insulating tape (such as ultra-high molecular weight plastic) may be placed at the specimen contact points. This tape strain hardens, and after an initial loading, has only a small effect on system compliance and may be reused several times before replacement.

A18.7 Wire Selection and Attachment

A18.7.1 Careful selection and attachment of current input and voltage measurement wires can avoid many problems

associated with the electric potential difference method. This is particularly important in aggressive test environments such as elevated temperature where the strength, melting point, and oxidation resistance of the wires must be taken into account.

A18.7.2 Depending on the specimen size and configuration, the voltage measurement wires and other optional measurement transducers can be mounted either before or after placing the specimen in the test machine. This is mostly a matter of operator convenience (see Note A18.3).

A18.7.3 *Current Input Wires*—Selection of the current input wires shall be based on current carrying ability, and ease of attachment (weldability, connector compatibility). Wires shall be of sufficient gage to carry the required current under the test conditions and may be mechanically fastened or welded to the specimen. Symmetric locations relative to the crack plane and crack centerline are required.

A18.7.4 *Voltage Measurement Wires*—Voltage wires shall be as fine as possible to allow precise location on the specimen and minimize stress on the wire during testing which could cause detachment. For readily weldable materials, attaching probe wires using resistance spot welding works well. This attachment method allows the leads to be accurately located, uses little specimen space, and is relatively durable. For materials of low weldability (for example, certain aluminum alloys), lead wires may be fastened using mechanical fasteners provided that the size of the fastener is accounted for when determining the location of voltage sensing leads. Voltage sensing wires shall be located diagonally across the starter notch or crack tip in order to average measurements of non-uniform crack fronts. The probe wires are typically of very small diameter (for example, 30 gauge or 0.25 mm diameter)

so a terminal strip near the specimen for transition from the probe wires to a more permanent connection into the data acquisition system is recommended. Calibration relationships used to relate DCEPD measurements and crack size can be sensitive to the location of voltage wires on the test specimen. For a 25-mm thick C(T) specimen, attachment within ±0.5 mm of the locations for which the calibration relationship was developed will provide adequate accuracy in crack size measurement.

A18.7.4.1 When testing C(T) specimens of materials with a high toughness-to-strength ratio, such as austenitic stainless steels, large plastic strain can occur in the small section of material between the pin hole and the notch, which can introduce significant apparent crack extension measurements. To mitigate this, it is recommended to attach the voltage wires as shown in Fig. A18.2 (**38**).

A18.8 Resolution of Electric Potential Systems

A18.8.1 The effective resolution of DCEPD measurements depends on a number of factors including voltmeter resolution, amplifier gain, current magnitude, specimen geometry, voltage measurement and current input wire locations, and electric resistivity of the specimen material. Herein, effective resolution is defined as the smallest change in crack size which can be distinguished in actual test operation, not simply the best resolution of the recording equipment. For common laboratory specimens, a direct current in the range of 5 A to 50 A and voltage resolution of about ±0.1 µV or ±0.1 % of the initial voltage will yield a resolution in crack size better than 0.1 % of the specimen width. For highly conductive materials (that is, aluminum, copper) or lower current levels, or both, the resolution would decrease, while for materials with a higher
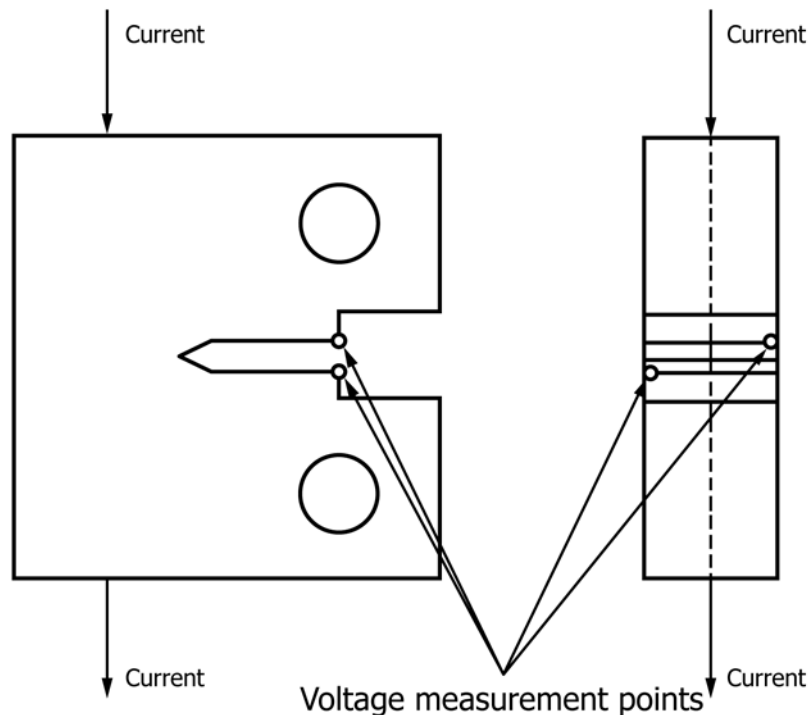

FIG. A18.2 Recommended voltage wire locations for materials with high toughness-to-strength ratio

resistivity (that is, titanium, nickel) resolutions better than 0.01 % of the specimen width have been achieved.

NOTE A18.5—The following is an example of the magnitude of voltages as measured at 20 °C on a non-standard C(T) specimen (thickness B = 7.7 mm, width W = 50 mm, a/W = 0.22) for a direct current of 10 A (**39**):

Material	Approximate DCEPD Measured at 10 A	Approximate Change in Crack Size for 1 µV Change in DCEPD
Aluminum	0.1 mV	300 µm
Steel	0.6 mV	50 µm
Titanium	3.5 mV	9 µm

A18.9 Techniques to Reduce Voltage Measurement Scatter

A18.9.1 Because of the low level of voltages which must be measured with the DCEPD method, a number of procedures should be followed to improve voltage measurement precision.

A18.9.2 *Induced EMF*—Voltage measurement lead wires should be as short as possible and should be twisted together to reduce stray voltages induced by changing magnetic fields. Holding them rigid also helps reduce the stray voltages which can be generated by moving the wires through any static magnetic fields that may exist near the test frame. In addition, routing the voltage measurement leads away from the motors, transformers, or other devices which produce strong magnetic fields is recommended.

A18.9.3 *Electric Grounding*—In order to mitigate the introduction of ground-loops, all devices used in the electric potential difference system, including test controllers, data-acquisition devices, power supplies, amplifiers, and relays, etc., shall be placed at a common electric ground.

A18.9.4 *Thermal Effects*—For DC systems, thermoelectric voltage measurement and correction are critically important. A minimum number of connections should be used and maintained at a constant temperature to minimize thermoelectric effects (see A18.3.5).

A18.9.4.1 All measuring devices (amplifiers/preamplifiers, voltmeters, analog-to-digital converters) and the specimen itself shall be maintained at a constant temperature. Enclosures to ensure constant temperatures throughout the test are generally beneficial.

NOTE A18.6—If there are concerns about signal fluctuations and/or drifts due to thermoelectric effects, it is helpful to monitor the stability of the DCEPD signals while the specimen is at the test temperature but before actually starting the test. If the stability is not deemed adequate, the use of a reference potential (see A18.3.3) or a tighter control of the test temperature, or both will be beneficial.

A18.9.5 *Selection of Input Current Duty Cycle*—The choice of input current duty cycle (see Note A18.7) shall be the result of a compromise. A 100 % duty cycle corresponds to a constant applied current throughout the test. This option allows for continuous monitoring of the DCEPD signal, however it may require a reduction of the input current magnitude and an associated drop in sensitivity in order to avoid significant specimen heating. A low-duty current cycle will minimize specimen heating, allowing for higher input current magnitude and for correction of thermal effects.

NOTE A18.7—The input current duty cycle is the ratio between the time the current is on and the total duration of the test, expressed in percentage.

A18.9.6 *Selection of Input Current Pulse Duration*—When using pulsed current, the duration of the input current pulse should be short enough to minimize specimen heating, and long enough to allow current stabilization (depending on the characteristics of the DC current source) and stable DCEPD measurements.

A18.9.7 *Selection of Input Current Magnitude*—The choice of current magnitude is an important parameter: too low a value may not produce measurable output voltages; too high a value may cause excessive specimen heating or arcing (**40**).

A18.9.7.1 To minimize these problems, current densities should be kept to the minimum value which can be used to produce the required crack size resolution. The maximum current that can be used with a particular specimen can be determined by monitoring the specimen temperature while increasing the current in steps, allowing sufficient time for the specimen to thermally stabilize. Particular care should be exercised when testing in vacuum, as convection currents are not available to help maintain the specimen at the test temperature.

A18.9.8 *DC Current Stabilization Period*—Allow a sufficient stabilization period after turning the DC current either on or off before making a voltage measurement. Most solid-state power sources can stabilize the output current within a period of 1 or 2 s for a step change in output. However, this should be verified for each particular specimen and experimental configuration. Measurements of DCEPD shall be taken once the current is stabilized.

A18.10 Effects of Plasticity on DCEPD

A18.10.1 Plastic deformation of the specimen can increase measured electric potential differences due to changes in material resistivity and specimen geometry (other than crack extension). It is therefore necessary to distinguish between changes in DCEPD due to plasticity and changes due to crack extension.

A18.10.2 Two methods to account for plasticity-induced DCEPD changes are described in A18.11 for the determination of crack size from DC electric potential differences. Both methods require establishing a value of DCEPD labelled V_0. Depending on the method used, V_0 is either a fixed value that corresponds to the DCEPD at the initiation of ductile crack extension (reference method, A18.11.1), or a force-dependent value that corresponds to the start of the test plus any DCEPD increase associated with the elastic deformation of the specimen (alternative method, A18.11.2).

A18.10.3 The analytical or experimental calibrations used for calculating crack size (A18.4-A18.5) do not account for the effects of plasticity on the measured DCEPD. Within the requirements of this annex, it is assumed that most, if not all, of the significant plasticity in the specimen occurs prior to the initiation of crack extension. For the reference method in A18.11.1, the change in DCEPD measured prior to the onset of crack extension shall be ignored, and the remainder of the DCEPD change shall be used to establish the ductile crack extension portion of the *J-R* curve. This method involves the

analysis of a plot of crack-mouth opening displacement or load-line displacement as a function of DCEPD (**41, 42**). The alternative method in A18.11.2, which has been shown to work satisfactorily for several steels (**43**), uses a plot of force as a function of DCEPD (**44**).

A18.11 Methods for determining V_0

A18.11.1 *Reference Method: Determination of V_0 from the CMOD/LLD versus DCEPD Record:* Construct a plot of CMOD (for SE(B) specimens) or LLD (for C(T) specimens) as a function of DCEPD, as shown in Fig. A18.3. The value of DCEPD corresponding to a change in slope corresponds to V_0. On the force versus displacement record of the test, the point corresponding to the change in slope shall fall between the elastic limit (end of the initial linear portion of the curve) and the maximum recorded force.

Note A18.8—The specific procedure used to identify the point corresponding to the change in slope is left to the user. Different methods, ranging from purely visual to analytical approaches, have been used (**43**).

Note A18.9—For some high-toughness materials, it might be difficult to unequivocally identify the point corresponding to the initiation of crack extension, particularly when the point of slope change is not clearly detectable (**37**). In these instances, it may be useful to run some tests interrupted before and just after the onset of crack extension to validate the determination of V_0 for a given material, preferably before the actual scheduled tests and after the confirmatory specimen mentioned in A18.16.3.

A18.11.2 *Alternative Method: Determination of V_0 from the Force versus DCEPD Record*—Construct a plot of force as a function of DCEPD, as shown in Fig. A18.4. Using force as the dependent variable and DCEPD as the independent variable, linearly fit the data corresponding to the steeply rising part of the record using the equation $V_0 = CF + D$, where F is applied force and C, D are fitting coefficients. Another key value of DCEPD, V_{el}, corresponds to the upper deviation from linearity in the force versus DCEPD curve (Fig. A18.4).

Note A18.10—Experience has shown that the alternative method in A18.11.2 tends to yield unconservative results when applied to high-toughness, high-ductility steels such as austenitic steels, where significant

deformation occurs prior to crack initiation (**37**). For such materials, the use of the reference method (A18.11.1) is recommended.

Note A18.11—The non-linear portion of the curve shown in Fig. A18.4 at the very beginning of the test, which is often observed, corresponds to the rapid increase of DCEPD after the specimen is loaded, caused by the separation of the fatigue precrack surfaces. This portion should not be included in the linear fit.

A18.12 Consideration of Crack-Tip Blunting in the Calculation of Crack Size

A18.12.1 Depending on the method used for the establishment of V_0, different approaches shall be used to account for crack-tip blunting before the onset of ductile crack extension.

A18.12.2 When using the reference method (A18.11.1), the crack size before the onset of ductile crack extension ($V \leq V_0$) shall be calculated as:

$$a_i = a_0 + \frac{J_i}{2\sigma_Y} \qquad (A18.1)$$

where J_i is calculated using a_0 in accordance with Annex A1 for SE(B) specimens or Annex A2 for C(T) specimens, respectively, and σ_Y is the effective yield strength at the test temperature. The blunting-corrected initial crack size at the initiation of ductile tearing ($V = V_0$), $a_{0,bl}$, is given by:

$$a_{0,bl} = a_0 + \frac{J_{V0}}{2\sigma_Y} \qquad (A18.2)$$

where J_{V0} is the *J*-integral value corresponding to V_0 and a_0. For $V > V_0$, a_i shall be calculated from DCEPD using a specific analytical or experimental relationship, for example one of those described in A18.14 or A18.15.

A18.12.3 When using the alternative method (A18.11.2), the crack size corresponding to $V \leq V_{el}$ shall be approximated by:

$$a_i = a_0 + \frac{J_{el,i}}{2\sigma_Y} \qquad (A18.3)$$
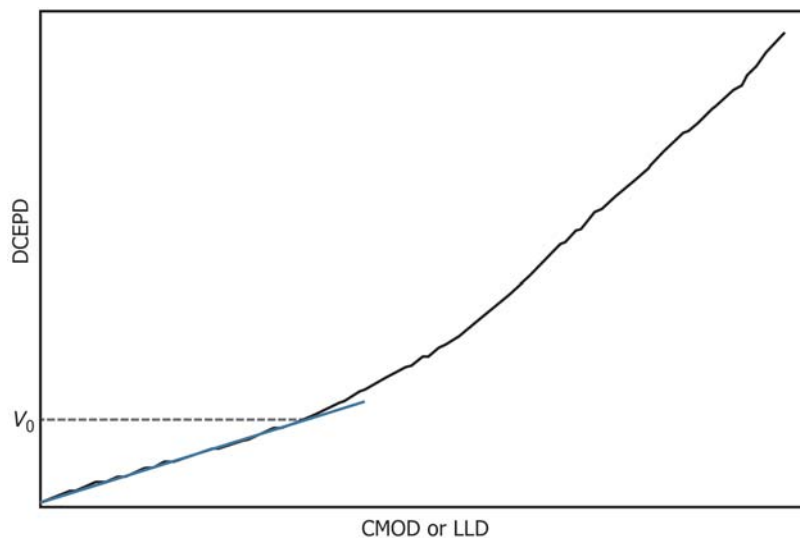
where $J_{el,i}$ is calculated as:

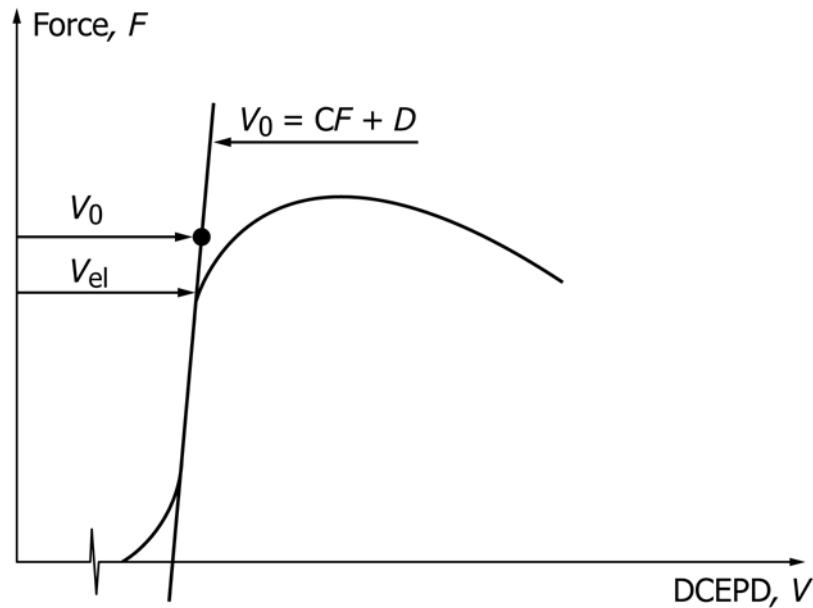**FIG. A18.3 Example of DCEPD versus CMOD or LLD Record for a Structural Steel**

FIG. A18.4 Example of Force versus DCEPD Test Record for a Structural Steel

$$J_{el,i} = \frac{K_i^2(1 - v^2)}{E} \qquad (A18.4)$$

and K_i is calculated according to A1.4.1 for SE(B) specimens or A2.4.1 for C(T) specimens, using the original crack size a_0. The approximate blunting-corrected initial crack size for $V = V_{el}$, $a_{0,bl}$, is given by:

$$a_{0,bl} = a_0 + \frac{J_{Vel}}{2\sigma_Y} \qquad (A18.5)$$

with J_{Vel} = J-integral corresponding to V_{el} and a_0. For $V > V_{el}$, a_i shall be calculated from DCEPD using a specific analytical or experimental relationship, for example one of those described in A18.14 or A18.15.

A18.13 Charateristics of DCEPD versus Crack Size Relationships

A18.13.1 Some closed-form solutions for the relationship between DCEPD and crack size are described in A18.14 and A18.15 for C(T) and SE(B) specimens, respectively. These relationships are sensitive to the location of current and voltage wires, but they are not sensitive to test temperature, as long as temperature variations are accounted for (see Note A18.6). The relationships are also insensitive to specimen material and dimensions, provided that all dimensions vary in a proportional manner.

A18.13.2 When testing alternative geometries or with different current/voltage wire locations than those shown in A18.14 and A18.15, the relationship between DCEPD and crack size may be derived empirically or by numerical modelling (finite elements). Any such relationship shall be experimentally verified using post-test fracture surface measurements (that is, by comparing measured and predicted final crack sizes or extensions). It must be emphasized that a specific relationship between crack size and DCEPD is only valid for a specific combination of current and voltage wire locations.

NOTE A18.12—The placement of voltage wires is usually a compromise

between good sensitivity to crack size changes and freedom from errors caused by minor variations in lead location from specimen to specimen. Lead locations near the crack tip yield better sensitivity to changes in crack size or initiation of crack extension. The difficulty with this type of arrangement is that the electric field is, in general, highly non-uniform in the near-tip region. Thus, minor variations in lead placement from one specimen to the next may produce significant differences in measured voltage for the same crack size (45). In most cases, those positions which give greatest sensitivity to crack size changes also have the greatest sensitivity to variations in lead wire positioning.

NOTE A18.13—Current input wire locations also represent a compromise between uniformity and sensitivity. Placement of the current input wires near the crack tip region focuses the current streamlines there, resulting in increased sensitivity to crack initiation. Placement of the current leads remote from the crack plane tends to provide a more uniform current field for the measurement of crack extension (see, for example, Figs. A18.5-A18.9).

A18.13.3 A closed-form analytical solution for the relationship between voltage difference and crack size was established by Johnson (46) for the M(T), middle-cracked tension, specimen. It has been shown that this relationship may also be applied to a wide range of specimen geometries, including C(T) and SE(B) specimens (47).

A18.13.4 *General Form of the Relationships*—Relationships between crack size and DCEPD are generally of the form:

$$\frac{a}{W} = f\left(\frac{V}{\bar{V}}\right), \qquad (A18.6)$$

or alternatively

$$\frac{a - \bar{a}}{\bar{a}} = f\left(\frac{V - \bar{V}}{\bar{V}}\right), \qquad (A18.7)$$

where:
V = DCEPD signal,
$\bar{V}$ = DCEPD signal corresponding to a specific crack size $\bar{a}$,
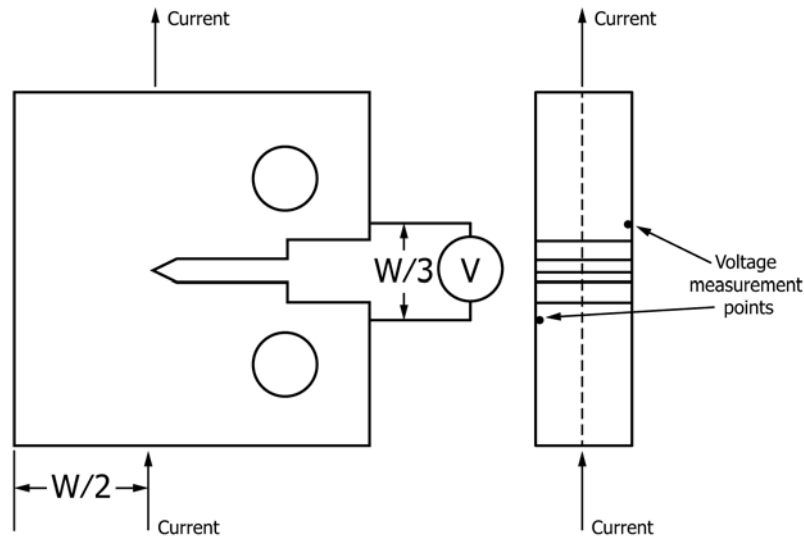a = crack size, and
W = specimen width.

FIG. A18.5 Possible C(T) Specimen configuration for Eq. A18.8, with $2y = W/3$.
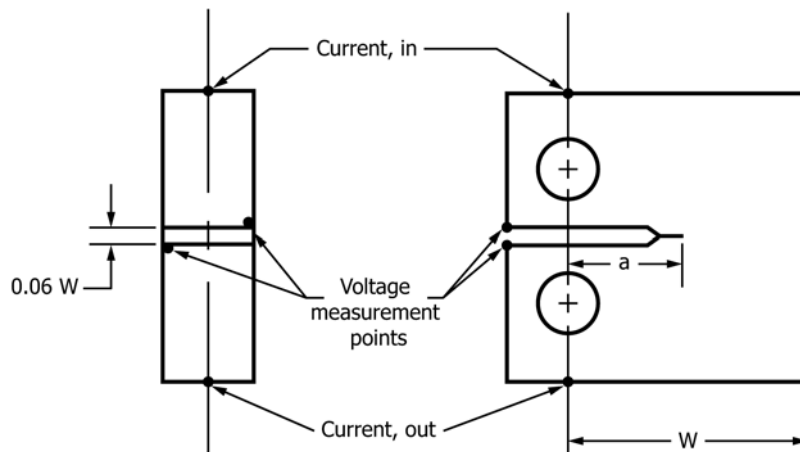

FIG. A18.6 Schematic of C(T) Specimen DC Current and Potential Lead Connections for Eq. A18.9

A18.13.5 In some analytically derived calibration functions, for example, Eq A18.8, it is possible to select convenient values of $\bar{V}$ and $\bar{a}$ such that, $\bar{V} = V_0$ and $\bar{a} = a_{0,bl}$, where V_0 is obtained using the reference method (A18.11.1) or the alternative method (A18.11.2), and $a_{0,bl}$ is the blunting-corrected initial crack size, calculated by means of Eq A18.2 for the reference method or Eq A18.5 for the alternative method.

A18.13.6 For calibration functions which are derived numerically or empirically, for example Eq A18.9, Eq A18.10, and Eq A18.13, the value of $\bar{a}$ is usually predefined, so the corresponding value of $\bar{V}$ can be calculated from V_0 and $a_{0,bl}$, using, for example, Eq A18.10, Eq A18.12 and Eq A18.14.

A18.13.7 The equations listed in the following sections (A18.4 for C(T) specimens and A18.5 for SE(B) specimens)

have been derived under DC conditions for sharp cracks in the respective specimen geometries using either closed-form or experimental calibrations.

A18.13.8 Regardless of the relationship between DCEPD and crack size used, the use of a reference probe is recommended (see A18.3.3). When employing such a reference probe, the DCEPD measurements made for crack size determination shall be divided by the ratio $V_{ref}/V_{ref,0}$,

where:

V_{ref} = the reference probe voltage measured at the same time as the DCEPD test specimen probe voltage, and
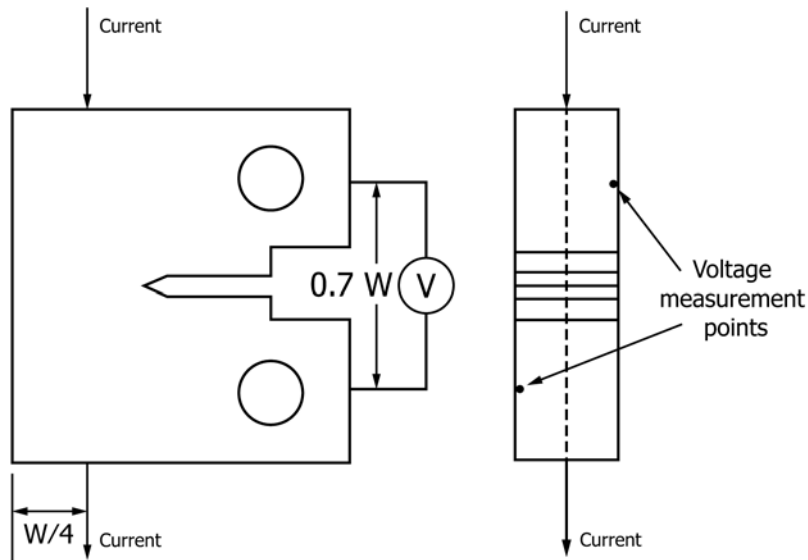
$V_{ref,0}$ = the initial reference probe voltage.

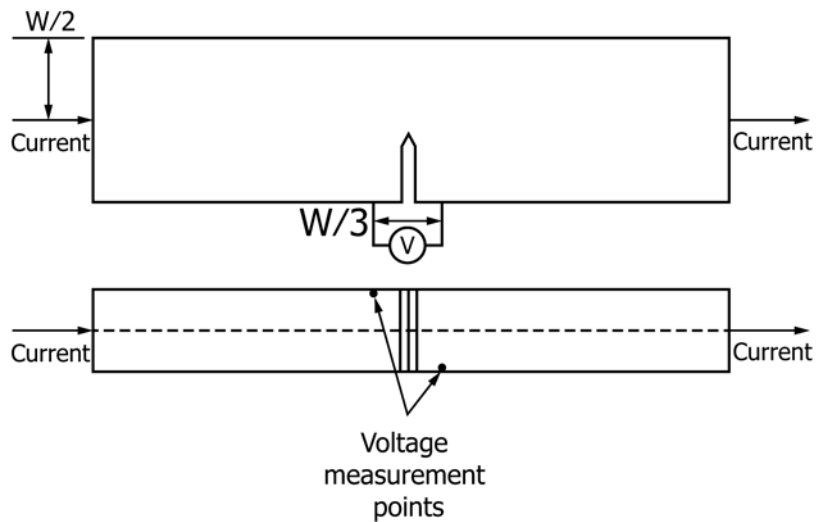**FIG. A18.7 Alternative C(T) Specimen DC Potential Lead Connections for Eq. A18.11.**

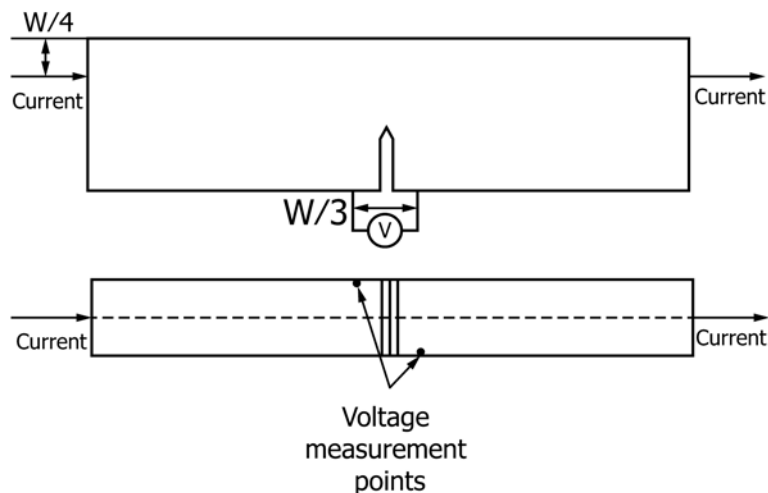**FIG. A18.8 Schematic of SE(B) Specimen DC Potential Lead Connections for Eq. A18.8**

FIG. A18.9 Alternative SE(B) Specimen DC Potential Lead Connections for Eq. A18.13

A18.14 Examples of Relationships between DCEPD and Crack Size for C(T) Specimens

A18.14.1 A closed-form analytical expression (**46**) that can be used for the C(T) geometry is the following:

$$\frac{a}{W} = \frac{2}{\pi} \cos^{-1}\left[\frac{\cosh\left(\frac{\pi y}{2W}\right)}{\cosh\left\{ \frac{V}{V_0} \cosh^{-1}\left[\frac{\cosh\left(\frac{\pi y}{2W}\right)}{\cos\left(\frac{\pi a_{0,bl}}{2W}\right)} \right] \right\}} \right] \tag{A18.8}$$

where y is the half-distance between the voltage measurements points. A possible configuration for a C(T) specimen with $2y = W/3$ is shown in Fig. A18.5.

A18.14.2 Another closed-form analytical relationship for the C(T) specimen, developed from finite element analyses and verified through experimental techniques (**48**), is the following:

$$\frac{a}{W} = B_0 + B_1\left(\frac{V}{\bar{V}}\right) + B_2\left(\frac{V}{\bar{V}}\right)^2 + B_3\left(\frac{V}{\bar{V}}\right)^3 \tag{A18.9}$$

$$\text{for } 0.24 \leq \frac{a}{W} \leq 0.7$$

where:

V = DCEPD signal,
$\bar{V}$ = DCEPD signal corresponding to $\bar{a} = 0.241W$
B_0 = -0.5051,
B_1 = 0.8857,
B_2 = -0.1398, and
B_3 = 0.0002398.

$$\bar{V} = \frac{V_0}{A_0 + A_1\left(\frac{a_{0,bl}}{W}\right) + A_2\left(\frac{a_{0,bl}}{W}\right)^2 + A_3\left(\frac{a_{0,bl}}{W}\right)^3} \tag{A18.10}$$

where:

A_0 = 0.5766
A_1 = 1.9169,
A_2 = -1.0712, and
A_3 = 1.6898.

NOTE A18.14—When the reference method (A18.11.1) is used, Eq A18.10 yields a unique value of $\bar{V}$ for the whole test. Conversely, when the alternative method (A18.11.2) is used, since V_0 is force-dependent, Eq A18.10 provides a different value of $\bar{V}$ for each data point.

A18.14.3 An empirical relationship for the C(T) specimen was developed based on data from (**49**), which involved current inputs at the $W/4$ position, as shown in Fig. A18.7. The following power-law relationship was obtained in the range $0.45 \leq a/W \leq 0.8$:

$$\frac{a}{w} = \left[0.2864 \left(\frac{V}{\bar{V}} - 0.5 \right) \right]^{0.3506} \tag{A18.11}$$

where $\bar{V}$ corresponds to a $\approx 0.5W$, and is calculated from V_0 using the following relationship:

$$\bar{V} = \frac{V_0}{3.4916\left(\frac{a_{0,bl}}{W}\right)^{2.8523} + 0.5} \tag{A18.12}$$

NOTE A18.15—When the reference method (A18.11.1) is used, Eq

A18.12 yields a unique value of $\bar{V}$ for the whole test. Conversely when the alternative method (A18.11.2) is used, since V_0 is force-dependent, Eq A18.12 provides a different value of $\bar{V}$ for each data point.

A18.15 Examples of Relationships between DCEPD and Crack Size for SE(B) Specimens

A18.15.1 The same closed-form expression provided in A18.14.1, Eq A18.8, has been found to apply to SE(B) specimens when the current input leads and voltage wires are at the locations shown in Fig. A18.8.

A18.15.2 An empirical relationship for the SE(B) specimen was developed based on data from (**49**), which involved current input leads and voltage wires located as shown in Fig. A18.9. The following power-law relationship was obtained over the range $0.45 \leq a/W \leq 0.8$:

$$\frac{a}{w} = \left[0.4512 \left(\frac{V}{\bar{V}} - 0.5 \right) \right]^{0.4688} \tag{A18.13}$$

where $\bar{V}$ corresponds to $\bar{a} \approx 0.5W$, and is calculated from V_0 using the following relationship:

$$\bar{V} = \frac{V_0}{2.2163\left(\frac{a_{0,bl}}{W}\right)^{2.1331} + 0.5} \tag{A18.14}$$

NOTE A18.16—When the reference method (A18.11.1) is used, Eq A18.14 yields a unique value of $\bar{V}$ for the whole test. Conversely, when the alternative method (A18.11.2) is used, since V_0 is force-dependent, Eq A18.14 provides a different value of $\bar{V}$ for each data point.

A18.16 Validity Requirements

A18.16.1 The requirements of 9.1.4, 9.1.5.1, A9.9, A9.10, A11.9, and A11.10 shall be fulfilled.

A18.16.2 The final predicted crack extension, $\Delta a_{p,predicted}$, and the measured physical crack extension, Δa_p, shall not differ by more than $0.25 \Delta a_p$ for $\Delta a_p < 0.3 b_o$, and by more than $0.075 b_o$ thereafter.

A18.16.3 At least one additional, confirmatory specimen shall be tested under the same test conditions as the remaining specimens. The value of DCEPD corresponding to a crack extension of 0.5 mm shall be estimated from the analytical or experimental relationship used. The additional, confirmatory specimen shall then be tested to this DCEPD value, marked as prescribed in 8.5.1, broken open and the ductile crack extension shall be measured. The measured crack extension shall be 0.5 ± 0.25 mm in order for the subsequent tests to be qualified according to this method.

NOTE A18.17—The confirmatory specimen should be tested before the scheduled tests, as it can provide an indication of V_0 (constant or force-dependent), which can be used for a preliminary analysis of the following tests.

A18.17 Crack Size Adjustment

A18.17.1 After checking that all validity requirements in A18.16 are fulfilled, predicted crack sizes shall be adjusted based on the measured original crack size, a_0, and the measured physical crack extension, Δa_p, in order to improve the overall accuracy of the predictions.

A18.17.2 Each predicted crack size for $V > V_0$ (reference method, A18.12.2) or $V > V_{el}$ (alternative method, A18.12.3) shall be adjusted using:

$$a_{i,adj} = \frac{a_p - a_{0,bl}}{a_{p,\,predicted} - a_{0,bl}}(a_i - a_{0,bl}) + a_{0,bl}, \quad (A18.15)$$

where a_i is the unadjusted crack size.

A18.18 Report

A18.18.1 Section 10 describes the reporting requirements for this method. If the DCEPD method is used, the following additional items shall be reported.

A18.18.2 Details of the analytical or experimental relationship used to infer crack size from DCEPD measurements.

A18.18.3 If the reference method (A18.11.1) has been used, DCEPD versus CMOD or LLD record for each test, indicating the point of slope change used to determine V_0. Additionally, an explanation on how this point was established (visual examination, use of a slope determination algorithm, etc.) shall be included.

A18.18.4 If the alternative method (A18.11.2) has been used, force versus DCEPD record for each test, showing the linear fit established in the initial portion of the test. Additionally, an explanation on how the linear fit was established (visual examination, use of a slope determination algorithm, etc.) shall be included.

APPENDIXES

(Nonmandatory Information)

X1. FITTING OF EQUATION A9.1

X1.1 To fit Eq A9.1 to the J_i, a_i data using the method of least squares, the following equation must be set up and solved for a_{oq}, B, and C:

X1.2 This equation can be set up and solved using a standard spreadsheet or using a mathematical analysis program like MathCad, Maple, or Mathematica.

$$\begin{Bmatrix} \sum a_i - \dfrac{\sum J_i}{2\sigma_Y} \\[2mm] \sum a_i J_i^2 - \dfrac{\sum J_i^3}{2\sigma_Y} \\[2mm] \sum a_i J_i^3 - \dfrac{\sum J_i^4}{2\sigma_Y} \end{Bmatrix} = \begin{bmatrix} n & \sum J_i^2 & \sum J_i^3 \\ \sum J_i^2 & \sum J_i^4 & \sum J_i^5 \\ \sum J_i^3 & \sum J_i^5 & \sum J_i^6 \end{bmatrix} \begin{Bmatrix} a_{oq} \\ B \\ C \end{Bmatrix} \quad (X1)$$

X2. GUIDELINES FOR MEASURING THE FRACTURE TOUGHNESS OF MATERIALS WITH SHALLOW CRACKS

X2.1 Significance and Use

X2.1.1 Fracture toughness measurements may be made using specimens with relatively shallow cracks, $0.05 < a/W < 0.45$, which are not permitted by the standard test method. The resulting measures of fracture toughness, designated $J_{xSC()}$ and $\delta_{xSC()}$, will be dependent upon the size of the specimen and the crack length. The fracture toughness determined from specimens with shallow cracks is usually non-conservative when compared to the fracture toughness determined from standard, deep crack specimen geometries and may exhibit considerably more scatter, particularly in the ductile to brittle transition region for ferritic materials. The J resistance curves determined

according to this appendix are not corrected for crack growth and will be non-conservative relative to crack growth corrected resistance curves.

X2.1.2 This appendix is provided to give recommended procedures for conducting fracture toughness tests of specimens containing shallow cracks. Special requirements for the instrumentation, specimen, testing procedure and data analysis are described.

X2.1.3 Particular care must be exercised when using these non-standard measures of fracture toughness for structural integrity assessments. The user is cautioned that differences may exist between laboratory test and field conditions and that

the fracture toughness of a shallow crack specimen may be strongly influenced by the size of the crack and the specimen geometry.

X2.2 Terminology

X2.2.1 All of the following parameters describe various measures of fracture toughness determined using specimens containing shallow cracks. These parameters are similar to the corresponding parameters for standard specimens except that they include the subscript $SC(a_0/W)$ to indicate a shallow crack specimen. The number in the parentheses is the original crack size to specimen width ratio for the shallow crack specimen.

X2.2.1.1 $\delta_{IcSC()}$ [L]— is a value of CTOD near the onset of slow stable crack extension in a specimen with a shallow crack, here defined as occurring at $\Delta a_p = 0.2$ mm (0.008 in) + $0.7\delta_{Ic}$.

X2.2.1.2 $\delta_{SC()}$ [L]—is the value of CTOD at the onset of unstable crack extension (see 3.2.36) or pop-in (see 3.2.22) in a specimen with a shallow crack when $\Delta a_p < 0.2$ mm (0.008 in) + $0.7\delta_{cSC()}$. $\delta_{cSC()}$ corresponds to the force P_c and clip-gage displacement v_c (see Fig. 1).

X2.2.1.3 $\delta_{uSC()}$ [L]—is the value of CTOD at the onset of unstable crack extension (see 3.2.36) or pop-in (see 3.2.22) in a specimen with a shallow crack when the event is preceded by $\Delta a_p \geq 0.2$ mm (0.008 in) + $0.7\delta_{uSC()}$. $\delta_{uSC()}$ corresponds to the force P_u and the clip gage displacement v_u (see Fig. 1). It may be size dependent and a function of test specimen geometry. It can be useful to define limits on ductile fracture behavior.

X2.2.1.4 $J_{IcSC()}$ [FL^{-1}] - The property J_{Ic} determined by this test method characterizes the fracture toughness of materials in a specimen with a shallow crack near the onset of stable tearing crack extension here defined as occurring at $\Delta a_p = 0.2$ mm (0.008 in) + $J_{IcSC()}/2\sigma_Y$.

X2.2.1.5 $J_{cSC()}$ [FL^{-1}]—The property J_c determined by this test method characterizes the fracture toughness of materials at fracture instability prior to the onset of significant stable tearing crack extension, $\Delta a_p < 0.2$ mm (0.008 in) + $J_{cSC()}/2\sigma_Y$, in a specimen with a shallow crack.

X2.2.1.6 $J_{uSC()}$ [FL^{-1}] The quantity J_u determined by this test method measures fracture instability after the onset of significant stable tearing crack extension, $\Delta a_p \geq 0.2$ mm (0.008 in) + $J_{uSC()}/2\sigma_Y$, in a specimen with a shallow crack.

X2.3 Specimen Size and Configuration

X2.3.1 *Recommended Specimen*—The recommended specimen is a single-edge notch, bend specimen SE(B), similar to that shown in Fig. A1.1.

X2.3.1.1 The initial crack size to specimen width shall be $0.05 \leq a/W \leq 0.45$ and the specimen width to thickness shall be in the range $1 \leq W/B \leq 4$.

X2.3.1.2 The narrow notch configuration of Fig. 6 is recommended; however, the notch opening at the front face of the specimen may need to be modified from the dimensions shown in Fig. 7, particularly for specimens with a/W < 0.2. The notch opening should be made as small as practical to minimize the influence of the machined notch on the elastic compliance of the specimen and the fracture response of the specimen. Notches produced using the wire electrical discharge machining process with a wire diameter less than 0.25 mm (0.010 in.) usually produce satisfactory results.

X2.3.1.3 An alternative method for producing a shallow crack specimen involves machining an SE(B) specimen with an over-sized W dimension. A fatigue crack is extended from the starter notch and then the specimen is remachined to remove the starter notch leaving a specimen with only a fatigue crack. Integral knife edges may subsequently be machined into the specimen.

X2.3.1.4 Integral knife edges or features for the seating of the crack mouth opening displacement gage may be particularly advantageous for specimens containing shallow cracks. Suggested configurations are shown in Fig. X2.1. The square notch configuration along with the ring-type crack mouth opening displacement gage of Fig. X2.2 is well-suited to small specimens and shallow cracks. The integral knife edges shown in Fig. X2.1 may not be suitable for very small cracks, a < 2 mm (0.079 in.).

X2.4 Apparatus

X2.4.1 Apparatus is required for the measurement of the applied force and the crack mouth opening displacement. Standard force transducers as described in 6.3 are satisfactory. Load-line displacement measurements are not required for the shallow crack SE(B) specimens.
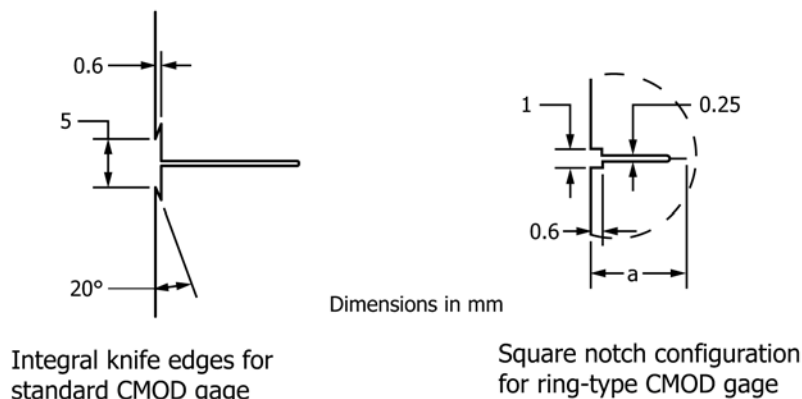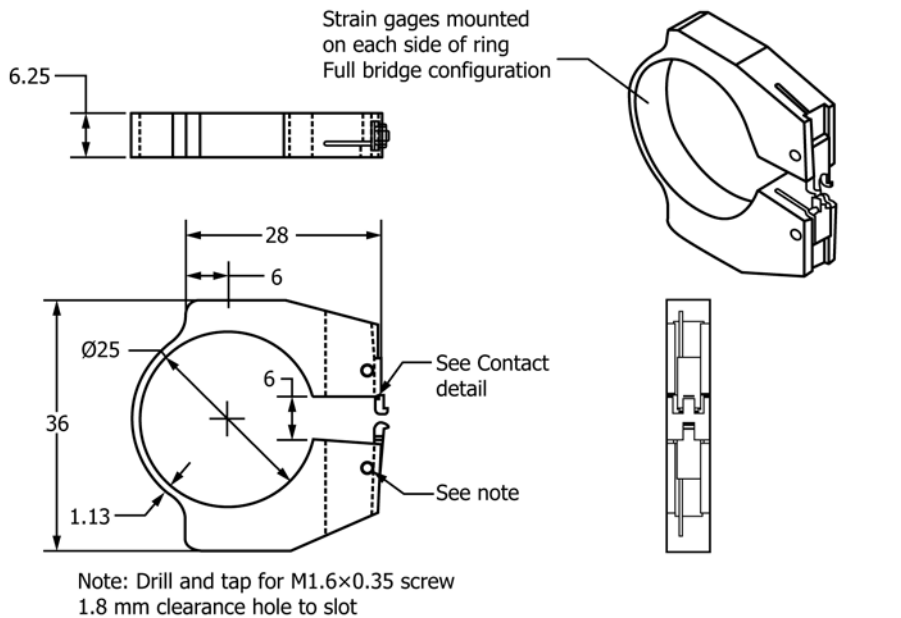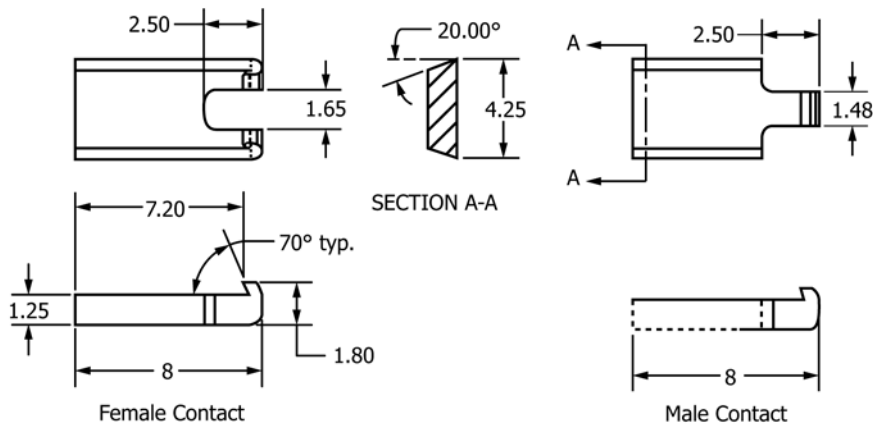

FIG. X2.1 Recommended Notch Configurations with Integral Features for Mounting Crack Mouth Opening Displacement Gages. These Notch Configurations Are Only Recommended for a $\geq$ 2mm (0.079 in.)

6.25

Strain gages mounted
on each side of ring
Full bridge configuration

28

6

Ø25

36

6

1.13

See Contact
detail

See note

Note: Drill and tap for M1.6×0.35 screw
1.8 mm clearance hole to slot

25 mm Crack Mouth Opening Displacement Ring Gage
Gage body machined from 7075-T6 AI

2.50

1.65

20.00°

4.25

A

2.50

1.48

A

SECTION A-A

7.20

70° typ.

1.25

8

1.80

8

Female Contact

Male Contact

Contact Detail
Contacts machined from Titanium 6AI-4V

All dimensions are in mm.

FIG. X2.2 Alternative crack opening displacement gage suitable for use with very narrow Notches.

X2.4.1.1 *Crack Mouth Opening Displacement Gages*—The standard gage described in 6.2.2 may be suitable for measuring the CMOD on specimens which have a notch opening that is large enough to accommodate the arms of the gage. For small specimens and for specimens with very shallow cracks, an alternative gage design such as the ring gage in Fig. X2.2 is recommended. Alternative means for measuring CMOD may be required for specimens with very shallow cracks, a < 2 mm (0.079 in.).

X2.4.1.2 The bend-test fixture recommended in 6.5.1 is suitable for testing SE(B) specimens with shallow cracks.

X2.5 Specimen Preparation

X2.5.1 The requirements of Section 7 are generally applicable with the following notable exceptions.

X2.5.1.1 *Crack Starter Notch Configuration*—Only the straight through notch configuration of Fig. 5 is recommended for the shallow crack SE(B) specimen.

X2.5.1.2 *Fatigue crack length*—The crack size, total length of the starter notch plus the fatigue crack, shall be between 0.05W and 0.45W.

X2.5.1.3 *Fatigue Loading Requirements*—In order to promote early fatigue crack initiation it is recommended that the

60

specimen be statically preloaded in such a way that the notch tip is compressed in a direction normal to the intended crack plane (not to exceed a force equal in magnitude to $2P_f$). The fatigue crack shall be grown a minimum of 1.5× the size of the plastic zone resulting from the compression preload, r_p, where:

$$r_p = \frac{1}{3\pi}\left(\frac{K}{\sigma_{ys}}\right)^2 \qquad (X2.1)$$

with K evaluated using the expression in A1.4.1 and the maximum compressive force used to preload the notch.

X2.6 Procedure

X2.6.1 The requirements of Section 8 for the SE(B) specimen are generally applicable for conducting the tests. The resistance curve procedure is recommended. It may be necessary to use unload/reload cycles near the maximum recommended range of either 50 % of P_f or 50 % of the current force, whichever is smaller, in order to get accurate estimates of the specimen compliance.

X2.6.2 The user is cautioned that specimens with shallow cracks can store greater amounts of elastic energy than the standard deeply cracked specimen. If the specimen fails in an unstable manner, the broken halves of the specimen may be forcefully ejected from the testing machine and suitable restraints should be fashioned.

X2.7 Calculation

X2.7.1 *Calculation of K*—The stress intensity factor, K, is calculated using the expression in A1.4.1.

X2.7.2 *Calculation of J:*

X2.7.2.1 *J Calculation for the Basic Method*— J is calculated according to A1.4.2 except that the crack growth correction of Annex A16 shall not be employed because it is not applicable to shallow cracks.

X2.7.2.2 *J Calculations for the Resistance Curve Method*— At a point corresponding to $v_{(i)}$, $P_{(i)}$ on the force versus crack-mouth opening displacement record, calculate J as follows:

$$J = \frac{K_{(i)}^2\left(1 - v^2\right)}{E} + J_{pl} \qquad (X2.2)$$

where $K_{(i)}$ is from A1.4.1 and

$$J_{pl(i)} = J_{pl(i-1)} + \frac{\eta_{CMOD(i-1)}\left[A_{CMODpl(i)} - A_{CMODpl(i-1)}\right]}{B_N b_{(i-1)}} \qquad (X2.3)$$

In Eq X2.3, the quantity $A_{CMODpl(i)} - A_{CMODpl(i-1)}$ is the increment of area under the force versus plastic component of CMOD record between lines of constant displacement at i-1 and i as shown in Fig. A1.3. The quantity $A_{CMODpl(i)}$ can be evaluated from the following equation:

$$A_{CMODpl(i)} = A_{CMODpl(i-1)} + \frac{\left(P_i + P_{i-1}\right)}{2}\left(v_{pl(i)} - v_{pl(i-1)}\right) \qquad (X2.4)$$

where:

$v_{pl(i)}$ = plastic part of the CMOD = $v_{(i)}$- P_iC_i and
C_i = slope $(\Delta v_m/\Delta P)_i$ of the current unload/reload cycle.

In Eq X2.3, η_{CMOD} is a function of crack size and is given by the following expression:

$$\eta_{CMOD\,(i-1)} = 3.667 - 2.199\left(\frac{a}{w}\right) + 0.437\left(\frac{a}{w}\right)^2 \qquad (X2.5)$$

X2.7.2.3 For a resistance curve test method using an elastic compliance technique with crack mouth opening displacement measured at the notched edge of a shallow crack specimen with $0.05 \le a/W \le 0.45$, the crack length is given as follows (50):

$$\frac{a}{W} = 1.01878 - 4.5367u + 9.0101u^2 - 27.333u^3 + 74.4u^4 - 71.489u^5 \qquad (X2.6)$$

where:

$$u = \frac{1}{\left[\dfrac{B_e WEC_i}{S/4}\right]^{1/2} + 1}$$

C_i = $(\Delta v_m/\Delta P)$ on an unloading/reloading sequence, and
B_e = = B - (B-B_N)^2/B.

X2.7.3 *Calculation of CTOD:*

X2.7.3.1 For the shallow crack SE(B) specimen, calculations of CTOD for any point on the force-displacement record are made using A1.4.5 except that J values shall not be crack growth corrected when using equations Eq A1.15 or Eq A1.17.

X2.8 Analysis of Results

X2.8.1 The data shall meet the following requirements to be qualified according to this method. If the data do not pass these requirements no fracture toughness measures can be determined according to this method.

X2.8.1.1 All requirements on the test equipment in 6 or as modified in X2.4 shall be met.

X2.8.1.2 All requirements on machining tolerance and pre-cracking in Section 7 or as modified in X2.5 shall be met.

X2.8.1.3 All requirements on fixture alignment, test rate, and temperature stability and accuracy in 8 shall be met.

X2.8.1.4 The crack size requirements in 9.1.4 and 9.1.5 shall be met for shallow crack fracture toughness tests.

X2.8.2 *Fracture Toughness Calculation*—The reported fracture toughness values for shallow crack specimens shall include the subscript SC(a_0/W) where a_0/W is replaced by the original crack size to specimen width ratio. When the test terminates with fracture instability, evaluate whether the fracture occurred before significant stable tearing or after significant stable tearing. The beginning of significant stable tearing is defined in A6.3 and A7.3. For fracture instability, proceed to Annex A6 and Annex A7 to evaluate the toughness values in terms of J or CTOD. For fracture instability occurring after significant stable tearing, proceed to Annex A6 and Annex A7 to evaluate toughness values and then go to Annex A8 and Annex A10 to develop R-curves. Proceed to Annex A9 and Annex A11 to develop initiation values of toughness.

X2.8.2.1 The maximum crack extension capacity for a specimen in A8.3.2 and A10.3.2 is limited to $\Delta a_{max} = 0.1b_0$ for a shallow crack specimen.

X3. RECOMMENDED BEST PRACTICES FOR ESTIMATING CRACK SIZE USING ELASTIC COMPLIANCE

X3.1 This test method does not prescribe specific practices for performing elastic compliance estimates of crack size. This appendix provides recommendations for analyzing the compliance data from unload/reload sequences and provides a method for quantifying the uncertainty in J_{Ic} due to uncertainty in the compliance estimate.

X3.2 It is not uncommon for there to be some non-linearity in the test record at the start and end of an unload; therefore, the following recommendations are made to exclude data near the displacement reversals at the start and end of an unload from the compliance calculation. The start of an unload is defined as the point at which the crack opening displacement first decreases. If the specimen is held at constant displacement to allow stress relaxation per 8.6.4, the displacement decrease would occur after completing the hold period. The force at the start of the unload is P_1. The end of an unload is defined as the point at which crack opening displacement first increases again to start reloading. The force at the end of the unload is P_2 and $\Delta P = (P_1 - P_2)$. Selection of data for linear regression of the unload should start with the first point that falls below P_1-0.05ΔP (point a in Fig. X3.1) and stop with the last point

before the force first falls below $P_1 - 0.95\Delta P$ (point b in Fig. X3.1). Selection of data for regression of the reload should start when the force exceeds $P_1 - 0.95\Delta P$ (point c in Fig. X3.1), and stop with the last point before the force exceeds P_1-0.05ΔP (point d in Fig. X3.1). After the data first crosses a limit to start an unload or reload, all subsequent data is included in the regression analysis until the data first crosses the other limit to end the unload or reload.

X3.2.1 Nonlinearity in the test record can result from stress relaxation and ductile tearing among other possible causes. It may be necessary to exclude data from a larger region than the upper and lower 5% of the load range as specified in X3.2. A plot of the residuals from the regression analysis may be useful to determine an appropriate range of linear data to include in the compliance estimate.

X3.3 Conduct linear regression on the data selected for the unload and reload separately. The independent variable (x) is taken as the force and the dependent variable (y) is displacement so that the slope from the regression analysis is the compliance. It is recommended that crack sizes be calculated
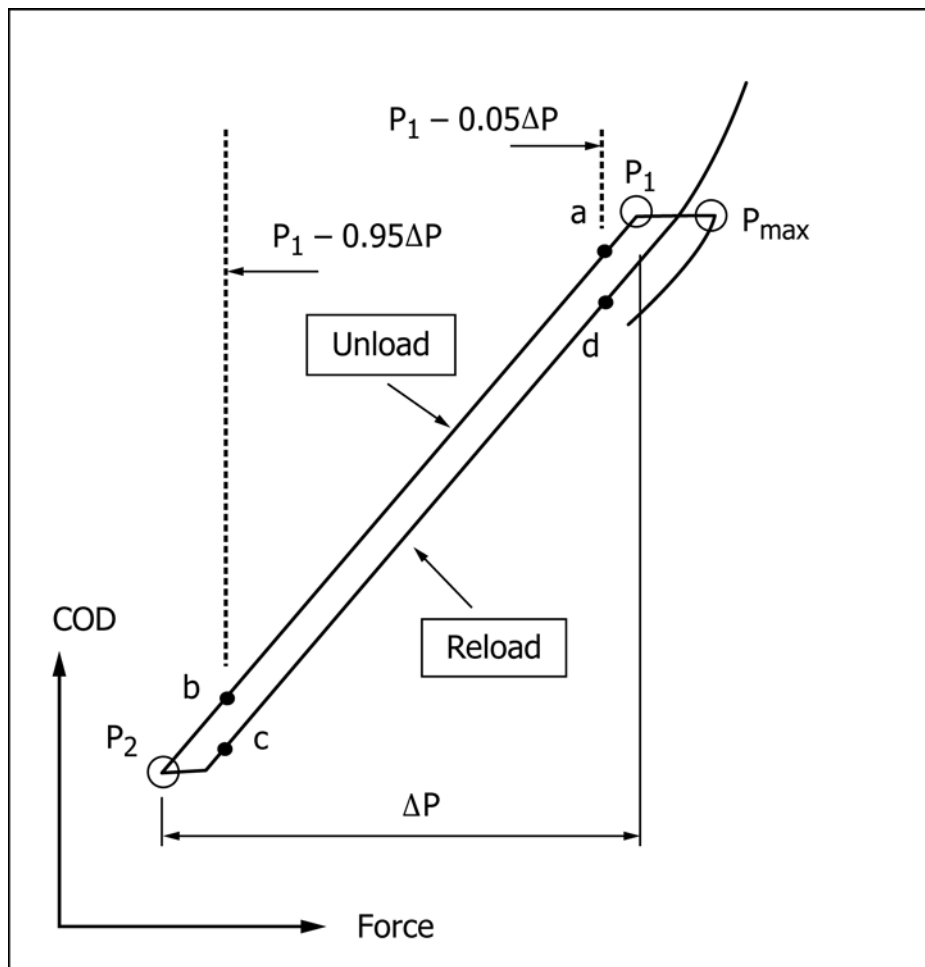

FIG. X3.1 Unload-reload sequence for compliance measurements (offset exaggerated for clarity)

using just the unload compliances for each unload/reload sequence. As an alternative it is permissible to calculate crack sizes using the reload compliances or to average the unload and reload compliances and calculate crack sizes from the average.

NOTE X3.1—Averaging the unload and reload compliances may give a different result than performing regression on all of the unload and reload data as a single data set. This distinction is important when quantifying the uncertainty in J_{Ic}.

X3.4 For each linear regression, also calculate the standard error of the compliance using equation Eq X3.1. This is a measure of the uncertainty in the slope measurement and can be used to estimate uncertainty in J_{Ic}.

$$S_{\beta_1} = \sqrt{\frac{\frac{1}{n-2}\Sigma\left[y_i - \left(\hat{\beta}_0 + \hat{\beta}_1\, x_i\right)\right]^2}{\Sigma(x_i - \bar{x})^2}} \qquad (X3.1)$$

where:

s_{β_1} = standard error of the compliance
$\hat{\beta}_0$ = estimate of intercept
$\hat{\beta}_1$ = estimate of compliance
$\bar{x}$ = mean of x-values
x_i = force values
y_i = displacement values
n = number of points used in compliance calculation

If the average compliance is used to calculate the crack size, calculate the root-mean square of the standard errors of the unload and the reload compliances to obtain a standard error of the average compliance.

X3.5 Uncertainty in J_{Ic} is related to uncertainty in compliance and can be estimated from the non-dimensionalized root-mean-square (rms) of the standard error of the compliance for all $(\Delta a, J)$ data pairs used in the power law fit of section A9.6.5. The non-dimensionalized root-mean-square of the standard error of the compliance is calculated as follows:

X3.5.1 Calculate the root-mean-square of the standard error of the compliances (from Eq X3.1) corresponding to the n (Δa, J) points selected for the power law fit in A9.6.5.

$$e = \sqrt{\frac{\Sigma_{i=1}^{n}\left(s_{\beta_1}\right)_i^2}{n}} \qquad (X3.2)$$

X3.5.2 Non-dimensionalize the rms standard error, e, from X3.5.1 by multiplying it by the product of the elastic modulus of the material, the specimen effective thickness, and the specimen width (EB_eW), then dividing by 0.0254 mm (0.001 in).

$$\tilde{e} = e\, \frac{EB_eW}{0.0254\ \text{mm}\ (0.001\ \text{in.})} \qquad (X3.3)$$

X3.5.3 Analysis of data from a round robin has shown that the uncertainty in J_{Ic} due to noise in the unload/reload data is less than 4% of J_{Ic} when the non-dimensionalized rms standard error of the compliances, $\tilde{e}$, for all points used in the power law fit is less than 400 (51). It is recommended that the non-dimensionalized rms standard error of the compliance corresponding to the unload/reload points used in the power law fit not exceed 400. If this value is exceeded, the data acquisition system should be checked to make sure enough data is being collected during an unload (reload), digital resolution is sufficient, and noise is not excessive. See Guide E1942 for guidance on evaluating a data acquisition system. See also the transducer requirements in 6.2.3 and 6.3.2. The limits used for data selection in X3.2 should also be checked to make sure data is being selected from the linear region of the unload (reload). The load train alignment, movement of pins in clevis holes, and seating of clip gage on knife edges should also be checked for these are possible sources of nonlinearity in the unload (reload). It is possible that reloads may have consistently lower standard errors, or vice versa, so examining the standard errors for both will help determine what data to use for crack size determination in order to reduce uncertainty in the resulting J_{Ic}.

NOTE X3.2—The standard error of the compliance can be decreased by increasing the number of points acquired during an unload (reload).

X3.6 Report the non-dimensionalized rms standard error of all points used in the power-law fit of A9.6.5; whether unload, reload or the average of unload and reload was used for crack size estimates; and the average number of points in the regression analyses of the unloadings to determine the compliances.

REFERENCES

(1) Rice, J. R., *Journal of Applied Mechanics*, Vol. 35, 1968, p. 379.

(2) Joyce, J. A., and Tregoning, R. L., "Development of Consistent Size Criteria for ASTM Combined Fracture Mechanics Standards," *Fatigue and Fracture Mechanics*, Vol 30, ASTM STP 1360, P. C. Paris, et al, eds., ASTM, West Conshohocken, PA, 1999.

(3) Joyce, J. A., "Manual on Elastic-Plastic Fracture: Laboratory Test Procedures," *ASTM Manual Series MNL 27*, 1996.

(4) Dawes, M. G.," Elastic-Plastic Fracture Toughness Based on the COD and *J*-Integral Concepts," *Elastic-Plastic Fracture, ASTM STP 668*, J. D. Landes, J. A. Begley, and G. A. Clarke, eds., ASTM, 1979, pp. 307–333.

(5) Willoughby, A. A., and Garwood, S. J., "On the Loading Compliance Method of Deriving Single Specimen *R*Curves in Three Point Bending," *Elastic-Plastic Fracture: Second Symposium, Volume II—Fracture Resistance Curves and Engineering Applications, ASTM STP 803*, C. F. Shih and J. P. Gudas, eds., ASTM, 1983, pp. II-372–II-397.

(6) Hackett, E. M., and Joyce, J. A., "Dynamic *J-R* Curve Testing of a High Strength Steel Using Key Curve and Multi-Specimen Techniques," *Fracture Mechanics, Seventeenth Volume, ASTM STP 905*, ASTM, 1986, pp. 741–774.

(7) Hellman, D., Rohwerder, G., and Schwalbe, K. H.," Development of a Test Setup for Measuring Deflections of Single Edge Notched Bend (SENB) Specimens," *Journal of Testing and Evaluation*, Vol 12 , No.

1, January 1984, pp. 62–64.

(8) KarisAllen, K. J. and Mathews, J. R., "The Determination of Single Edge-Notched Bend Specimen Load-Line Displacement from Remotely Located Sensors in Elastic-Plastic Fracture Testing," *Journal of Testing and Evaluation*, JTEVA, Vol 22, No. 6, Nov. 1994, pp. 581-583.

(9) Begley, J. A., Clarke, G. A., and Landes, J. D., "Results of an ASTM Cooperative Test Program on the J_{Ic} Determination of HY-130 Steel," *Journal of Testing and Evaluation*, Vol 8, No. 5, September 1980.

(10) Gudas, J. P., and Davis, D. A., "Evaluation of the Tentative J_I-R Curve Testing Procedure by Round Robin Tests of HY-130 Steel," *Journal of Testing and Evaluation*, Vol 10, No. 6, November 1982, pp. 252–262.

(11) Wallin, K., and Laukkanen, A., "Improved Crack Growth Corrections for J-R Curve Testing," *Engineering Fracture Mechanics*, 71, 2004 , pp. 1601–1614.

(12) Pisarski, H. G., "Measurement of Heat Affected Zone Fracture Toughness," Paper TS31, Steel in Marine Structures, C. Noordhoek and J. de Back, eds., Proceedings of 3rd International ECSC Conference, Delft, June 15-18, 1987, Elsevier Science Publishers B.V., Amsterdam, 1987, pp. 647–656.

(13) Srawley, J. E., "Wide Range Stress Intensity Factor Expressions for ASTM E399 Standard Fracture Toughness Specimens," *International Journal of Fracture*, Vol 12, June 1976, pp. 475–476.

(14) Newman, J. C., Jr., "Stress Analysis of the Compact Specimen Including the Effects of Pin Loading," *ASTM STP 560*, 1974, pp. 105–121.

(15) Newman, J. C., Jr., "Stress Intensity Factors and Crack Opening Displacements for Round Compact Specimens," *International Journal of Fracture*, 17(6), December 1981, pp. 567–578.

(16) Underwood, J. H., Kapp, J. A., and Baratta, F. I., "More on Compliance of the Three-Point Bend Specimen," *International Journal of Fracture*, Vol 28, 1985, pp. R41–R45.

(17) Saxena, A., and Hudak, S. J., "Review and Extension of Compliance Information for Common Crack Growth Specimens," *International Journal of Fracture*, Vol 14, October 1978, pp. 453–468.

(18) Yoon, K. K., Gross, L. B., Wade, C. S., and VanDerSluys, W. A., "Evaluation of Disk-Shaped Specimen for Determining J-R Curves," *Fracture Mechanics: 26th Volume, ASTM STP 1256*, W. G. Reuter, J. H. Underwood, and J. C. Newman, eds., American Society for Testing and Materials, Philadelphia, 1995.

(19) Nakamura, T., Shih, C. F., and Freund, L. B., "Analysis of a Dynamically Loaded Three-Point-Bend Ductile Fracture Specimen," *Engineering Fracture Mechanics*, Vol 25, No. 3, 1986, pp. 323–339.

(20) Joyce, J. A., and Hackett, E. M., "An Advanced Procedure for J-R Curve Testing Using a Drop Tower," *Nonlinear Fracture Mechanics: Vol 1–Time Dependent Fracture, ASTM STP 995*, A. Saxena, J. D. Landes, and J. L. Bassani, Eds., ASTM, Philadelphia, 1989, pp. 298–317.

(21) Irwin, G. R., " Crack-Toughness Testing of Strain-Rate Sensitive Materials", *Journal of Engineering for Power*, Trans. ASME, Oct 1964, pp. 444-450.

(22) Shoemaker, A. K., "Factors Influencing the Plane-Strain Crack Toughness Values of a Structural Steel," Transactions of the ASME, *Journal of Basic Engineering*, Sep 1969, pp. 506-511.

(23) Joyce, J. A., "Analysis of the E08.02 High Rate Round Robin," *Journal of Testing and Evaluation*, JTEVA, Vol 29. No. 4. July 2001, pp. 329–351.

(24) Herrera, R., and Landes, J. D., "Direct J-R Curve Analysis: A Guide to the Methodology," *Fracture Mechanics: Twenty-First Symposium, ASTM STP 1074*, J.P. Gudas, J.A. Joyce, and E.M. Hackett, Eds., ASTM, Conshohocken, PA, 1990, pp 24–43.

(25) Landes, J. D., Zhou, Z., Lee, K., and Herrera, R., "Normalization Method for Developing J-R Curves with the LMN Function," *Journal of Testing and Evaluation*, JTEVA, Vol 19, No. 4, July 1991, pp. 305–311.

(26) Lee, Kang, "Elastic-Plastic Fracture Toughness Determination Under Some Difficult Conditions," Ph.D Dissertation, The University of Tennessee, Knoxville, August, 1995.

(27) Linares, A.E., et al., "Using Automated J-R Curve Analysis Software To Simplify Testing And Save Time," *Advanced Materials & Processes*, Feb/Mar 2019, Vol. 177, No.2, p27.

(28) Lucon, E., "On the Effectiveness of the Dynamic Force Adjustment for Reducing the Scatter of Instrumented Charpy Results," *Journal of ASTM International*, Volume 6, Issue 1 (January 2009).

(29) Manahan, M. P., and Stonesifer, R. B., "The Difference Between Total Absorbed Energy Measured Using an Instrumented Striker and that Obtained Using an Optical Encoder," *Pendulum Impact Testing: A Century of Progress*, ASTM STP 1380, T. A. Siewert, ed., ASTM, 2000, pp. 181-197.

(30) Ireland, D. R., " Procedures and Problems Associated with Reliable Control of the Instrumented Impact Test," Instrumented Impact Testing, ASTM STP 563, T.S.,DeSisto, ed., ASTM, 1974, pp.3-29.

(31) Böhme, W., " *Experience with Instrumented Charpy Tests obtained by a DVM Round Robin and Further Developments*," ESIS 20, E. van Walle, ed., MEP Publications, London, 1996, pp. 1-23.

(32) Lucon, E., " The Use of the Normalization Data Reduction Technique for Measuring Upper Shelf Toughness Under Impact Loading Rates"," *Journal of ASTM International*, Vol. 8, No. 10, (pending release) November 2011.

(33) Lucon, E., "Estimating dynamic ultimate tensile strength from instrumented Charpy data," *Materials and Design*, Volume 97, May 2016, pp. 437-443.

(34) Hartman, G. A., and Johnson, D. A., "D-C Electric Potential Method Applied to Thermal/Mechanical Fatigue Crack Growth," *Experimental Mechanics*, March 1987, pp. 106–112.

(35) Pollock, D. D., "Thermoelectricity, Theory, Thermometry, Tool," ASTM STP 852, ASTM, 1985.

(36) Catlin, W. R., Lord, D. C., Prater, T. A., and Coffin, L. F., "The Reversing D-C Electrical Potential Method," *Automated Test Methods for Fracture and Fatigue Crack Growth*, ASTM STP 877, Cullen, W. H., Landgraf, R. W., Kaisand, L. R., and Underwood, J. H., Eds., ASTM, 1985, pp. 67–85.

(37) Bicego, V., Liviero, D., Fossati, C., and Lucon, E., "J-R curve testing utilizing the reversing direct current electrical potential drop method," *Application of Automation Technology to Fatigue and Fracture Testing*, ASTM STP 1092, Braun A.A., Ashbaugh, E., and Smith F.M., Eds., American Society for Testing and Materials, 1990, pp. 143-166.

(38) Tarnowski, K. M., Davies, C. M., Dean, D. W., and Nibkin, K. M., "The Influence of Plasticity on Crack Length Measurements Using the Potential Drop Technique," *Evaluation of Existing and New Sensor Technologies for Fatigue, Fracture and Mechanical Testing*, ASTM STP 1584, Kang J., Jablonski, D., and Dudzinski, D., Eds., American Society for Testing and Materials, 2015, pp. 73-96.

(39) Donald, J. K., and Ruschau, J., "Direct Current Potential Difference Fatigue Crack Measurement Techniques," *Fatigue Crack Measurement: Techniques and Applications*, K. J. Marsh, R. A. Smith, and R. O. Ritchie, Eds., EMAS, Warley UK, 1991, pp. 11-37.

(40) Dover, W. D., et al., "A.C. Field Measurement—Theory and Practice," from *The Measurement of Crack Length and Shape During Fracture and Fatigue*, Beevers, C. J., Ed., EMAS, Cradley Heath, UK, 1980, pp. 222-260.

(41) Wilkowski, G. M., Wambaugh, J. O., and Prabhat, K., "Single Specimen J-R Curve Evaluations Using the DCEP Method and a Computerized Data Acquisition System," *Fracture Mechanics*: Fifteenth Symposium, R. J. Sanford, Ed., ASTM, 1984, pp. 553-576.

(42) Marschall, C. W., Held, P. R., Landow, M. P., and Mincer, P. N., "Use of the Direct-Current Electric Potential Method to Monitor Large Amounts of Crack Growth in Highly Ductile Metals," *Fracture Mechanics: Twenty-First Symposium*, ASTM STP 1074, J. P. Gudas, J. A. Joyce, and E. M. Hackett, eds., ASTM, 1990, pp. 581-593.

(43) Lucon, E., "ASTM E08.07.09 Analytical Round-Robin on the Use of DC Electrical Potential Difference for the Measurement of Crack Size in Ductile Fracture Testing," *Materials Performance and Characterization*, Vol. 7, No. 2, April 2018.

(44) Schwalbe, K.-H., Hellmann, D., Heerens, J., Knaack, J., and Müller-Roos, J., "Measurement of stable growth including detection of initiation of growth using the DC potential drop and the partial unloading methods," ASTM STP 856, 1985, pp. 338-362

(45) Aronson, G. H., and Ritchie, R. O., "Optimization of the Electrical Potential Technique for Crack Monitoring in Compact Test Pieces Using Finite Element Analysis," *Journal of Testing and Evaluation*, JTEVA, Vol. 7, No. 4, July 1979, pp. 208–215.

(46) Johnson, H. H., "Calibrating the Electric Potential Method for Studying Slow Crack Growth," *Materials Research and Standards*, Vol. 5, No. 9, Sept. 1965, pp. 442–445.

(47) Tarnowski, K. M., Nibkin, K. M., Dean, D. W., and Davies, C. M., "A Unified Potential Drop Calibration Function for Common Crack Growth Specimens," *Experimental Mechanics*, published on line 25 May 2018, https://doi.org/10.1007/s11340-018-0398-z.

(48) Hicks, M. A., and Pickard, A. C., "A Comparison of Theoretical and Experimental Methods of Calibrating the Electrical Potential Drop Technique for Crack Length Determination," *Int. Journal of Fracture*, No. 20, 1982, pp. 91–101.

(49) Hackett, E. M., Kirk, M. T., and Hays, R. A., "An Evaluation of J-R Curve Testing of Nuclear Piping Materials Using the Direct Current Potential Drop Technique," NUREG/CR-4540, U.S. Nuclear Regulatory Commission, August 1986.

(50) Joyce, J.A., " J Resistance Curve Testing of Short Crack Bend Specimens Using Unloading Compliance," *Fracture Mechanics, Twenty-Second Symposium*, *Vol. 1, ASTM STP 1131*, American Society for Testing and Materials, West Conshohocken, PA, 1992, pp. 904-926.

(51) Graham, Stephen M., "Uncertainty in Ductile Fracture Initiation Toughness (J_{Ic}) Resulting From Compliance Measurement," *Application of Automation Technology in Fatigue and Fracture Testing and Analysis, STP 1571*, Peter C. McKeighan and Arthur A. Braun, Eds., pp. 134 – 152, ASTM International, West Conshohocken, PA 2014.